STUDY ON THE CONNEXIN 32 AND ITS ROLE IN THE RELEASE OF ATP

Eugènia Grandes Vilaclara

Barcelona, June 2008

Department of Pathology and Experimental Therapeutics.
Campus of Bellvitge, University of Barcelona

209. Nagy, J.I., Dudek, F.E. & Rash, J.E. Update on connexins and gap junctions in neurons and glia in the mammalian nervous system. *Brain Res Brain Res Rev* **47**, 191-215 (2004).
210. Okada, Y. et al. Receptor-mediated control of regulatory volume decrease (RVD) and apoptotic volume decrease (AVD). *J Physiol* **532**, 3-16 (2001).
211. Franco, R., Panayiotidis, M.I. & Ochoa de la Paz, L.D. Autocrine signaling involved in cell volume regulation: The role of released transmitters and plasma membrane receptors. *J Cell Physiol* (2008).
212. Elfgang, C. et al. Specific permeability and selective formation of gap junction channels in connexin-transfected HeLa cells. *J Cell Biol* **129**, 805-17 (1995).
213. Vogel, R., Valiunas, V. & Weingart, R. Subconductance states of Cx30 gap junction channels: data from transfected HeLa cells versus data from a mathematical model. *Biophys J* **91**, 2337-48 (2006).
214. Das Sarma, J., Das, S. & Koval, M. Regulation of connexin43 oligomerization is saturable. *Cell Commun Adhes* **12**, 237-47 (2005).
215. Eckert, R., Dunina-Barkovskaya, A. & Hulser, D.F. Biophysical characterization of gap-junction channels in HeLa cells. *Pflugers Arch* **424**, 335-42 (1993).
216. Hulser, D.F. & Webb, D.J. Relation between ionic coupling and morphology of established cells in culture. *Exp Cell Res* **80**, 210-22 (1973).
217. Dinter, A. & Berger, E.G. Golgi-disturbing agents. *Histochem Cell Biol* **109**, 571-90 (1998).
218. Bal-Price, A., Moneer, Z. & Brown, G.C. Nitric oxide induces rapid, calcium-dependent release of vesicular glutamate and ATP from cultured rat astrocytes. *Glia* **40**, 312-23 (2002).
219. North, R.A. Molecular physiology of P2X receptors. *Physiol Rev* **82**, 1013-67 (2002).
220. North, R.A. & Verkhratsky, A. Purinergic transmission in the central nervous system. *Pflugers Arch* **452**, 479-85 (2006).
221. Jun, D.J. et al. Extracellular ATP mediates necrotic cell swelling in SN4741 dopaminergic neurons through P2X7 receptors. *J Biol Chem* **282**, 37350-8 (2007).
222. Chow, S.C., Kass, G.E. & Orrenius, S. Purines and their roles in apoptosis. *Neuropharmacology* **36**, 1149-56 (1997).
223. James, G. & Butt, A.M. P2Y and P2X purinoceptor mediated Ca2+ signalling in glial cell pathology in the central nervous system. *Eur J Pharmacol* **447**, 247-60 (2002).
224. Veenstra, R.D. et al. Selectivity of connexin-specific gap junctions does not correlate with channel conductance. *Circ Res* **77**, 1156-65 (1995).
225. Musa, H. et al. Amino terminal glutamate residues confer spermine sensitivity and affect voltage gating and channel conductance of rat connexin40 gap junctions. *J Physiol* **557**, 863-78 (2004).
226. Trexler, E.B., Bukauskas, F.F., Kronengold, J., Bargiello, T.A. & Verselis, V.K. The first extracellular loop domain is a major

Programa de Doctorat de Neurobiologia

Bienni 2003-2005

STUDY ON THE CONNEXIN 32 AND ITS ROLE IN THE RELEASE OF ATP

Tesi Doctoral

Eugènia Grandes Vilaclara

Directors de Tesi

Dr. Carles Solsona Sancho Dr. Joan Blasi Cabús

Department of Pathology and Experimental Therapeutics.

Medicine School, Campus of Bellvitge, University of Barcelona

"The important thing in science is not so much to obtain new facts as to discover new ways of thinking about them."
(Sr. William Bragg, 1862-1942, Nobel Prize in Physics 1915)

I'd like to thank to everyone who has helped me in any way along this last five years. You know who you are, you know I'm grateful.

This work has been supported by Ministerio de Educación y Ciencia (MEC): BFI2001-3331, *SAF2005/736*, by La Marató de TV3, departament d'Universitats, recerca i Societat de la Informació de la Generalitat de Catalunya, agència de gestió d'ajuts Universitaris i de recerca (AGAUR): programa FI2004-07 and fondo social Europeo.

TABLE OF CONTENTS

ABBREVIATIONS

Å	Angstrom
AcA	Acetic acid
AsCx38	Connexin 38 antisense
AU	Arbitrary units
bp	base pairs
BFA	Brefeldin A
BSA	Bovine serum albumin
$CaCl_2$	Calcium chloride
cDNA	Complementary Deoxyribonucleic acid
CNS	Central nervous system
cRNA	Complementary Ribonucleic acid
Caspr	Contactin associated protein
Cx29	Connexin 29
Cx32	Connexin 32
Cx38	Connexin 38
Cx43	Connexin 43
Da	Daltons
DEPC	Dietil pirocarbonate
DMSO	Dimethyl sulfoxide
FBS	Foetal bovine serum
FFA	Flufenamic acid
G_j	Conductance
GJβ1	Gap Junction protein beta 1
GPCRs	G-protein coupled receptors
HCl	Hydrochloric acid
hCx32	human Connexin 32
HEPES	(4-(2-hydroxyethyl)-1-piperazineethanesulfonic acid)

HRP horseradish peroxidase

IBMX 3-Isobutyl-1-methylxanthine

IF Immunofluorescence

IP_3 Inositol 1,4,5-triphophate

KAc Potassium acetate

KCl Potassium chloride

KDa Kilo Daltons

LB Luria-Bertani media

LSM Laser scanning microscope

mA Milliamperes

$MnCl_2$ Manganese chloride

$MgSO_4$ Magnesium sulfate

mV Milli Volts

MΩ Mega Ohm

nA Nanoamperes

NaCl Sodium Chloride

NaMOPS Sodium 3-(N-morpholino)propanesulfonate

NaH_2PO_4 Sodium dihydrogenphosphate

Na_2HPO_4 Disodium hydrogenphosphate

NaOH Sodium hydroxide

NGS Normal goat serum

NSF *N*-ethylmaleimide-sensitive fusion protein

ON Over night

PANX Pannexin

PBS Phosphate buffered saline

PMSF phenylmethylsulphonyl fluoride**PNS**

Peripheral nervous system

RbCl	Rubidium chloride
pS	Pico Siemens
RT	Room temperature
s	seconds
SNAP 25	synaptosomal associated protein of 25 kDa
S1A	Syntaxin 1A
TBS	Tris buffered saline
TEVC	Two Electrode Voltage Clamp
Tris	trishydroxymethylaminomethane
UTP	Uridine triphospate
UTR	Untranslated region
V	Volts
V_j	Transjunctional voltage
V_m	Membrane potential
WT	Wild type
°C	Centigrade degree
µA	Microamperes

SUMMARY

La malaltia de Charcot-Marie-tooth (CMT) recull un seguit de neuropaties perifèriques les quals afecten tant la funció motora com la sensorial i tenen una elevada prevalència en la població (1:2500). Els símptomes més comuns són debilitat muscular dels peus i músculs inferiors de les cames, atrofia dels peus i deformitats com ara arcs alts i dits en martell. A més, la part inferior de les cames pot adquirir un aspecte "d'ampolla de xampany invertida" a causa de la pèrdua de massa muscular. La malaltia es progressiva i la debilitat muscular avança i acaba afectant també les mans. Avui en dia, la malaltia de CMT es classifica segons les característiques clíniques, electrofisiològiques, histopatològiques i genètiques en els subtipus CMT1, CMT2, CMT3, CMT4 i CMTX.

La forma de Charcot-Marie-Tooth lligada al cromosoma X (CMTX) ha estat relacionada amb mutacions de la connexina 32. Fins avui s'han trobat més de 290 mutacions diferents de gen de la Cx32 (GJβ1) relacionades amb aquesta malaltia. Aquest gen es troba al cromosoma X, per tant la malaltia té herència lligada al sexe, el que significa que els homes estan afectats de manera uniforme, mentre que les dones tenen una afectació variable: poden ser portadores sense patir la malaltia o expressar la malaltia amb afectació variable degut a la inactivació a l'atzar del cromosoma X.

Les mutacions de la connexina 32 (Cx32) poden donar lloc a CMTX de varies maneres ja que existeixen mutants de la Cx32 que afecten de manera diferent la proteïna, ja sigui trencant el trànsit de la proteïna al reticle endoplasmàtic o a l'aparell de

Golgi, o provocant defectes en el hemicanals de Cx32 de manera que no puguin formar unions gap o que la seva permeabilitat estigui alterada.

Les connexines són proteïnes que formen estructures hexamèriques a la membrana plasmàtica anomenades hemicanals o connexons. Aquests hemicanals tenen un porus central el qual permet el pas de molècules entre el citoplasma i l'espai extracel·lular. Cada connexina té quatre dominis transmembrana i els extrems amino i carboxi terminals són intracel·lulars. Les dues nanses extracel·lular resultants estan altament conservades i són les responsables de la unió de dos connexines expressades en la membrana de cèl·lules adjacents per formar una unió tipus gap. La nomenclatura de les connexines és "Cx" seguit del seu pes molecular esperat, així, la Cx32 pesa 32 KDa.

La funció clàssica de les connexines és la formació d'unions tipus gap entre cèl·lules, permetent l'acoblament elèctric i metabòlic de les cèl·lules mitjançant el pas directe entre elles d'ions i segons missatgers de fins a 1 KDa (com ara Na^+, K^+, Ca^{2+}, cAMP, IP_3, etc). Són canals no selectius i el moviments a través dels canals es a favor de gradient, modulat per la diferència de potencial. Tot i que al principi es creia que els hemicanals estaven tancats fins al moment de formar les unions tipus gap, estudis més recents indiquen que els hemicanals per si mateixos també tenen altres funcions dins del metabolisme cel·lular, com per exemple, la propagació d'onades de calci en astròcits. Fins ara s'han descrit varis mecanismes pels quals es

regula la obertura i tancament dels hemicanals, com són l'estat de fosforilació, estímuls mecànics, nivells de calci iònic, presència de quinina, el potencial de membrana o el pH.

La Cx32 va ser la primera connexina descrita i es troba al fetge, ronyons, intestí, pulmons, pàncreas, úter, cervell i nervis perifèrics. Tot i aquesta expressió tan ubiqua les mutacions en la Cx32 només afecten al sistema nerviós perifèric, el que indica que altres connexines dels altres òrgans podrien suplir la funció de la Cx32. Als nervis perifèrics la Cx32 s'expressa en les cèl·lules de Schwann (encarregades de formar les beines de mielina al sistema nerviós perifèric), concretament a les regions paranodals i a les incisures d'Schmidt-Lanterman de la beina de mielina, on la Cx32 forma unions reflexives que permetrien una via directe entre el citoplasma perinuclear i l'adaxonal de les cèl·lules de Schwann, facilitant així de distribució de nutrients, missatgers i retornant la concentració de K^+ a nivells basals després d'un potencial d'acció.

Els hemicanals de Cx32 tenen una conductància de 90 pS i s'activen per despolarització de la membrana i per absència de calci extracel·lular.

Al laboratori ens interessa estudiar la Cx32 en relació a l'alliberació d'ATP. L'alliberació cel·lular d'ATP ha estat investigada en les ultimes dècades i hi ha moltes hipòtesis sobre mecanismes relacionats amb l'alliberació d'ATP, com ara l'exocitosis, canals iònics, CD39, CFTR i els hemicanals de connexines.

Al nostre laboratori ja s'havien realitzat treballs sobre

l'alliberació d'ATP a través de la connexina endògena d'oòcits de *Xenopus* (Cx38). Per tal d'estudiar l'alliberació d'ATP a través d'hemicanals de Cx32, aquesta proteïna va ser expressada en oòcits de *Xenopus laevis* i posteriorment activada per despolarització mitjançant la tècnica de fixació de voltatge amb dos elèctrodes (TEVC). La connexina endògena dels oòcits (Cx38) va ser inhibida injectant un oligonucleòtid antisentit als oòcits juntament amb el cRNA que codificava per la hCx32. En resposta a l'estímul depolaritzant, vam registrar un corrent de sortida característica de la hCx32, i també alliberament d'ATP associat a una corrent de cua que apareixia quan el potencial de membrana tornava als valors basals i es tancava lentament. Hi havia una relació directament proporcional entre la càrrega elèctrica dels corrents generats i la quantitat d'ATP alliberat. Així vam poder constatar que la hCx32 expressada en oòcits de Xenopus s'activa per despolarització, i que es produeix una sortida d'ATP de la cèl·lula.

Com que la Cx32 s'expressa en cèl·lules de Schwann i havíem observat que els hemicanals d'aquesta connexina s'activen per depolarització, estàvem interessats en saber si la Cx32 també allibera ATP quan està expressada endògenament a les cèl·lules de Schwann. Per això vam utilitzar preparacions de nervi ciàtic de rata i ratolí, als quals vam aplicar estímuls elèctrics mitjançat un elèctrode de succió per estimular el nervis sencers imitant la despolarització que causa la transmissió d'un potencial d'acció a través del nervi. Utilitzant una camera de vídeo refrigerada d'alta sensibilitat i la reacció de la luciferina-luciferasa vam capturar la

sortida d'ATP del nervi ciàtic en resposta a estímuls elèctrics de 15 V, aplicats durant 10-30 minuts, amb una freqüència de 2-4 Hz. L'alliberament d'ATP capturat estava focalitzat en certs punts del nervi, que es repetien periòdicament al llarg del nervi, el que ens va portar a suposar que les regions on veiem aquest alliberament d'ATP més marcat podrien correspondre al les zones paranodals, en contacte amb els nodes de Ranvier, i on la Cx32 està altament expressada.

Esta descrit que la Cx32 s'expressa en zones paranodals i en les cissures d'Schmidt-Lanterman de la beina de mielina dels nervis perifèrics, per tal de constatar-ho en les nostres preparacions vam aplicar tècniques d'immunofluorescència per detectar la connexina 32 però també les dues altres connexines que està descrit que s'expressen a les cèl·lules de Schwann: la Cx29 i la Cx43. La Cx29 també s'expressa en regions paranodals i cissures d'Schmidt-Lanterman, en canvi la Cx43 ho fa en baixa quantitat al llarg de tota la beina de mielina. Els resultats de les nostres immunofluorescències van confirmar la presència de Cx32 i Cx29 a les regions paranodals i a les cissures d'Schmidt-Lanterman del nervi ciàtic de ratolí, però per la Cx43, tot i que l'expressió si que era baixa al llarg del nervi, vam trobar major expressió a les regions paranodals, com que hi ha pocs estudis sobre la localització de la Cx43 als nervis perifèrics, podem pensar que realment hi ha major expressió de Cx43 als paranodes.

La funció de la Cx29 i la Cx43 en la beina de mielina no es completament coneguda, s'ha proposat que la Cx29 podria tenir

un paper en la via directa que travessa les capes de mielina per unir el citoplasma perinuclear i adaxonal de la cèl·lula de Schwann conjuntament amb la Cx32, ja que els ratolins knock-out per la Cx32 no tenen interromput el transport radial de colorants de baix pes molecular, com seria d'esperar si aquesta via depengués exclusivament de la Cx32. De tota manera, els ratolins knock-out per la Cx32 acaben desenvolupant una neuropatia perifèrica amb símptomes similars als que pateixen els pacients de CMTX, indicant que la Cx29 no pot suplir completament la funció de la Cx32 en les cèl·lules de Schwann i, per tant, la Cx32 i la Cx29 tenen diferents funcions en la beina de mielina. Pel que fa a la Cx43, la seva funció es encara més desconeguda, altrament s'ha descrit que la seva expressió augmenta després d'una lesió en el nervi perifèric, indicant que tindria alguna funció en la degeneració Walleriana i en els processos de remielinització dels axons.

Després de veure l'alliberació d'ATP del nervi ciàtic després d'aplicar una estimulació elèctrica, i de veure l'expressió de les connexines a regions paranodals del nervi ciàtic de ratolí, (les quals es repeteixen periòdicament al llarg dels axons, com els punt d'alliberació d'ATP observats en els nervis estimulats elèctricament); volíem veure que l'alliberació d'ATP fos de les pròpies cèl·lules de Schwann, i no d'altres components del nervi. Per això vam posar a punt cultius primaris de cèl·lules de Schwann provinents de nervis ciàtics de ratolins adults joves. El primer que vam fer amb les cèl·lules en cultiu va ser comprovar mitjançant immunofluorescència si expressaven les connexins tot

i no estar formant mielina. Vam veure marca per les tres connexines: Cx32, Cx29 i Cx43. La Cx32 era la que mostrava una marca més intensa a tot el cos cel·lular, mentre que la Cx43 era la que tenia una expressió més baixa i la marca era més intensa a voltant del nucli.

Per tal d'estimular els hemicanals de Cx32 de les cèl·lules de Schwann en cultiu les vam sotmetre a un xoc hipotònic (un tipus d'estímul que s'ha descrit com activador d'obertura d'hemicanals) i vam detectar l'alliberament d'ATP utilitzant la reacció de la luciferina-luciferasa i un lector de plaques per luminiscència. Els cultius alliberaven de forma ràpida, immediata i curta després de rebre l'estímul. Les cèl·lules alliberaven $2,5x10^{-4}$ fmols d'ATP/10^4 cèl·lules després del xoc hipotònic, una quantitat significativament més gran ($p=0,024$, $n=7$) que l'ATP que alliberaven els grups control que no van rebre l'estímul hipotònic ($3,03x10^{-5}$ fmols/10^4 cèl·lules). Després d'aquests experiments hem arribat a la conclusió que les cèl·lules de Schwann en cultiu primari alliberen ATP després de rebre un estímul mecànic (xoc hipotònic), i que aquesta alliberació es ràpida i immediata. De tota manera no es pot demostrar que aquesta alliberació d'ATP hagi estat conseqüència de l'obertura d'hemicanals de Cx32.

Per tal de continuar la possible implicació dels hemicanals de Cx32 en aquesta alliberació d'ATP en resposta a hipotonicitat vam repetir els assaigs de xoc hipotònic però utilitzant la línia cel·lular HeLa, la qual s'utilitza sovint en estudis de connexina ja que de forma natural tenen una molt baixa expressió de connexines. El xoc hipotònic el vam realitzar utilitzant cèl·lules

HeLa normal com a controls i cèl·lules HeLa transfectades de forma estable amb la hCx32. Aquestes cèl·lules transfectades de forma estable es van generar durant una estança al laboratori del Dr. Klaus Willecke, a la Universitat de Bonn, Bonn, Alemanya. L'expressió de hCx32 en aquestes cèl·lules de forma constitutiva i elevada va ser comprovada per immunofluorescència, així com es va comprovar que aquestes cèl·lules són capaces de formar unions tipus nexe (gap) entre elles. La construcció amb la Cx32 per transfectar les cèl·lules també es va generar durant aquesta estada i serà explicat amb més detall més endavant en aquest resum.

En els assaigs d'hipotonicitat vam poder registrar alliberació d'ATP després d'un xoc hipotònic respecte a les cèl·lules que no rebien cap xoc. Però comparant les cèl·lules HeLa normals amb les transfectades amb la hCx32 no vam detectar diferències en la quantitat d'ATP alliberat entre els dos tipus de cèl·lules, ja que vam mesurar una alliberació d'ATP de l'ordre de 0.0117 fmols/10^4 cèl·lules en HeLa WT, i de 0.0102 fmols /10^4 cèl·lules en HeLa hCx32 en resposta al xoc hipotònic. Així, en aquests experiments sembla que en les cèl·lules HeLa la contribució d'hemicanals de hCx32 a l'alliberació d'ATP seria mínima o nula.

Després d'observar això vam voler comprovar si aquesta alliberació seria a través d'exocitosi i per això vam repetir els assaigs d'hipotonicitat però amb cèl·lules prèviament tractades amb brefeldina 1A (BFA), una droga que interromp el transport a través de l'aparell de Golgi i així acaba inhibint els processos d'exocitosi. Però després del tractament no hi havia inhibició en

la quantitat d'ATP alliberat així que podem descartar l'exocitosi com a via d'alliberació d'ATP en resposta a un xoc hipotònic. En els nostres experiments vam mesurar una alliberació d'ATP de 0.029 fmols/ 10^4 cèl·lules en cèl·lules HeLa WT preincubades amb BFA, i de 0.034 fmols/ 10^4 cèl·lules en HeLa WT sense preincubació (p=0.146). Per cèl·lules HeLa hCx32 vam mesurar un alliberació mitjana d'ATP de 0.033 fmols/ 10^4 cèl·lules per HeLa hCx32 no preincubades, i de 0.0211 fmols/ 10^4 cèl·lules per HeLa hCx32 preincubades amb BFA (p=0.75). Per altra banda vam observar que els controls (cèl·lules no sotmeses a xoc hipotònic) preincubats amb BFA alliberaven menys ATP que els que no van ser preincubats amb BFA, el que ens indica que l'alliberació basal d'ATP que enregistràvem en els controls degut a la injecció de solucions en els experiments es bàsicament deguda a exocitosi. Per HeLa WT l'ATP alliberat va passar de ser de l'ordre de 0.0173 fmols / 10^4 cèl·lules en els controls sense preincubar a ser de 9.49×10^{-3} fmols/ 10^4 cèl·lules en els controls preincubats prèviament amb BFA. Per HeLa transfectades de forma estable amb hCx32 la disminució va ser menor i va passar de 0.0189 fmols/ 10^4 cèl·lules per controls no preincubats a 7.33×10^{-3} fmols/ 10^4 cèl·lules en controls si van ser prèviament tractats amb BFA.

Tot i que aquest estudi deixa moltes portes obertes sobre el mecanisme d'alliberació d'ATP a través d'hemicanals de Cx32 i la seva possible implicació amb la malaltia de CMTX, també deixa eines per seguir la recerca sobre aquesta qüestió. Durant una

estada de sis mesos a la Universitat de Bonn a Alemanya, i sota la supervisió del Dr. Klaus Willecke, vam generar una sèrie de construccions de la Cx32 humana amb mutacions descrites en pacients de CMTX. Les mutacions que es van obtenir al laboratori són les següents: **Cx32^{S26L}**, la mutació es troba al primer domini transmembrana i provoca una reducció del porus de l'hemicanal de 7Å a menys de 3Å; **Cx32^{P87A}**, la mutació es troba en aquesta prolina situada en el segon domini transmembrana està molt conservada i ha estat relacionada amb l'obertura depenent de voltatge de l'hemicanal, una mutació així pot afectar a la permeabilitat dels hemicanals; **Cx32$^{del111-16}$**, delació d'una part del segment intracel·lular, implicat en l'obertura per pH; **Cx32^{D178Y}**, una mutació puntual que altera la detecció del calci, i **Cx32^{R220St}**, una mutació que elimina la part final del domini carboxi terminal, eliminant la possible interacció amb altres proteïnes. Totes aquestes construccions i també la forma normal de la hCx32 es van generar i inserir en dos plàsmids diferents, un, pBxG, que conté la seqüència de la β-globina de *Xenopus* i potencia l'expressió (traducció) de proteïna en oòcits de *Xenopus*, i l'altre, pMJgreen, que conté el promotor de CMV humà per l'expressió en cèl·lules eucariotes, preferentment humanes. Tot això són eines per estudiar la Cx32 i la seva implicació en l'alliberació cel·lular d'ATP.

Les construccions en pBxG estan llestes per obtenir cRNA per injectar a oòcits i mesurar els corrents de sortida i l'alliberació d'ATP que provoca un estímul despolaritzant. Com que ja hem fet experiments per veure com es comporta la Cx32 normal

podrem comparar el comportament de les mutacions i saber així, si alguna (o totes) alteren la permeabilitat per l'ATP, i si es així, si aquesta característica juga algun paper en el desenvolupament de la malaltia de CMTX.

Les construccions en pMJgreen poden ser transfectades a cèl·lules eucariotes com HeLa, Neuro 2A o C6, típiques línies utilitzades per estudiar connexines degut a la baixa expressió endògena de connexines que presenten, i poder fer més assaigs, tant d'hipotonicitat com d'altres característiques, per tal de seguir estudiant les característiques de les mutacions de Cx32 que donen lloc a la simptomatologia típica de CMTX. Totes aquestes mutacions que hem clonat arriben a la membrana plasmàtica i l'efecte no és, per tant, degut a la falta de proteïna, sinó a una alteració de les seves funcions.

Al nostre laboratori treballem amb la hipòtesi que l'alteració de l'alliberació d'ATP afecta a la cèl·lula de Schwann, la qual reaccionaria demielinitzant els axons i morint (o viceversa), com passa als pacients de CMTX. Ja s'ha descrit en la literatura que les cèl·lules de Schwann alliberen ATP en resposta a estímuls com ara el glutamat o UTP, i aquesta alliberació ha estat associada a exocitosi i obertura de canals aniònics. Nosaltres pensem que, a més d'altres mecanismes, les cèl·lules de Schwann també poden alliberar ATP a través d'hemicanals de Cx32. Com ja s'ha mencionat anteriorment, la Cx32 en cèl·lules de Schwann s'expressa en les regions paranodals, que estan en contacte íntim amb l'axó i a prop dels nodes de Ranvier, on es

produeix la despolarització quan es transmet un potencial d'acció. Aquesta despolarització també afecta per tant la membrana de la cèl·lula de Schwann en les regions paranodal i podria activar hemicanals de la Cx32, que s'obririen i alliberarien ATP al medi després d'un potencial d'acció i de l'acció mecànica del moviment. Aquest ATP alliberat activaria els receptors purinèrgics $P2X_7$ i $P2Y_2$, ambdós expressats també per les cèl·lules de Schwann (l'ATP tindria per tant, un paper de missatger autocrí). De tota manera el receptor $P2X_7$ necessita concentracions d'ATP de l'ordre de mil·limolar, pel que en general restaria inactiu, mentre que el receptor $P2Y_2$ s'activa a concentracions d'ATP més baixes, i provocaria augment de calci intracel·lular, activant cascades de senyals intracel·lulars, algunes implicades en la supervivència de les cèl·lules de Schwann.

Si considerem aquestes dades, quan la Cx32 està mutada, com passa a la malaltia de CMTX, es podrien produir dos tipus d'alteració en relació a l'alliberació d'ATP: un augment o una disminució de l'alliberació.

Per una banda, mutacions que afectin el trànsit de la proteïna i provoquin que no s'expressi a la membrana, o permetin la formació d'hemicanals a la membrana però aquests no siguin funcionals provocarien una disminució de l'alliberació d'ATP al medi, i per tant hi hauria menys senyals a través dels receptors $P2Y_2$, produint la mort cel·lular per falta de senyals de supervivència.

D' altra banda, en mutacions de la Cx32 que portessin a la formació d'hemicanals funcionals però amb una probabilitat

d'obertura anormalment augmentada augmentaria la sortida d'ATP, incrementant la concentració d'ATP extracel·lular, els que activaria no només els receptors $P2Y_2$, sinó també el receptors $P2X_7$, la sobreactivació dels quals ha estat relacionada amb processos d'apoptosi i necrosi cel·lular.

Una hipòtesi similar ja ha estat proposada per explicar la resposta a una lesió que presentarien les cèl·lules glials del sistema nerviós central. Per tant, poder caracteritzar les mutacions generades respecte a la seva capacitat per alliberar ATP seria interessant de cara a dilucidar si realment l'ATP té un paper de senyalitzador en la supervivència de les cèl·lules de Schwann, obrint així un nou camp de recerca per als mecanismes que provoquen la CMTX.

Per últim, a més de l'alliberació d'ATP a través d'hemicanals de Cx32, s'ha estudiat una mica la possible interacció amb una altra proteïna: la sintaxina 1A (S1A). La S1A es una proteïna SNARE, juntament amb la sinaptobrevina/VAMP1 i SNAP25. Aquestes tres proteïnes han estat relacionades amb l'ancoratge de les vesícules d'exocitosi a la membrana plasmàtica i amb la fusió de la membrana plasmàtica amb la de les vesícules en els processos d'exocitosi a través de la formació del complex SNARE. La S1A i SNAP25 s'expressen a la membrana plasmàtica (t-SNAREs) i la sinaptobrevina/VAMP1 a la membrana de les vesícules (v-SNARE), i es reconeixen entre elles per formar el complex SNARE.

A més del seu paper en l'exocitosi, la S1A ha estat

relacionada amb funcions reguladores de canals que s'expressen a la membrana plasmàtica, com ara canals de calci dels subtipus N, L i R, canals de potassi (Kv2.1), canals de potassi activats per calci (BK_{Ca}), canals de sodi epitelials (ENaC), CFTR, així com treballs previs en el nostre laboratori demostren la interacció entre la sintaxina 1A i els hemicanals de Cx38, la connexina endògena dels oòcits de *Xenopus laevis* (pendent de publicació).

Amb aquests antecedents vam voler veure si la S1A podia afectar altres connexines a més de la Cx38. Per això es van fer experiments amb oòcits de Xenopus injectant cDNA per la hCx32 i també per la S1A i es van realitzar experiments de TEVC activant els hemicanals de hCx32 per despolarització i registrant el corrent de sortida generat i l'alliberació d'ATP. Les interferències de la Cx38 endògena es van abolir injectant un oligonucleotid antisentit per la Cx38 al oòcits. Els resultats obtinguts es van comparar amb els d'oòcits injectats només amb la hCx32 i es va poder observar una inhibició parcial dels corrents de sortida generats, de l'ordre del 15%, tot i que el que més ens va sorprendre va ser que la inhibició de l'ATP alliberat i del corrent de carrega dels corrents de cua eren majors, de l'ordre del 45% i 52% d'inhibició respectivament, comparats amb els oòcits que no expressaven S1A però si havien estat injectats amb cRNA de hCx32 i oligonucleòtid antisentit per inhibir la Cx38 endògena.

Tot i que les connexines són canals típicament no selectius, i s'ha publicat que deixarien passar qualsevol compost més petit de 1000 Da, també s'ha descrit que diferents connexines tenen

diferents permeabiltats (diferents valors de conductància), el que permetria una certa discriminació d'ions i segons missatgers. En algunes connexines, s'ha publicat que certes càrregues a l'extrem amino-terminal i les nanses extracel·lulars podrien contribuir a la generar una certa selectivitat per certs ions i metabòlits. Altres estudis donen suport a la idea que la permeabilitat no depèn només de la mida del porus, i suggereixen que algunes càrregues dels aminoàcids de l'interior del porus podrien interaccionar amb els "permeants", o bé la pròpia estructura tridimensionals dels citats permeants influiria en la seva habilitat per travessar els porus de les connexines. Així, tot i que la Cx32 ha estat descrita com una de les connexines amb el porus més gran, també s'ha observat que te certa especificitat per l'adenosina i, en menor mesura, per l'ATP. Juntament amb el fet que la connexina es un canal més aviat aniònic, i que l'ATP té càrrega negativa, els nostres resultats podrien explicar-se per alguna característica especial de la Cx32 que li permetés alliberar ATP i que fos aquesta la que es veiés alterada per la presència de la S1A en una forma més complexa que provocant el tancament del porus de l'hemicanal.

A més a més, vam realitzar deteccions immunohistquímiques que demostren que tant la Cx32 com la S1A es localitzen en zones molt properes en algunes regions del nervi ciàtic de ratolí. Les nostres imatges són compatibles amb que probablement la S1A estaria prou a prop per interactuar (de forma directa o indirecta) amb la Cx32 expressada en la beina de mielina, i podria afectar així la permeabilitat dels hemicanals de la Cx32.

Per intentar obtenir més informació sobre aquesta possible interacció vam transfectar cèl·lules HeLa que expressen de forma estable hCx32 amb S1A i al cap de 24 hores es van activar els hemicanals de Cx32 mitjançant un xoc hipotònic. No es van detectar diferències significatives en la resposta al xoc hipotònic entre les cèl·lules transfectades amb la S1A i les sense transfectar tant en cèl·lules HeLa WT, les quals van alliberar una mitjana de $6.41x10^{-3}$ fmols/ 10^4 cèl·lules les no transfectades i $7.49x10^{-3}$ fmols/ 10^4 cèl·lules les que van ser transfectades amb S1A 24 hores abans (p=0.34), com per les cèl·lules HeLa hCx32, les quals van alliberar una mitjana de $8.49x10^{-3}$ fmols/ 10^4 cèl·lules les no transfectades i $6.36x10^{-3}$ fmols/ 10^4 cèl·lules les que van ser transfectades amb S1A 24 hores abans (p=0.44). Per altra banda, al mesurar l'ATP que alliberaven els grups controls (que no van rebre xoc hipotònic) vam veure que en les cèl·lules transfectades amb S1A es produïa un augment en l'alliberació d'ATP ja que en les cèl·lules HeLa WT vam mesurar una alliberació mitjana d'ATP de $2.71x10^{-3}$ fmols/ 10^4 cèl·lules per les no transfectades i aquest valor pujava a $5,63x10^{-3}$ fmols/ 10^4 cèl·lules en les que van ser transfectades amb S1A. Per les HeLa hCx32 l'ATP mesurat passava de $1.64x10^{-3}$ fmols/ 10^4 cèl·lules per les cèl·lules control sense transfectar a $4.15x10^{-3}$ fmols/ 10^4 cèl·lules per les cèl·lules control que havien estat transfectades amb S1A 24 hores abans.

Després d'analitzar la resposta de les cèl·lules HeLa WT i hCx32 transfectades amb S1A, i tenint en compte que tampoc vam detectar diferències significatives en els xocs hipotònics

realitzats a cèl·lules HeLa que expressen hCx32 i cèl·lules HeLa WT, es pot considerar que la obertura d'hemicanals de Cx32 no representa el mecanisme majoritari d'alliberació d'ATP d'aquestes cèl·lules quan són sotmeses a un xoc hipotònic, i la seva acció (si hi és) estaria emmascarada per algun altre mecanisme d'alliberació d'ATP que s'activa també per un xoc hipotònic. Així, que no hi hagi diferencies significatives en l'alliberació d'ATP entre les cèl·lules HeLa hCx32 transfectades amb la S1A i sense transfectar en aquest cas no ens indica que no es produeixi cap mena d'interacció entre elles, sinó que ens indica que no és un bon model per estudiar l'alliberació d'ATP a través d'hemicanals de Cx32 i, per tant, la possible interacció entre la Cx32 i la S1A. S'haurien de realitzar noves aproximacions experimentals per determinar o excloure aquesta interacció.

INTRODUCTION

The two main leading roles in this Thesis are Connexin32 and ATP. Connexin 32 is one of the best-known connexins, as it was the first connexin ever cloned, and has been described to be expressed in many different tissues. However, its impairment has been related only to Schwann cell dysfunction, suggesting that other connexins could supply its function in other cells types but not in Schwann cells, where it seems to be essential for its survival and, in consequence, for the maintenance of peripheral nerves.

ATP is a well-known molecule, which has been related to a wide variety of different functions such as cellular homeostasis, maintenance of ionic gradients, maintenance of pH in some organules, energetic storage, regulator of actin-myosin interaction, etc. Moreover, ATP can act as a signalling molecule through P2X and P2Y purinergic receptors

As ATP is very hydrophilic, it is believed that it can not cross the plasma membrane, which has very hydrophobic moiety. That's why one of the most accepted pathways for ATP release from cells is through vesicular exocytosis. Anyway, ATP can also cross the plasma membrane through transporters and channels, and Cx32 hemichannels could be one of these channels that can release ATP, which could act as a signalling molecule upon cells expressing purinergic receptors.

The following introduction aims to give information about all aspects involved in this study, starting with general information about the Charcot-Marie-Tooth disease, especially the X-linked form which has been related with Cx32. The second section

gives information about Connexins, either when their form hemichannels or gap junctions, focusing on the peripheral nervous system connexins, especially Cx32, the subject of this work, its relation to CMTX, and the available information from Cx32-null mice. The third section gives a quick glimpse to SNARE proteins, especially Syntaxin 1A, which has been described as a multiple channel modulator and can also have an effect on Connexin Hemichannels. The fourth section is focused on ATP, its release mechanisms and its possible relation with connexin hemichannels, as well as its role as a signalling molecule and its interaction with purinergic receptors. The last section is dedicated to Schwann cells and the connexins, as Cx32 is the main connexin in this particular cell type, and it's the main cell type affected in CMTX disease.

1. Charcot-Marie-Tooth disease

1.1 The disease

The neurologists Jean Martin Charcot, Pierre Marie and Howard Henry Tooth described for the first time in 1886 the main clinical features of a disease now known as Charcot-Marie-Tooth (CMT). This name is nowadays synonym of inherited peripheral neuropathies that affect both motor and sensory nerves and has a high prevalence among the population (1:2500). Although CMT is characterized by distal muscle weakness and atrophy and foot deformities as claw toes (*Figure I1-1*), it is nowadays classified into different variants according

to clinical, electrophysiological, histopathological and genetic features. Moreover, many forms of CMT have been related to specific proteins (*Figures I1-2&I1-3*) and transgenic and knock out mice have been generated to further study the mechanisms that lead different protein defects to cause the same syndrome with similar symptoms[1-3].

Figure I1-1 **|** Foot deformities characteristic from CMT patients.

Table 1. Major genes responsible for CMT and related diseases

Gene symbol	Chromosome	OMIM	Major mutations*	Mouse models
PMP22	17p13-p12	601097	CMT1A	Tr, Trl, tg, tg (tTA)
			PNPP	KO
			DSS	ENU mutants
			CMT and deafness	
MPZ	1q22	159440	CMT1B	KO, tg
			DSS	
			CH	
PRX	19q13.1-q13.2	605725	CMT4F	KO
			DSS	
Gjb1; Cx32	Xq13.1	304040	CMTX	KO
MTMR2	11q22	603557	CMT4B	
NDRG1; Proxy1	8q24.3	605262	HMSNL	
KIF1B	1p36.2	605995	CMT2A	KO
NFL	8p21	162280	CMT2E	KO, tg
GDAP1	8q13-q21.1	606598	CMT4A	
			Neuropathy with vocal cord paralysis	
LMNA	1q21.2	150330	CMT2B1	KO
			Emery-Dreifuss Muscular Dystrophy	
			Dilated Cardiomyopathy	
			Limb Girdle Muscular Dystrophy	

*Major mutations were obtained from the OMIM database, available online at http://www.ncbi.nlm.gov/OMIM/searchomim.html. Abbreviations: CMT, Charcot-Marie-Tooth disease; PNPP, peripheral nerve pressure palsy; DSS, Dejurine-Sottas syndrome; CH, congenital hypomyelination; HMSNL, hereditary motor and sensory neuropathy, Lom-type; KO, knockout; tg, transgenic.

Figure I1-2 **|** General table of genes (and proteins) related to major types of CMT disease. (From Tanaka & Hirokawa, 2002).

In the classical classification there are two main types of CMT: CMT1 or demyelinating and CMT2 or axonal.

1.2 CMT1

CMT1 typically starts on the 1st or 2nd decade of life and it is mainly characterized by demyelization, remyelinization and onion-bulb formation on peripheral nerves that reduce nerve conduction velocities.

There are various proteins related to CMT1 variants but duplications of Peripheral Myelin protein (PMP22) is the most frequent and cause CMT1A or HNPP (hereditary neuropathy with liability to pressure palsies). This neuropathy presents vulnerability to pressure trauma leading to temporary nerve palsies and is associated with focal hypermyelinization. It is not progressive and most patient show the classic features of CMT1. Moreover, some point mutations of PMP22 have been related to CMT, some lead to HNPP (described above) but most of them are associated to transmembrane domains of the protein and cause a more severe phenotype called Déjérine-Sottas syndrome (DSS). How this point mutations lead to disease remains unclear.

Other proteins related to CMT1 are: Myelin protein zero (MPZ) related to CMT1B, LITAF/SIMPLE related to CMT1C, and Connexin 32 related to CMT1X among others.

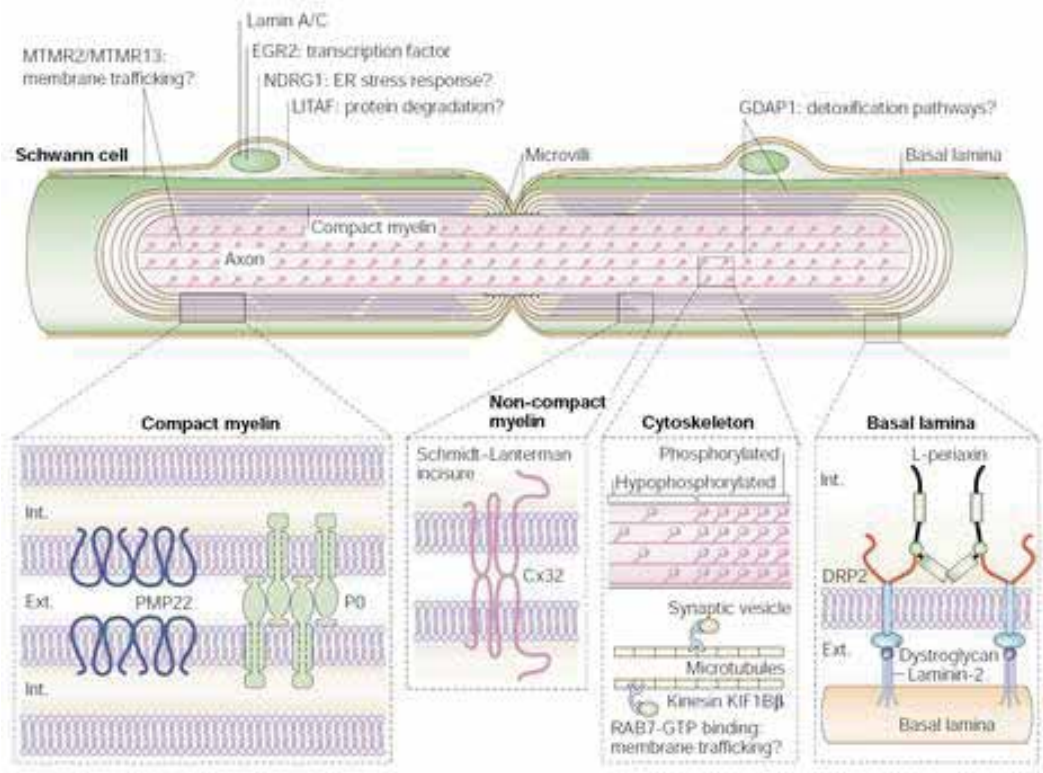

Figure I1-3 **|** Schematic overview of the molecular organization of myelinated axons highlighting the proteins affected in Charcot-Marie-Tooth disease. The figure depicts the localization of the wild type proteins encoded by the genes that are mutated in CMT. Cx: connexin, EGR: early growth response, ER: endoplasmatic reticulum, Ext.: extracellular, GDAP: ganglioside-induced differentiation-associated protein, Int.: intracellular, KIF: kinesin family member, LITAF: lipopolysaccharide-induced tumor-necrosis factor (TNF)-α factor, MTMR: myotubularin-related protein, NDRG: N-myc downstream-regulated gene, PMP: peripheral myelin protein. (From Suter & Scherer, 2003).

1.3 CMTX

There are more than 290 mutations on Gap Junction β-1 (GJβ1) gene described and related with X-linked form of Charcot-Marie-Tooth disease. GJβ1 gene codifies for hCx32 and is located in the X-chromosome, what leads CMTX to have an X-linked inheritance. Males are uniformly affected but female carriers show variable clinical features due to random X-chromosome inactivation.

CMTX is the second most frequent form of CMT1 (10-15%) and clinical manifestations are the same as in CMT1A or CMT1B. Many different mutations have been linked to this neuropathy but, although this genetic heterogeneity, the severity is similar in all affected patients. These mutations can, however, lead to disease in different manners which can include trafficking mutants that are retained in ER or Golgi apparatus, other that reach the plasma membrane but form defective channels or are unable to form gap junctions and others that have been predicted to disrupt the radial pathway that Cx32 gap junctions establish between adjacent layers of the myelin sheath [4].

1.4 CMT2

CMT2 or Axonal form of CMT is characterized by normal nerve conduction velocities and loss of myelinated axons. Some proteins related to CMT2 are Kinesin 1(KiR 1B), which leads to defects in axonal transport and is related to CMT2A, RAB7 related to CMT2B, Laminin A/C (LMNA) related to CMT2B1 and neurofilament light chain (NFL) related to CMT2E [5].

2. Connexins

2.1 Connexin genetics and structure

21 human genes and 20 mouse genes for connexins have been identified until now. Each connexin is expressed in specific tissues or cell types and many cell types express more than one connexin (*Figure I2-1*). Even in the same tissue, the expression

pattern of each connexin shows cell-type specificity and developmental changes, suggesting a tight control mechanism for the regulation of connexin expression. Connexin expression can be regulated during transcription, RNA processing, transport and localization, translation, mRNA degradation and protein activity control. However, transcriptional control is the most important.

Table 1
Connexin genes and their expression

Human			Mouse	Major expressed organ or cell types
Name		Chromosomal locus	Name	
Molecular mass nomenclature	HUGO (Greek letter) nomenclature		Molecular mass nomenclature	
hCx23		?	mCx23	–
hCx25	–	6	–	–
hCx26[a]	GJB2	13q11–q12	mCx26[a]	Breast, cochlea, placenta, hepatocytes, skin, pancreas, kidney, intestine
hCx30	GJB6	13q12	mCx30	Brain, cochlea, skin
hCx30.2	GJE1	7q22.1	mCx29	Brain, spinal cord, Schwann cells
hCx30.3	GJB4	1p35–p34	mCx30.3	Skin, kidney
hCx31	GJB3	1p34	mCx31	Cochlea, placenta, skin
hCx31.1	GJB5	1p35.1	mCx31.1	Skin
hCx31.9	GJC1 (GJA11)	17q21.1	mCx30.2	–
hCx32	GJB1	Xq13.1	mCx32	Hepatocytes, secretory acinar cells, Schwann cells
–	–	–	mCx33	Sertoli cells
hCx36	GJA9	15q13.2	mCx36	Neurons, pancreatic β-cells
hCx37	GJA4	1p35.1	mCx37	Endothelium, granulosa cells, lung, skin
hCx40	GJA5	1q21.1	mCx40	Cardiac conduction system, endothelium, lung
hCx40.1	–	–	mCx39	–
hCx43	GJA1	6q21–q23.2	mCx43	Many cell types
hCx45	GJA7	17q21.31	mCx45	Cardiac conduction system, smooth muscle cells, neurons
hCx46	GJA3	13q11–q12	mCx46	Lens
hCx47	GJA12	1q41–q42	mCx47	Brain, spinal cord
hCx50	GJA8	1q21.1	mCx50	Lens
hCx59	GJA10	1p34	–	–
hCx62	–	6q15–q16	mCx57	Retinal horizontal cells

[a] Orthologous genes of human and mouse connexin genes are listed in the same line.

Figure I2-1 **|** Table of connexin genes and their expression. hCx30.2 (equivalent to mouse Cx29), hCx32 and hCx43 are expressed on Schwann cells. (From Oyamada et al.,2005)

The general genomic structure of connexins is simple and consists of a 5'-UTR on exon 1 separated from the exon 2, which includes the complete connexin coding region and the 3'-UTR [6]. Many splice isoforms have been identified, indicating that different 5'-UTR can be spliced in different manners although these transcript isoforms vary only in their untranslated form. Some connexins also have introns within the coding region

(Cx36, Cx39 and Cx57).

Transcription binding sites for ubiquitous and cell-type dependent transcription factors have been described, For instance: Sp-1 (important for Cx32 and other connexins basal expression), AP-1 (Cx43), cAMP (Cx43) and retinoids have been described as ubiquous transcription factors, while for the cell-type specific transcription factors, NKx2 to 5 are important for connexin expression in the heart, estrogens are related to Cx43 expression in the uterus, thyroid and parathyroid hormones are also related to connexin expression, etc [7].

Connexin genes are translated to proteins that form hexameric structures in the plasma membrane called hemichannels or connexons, harbouring a central pore that permit the passage of ions and small molecules between cytoplasm and extracellular surroundings. Different connexins are designated by "Cx" plus the molecular weight, connexin proteins have four transmembrane domains that allow them to be anchored in the plasma membrane, carboxy and amino ends are cytoplasmatic, and the carboxy terminus interacts with other proteins. The two extracellular loops are highly conserved and necessary for docking of two hemichannels of adjacent cells to form gap junctions. A set of three cysteine residues in each of the extracellular loops may help to maintain the tertiary structure necessary for this docking of two hemichannels, allowing the exchange of small molecules between cells [8] (*Figure I2-2*).

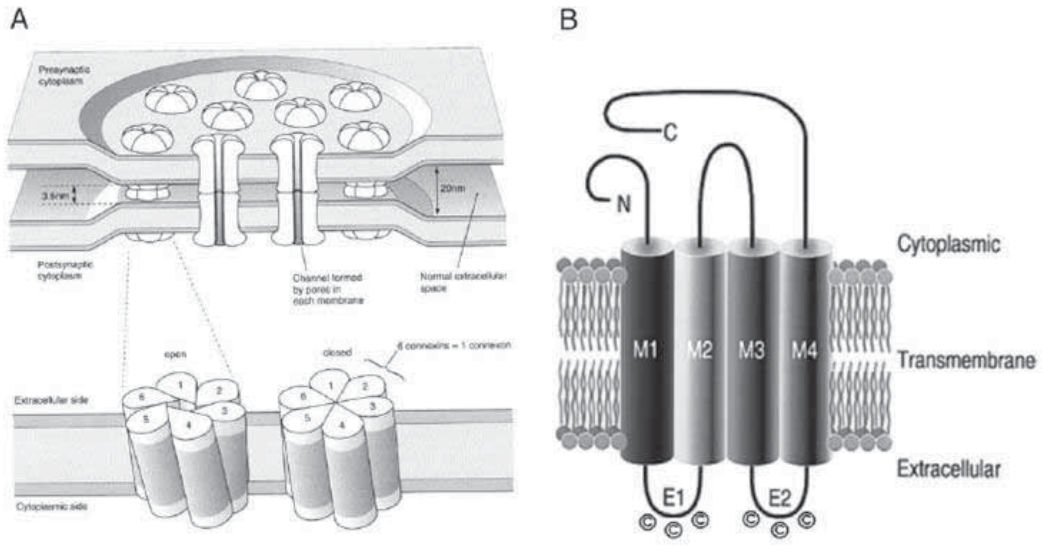

Figure I2-2 **| A** Schematic drawing of Gap Junction channels. Each apposed cell contributes a hemi-channel to the complete gap junction channel. Each hemichannel is formed by six protein subunits, called connexins. The darker shading indicates the portion of the connexon embedded in the membrane. **B** Topological model of a connexin. The cylinders represent transmembrane domains (M1– M4). The loops between the first and the second, as well as the third and fourth transmembrane domains, are predicted to be extracellular (E1 and E2, respectively), each with three conserved cysteine residues (from Söhl & Willecke, 2004).

Recent studies show that connexin function is not only related to non specific channels but they are involved in other activities such as growth control, adhesion and control of gene expression.[9]

2.2 Gap Junctions

Gap junctions are cell-cell communicating channels formed by the docking of two hemichannels of adjacent cells, multiple gap junction channels, in turn, cluster in the membrane to form gap junction plaques (*Figure I2-2*). Gap junctions allow electrical coupling and mediate exchange of low molecular weight metabolites and ions up to 1 KDa (such as Na^+, K^+, Ca^{2+}, ATP, cAMP, IP_3, etc.); they are relatively unspecific and movement

through the channels occurs by passive diffusion. These junctions exist in all vertebrate and invertebrate animals, and higher plants cells have a similar mechanism for cell-cell communication [8]. Gap junctions are hypothesized to play a role in homeostasis, morphogenesis, cell differentiation and growth control. There is a growing evidence that a single gap junction channel can be made of different connexins, i.e., two connexons each consisting of different types of connexins can form a heterotypic gap junction channel, whereas one connexon containing different types of connexins can form a heteromeric gap junction channel [8] (*Figure I2-3*).

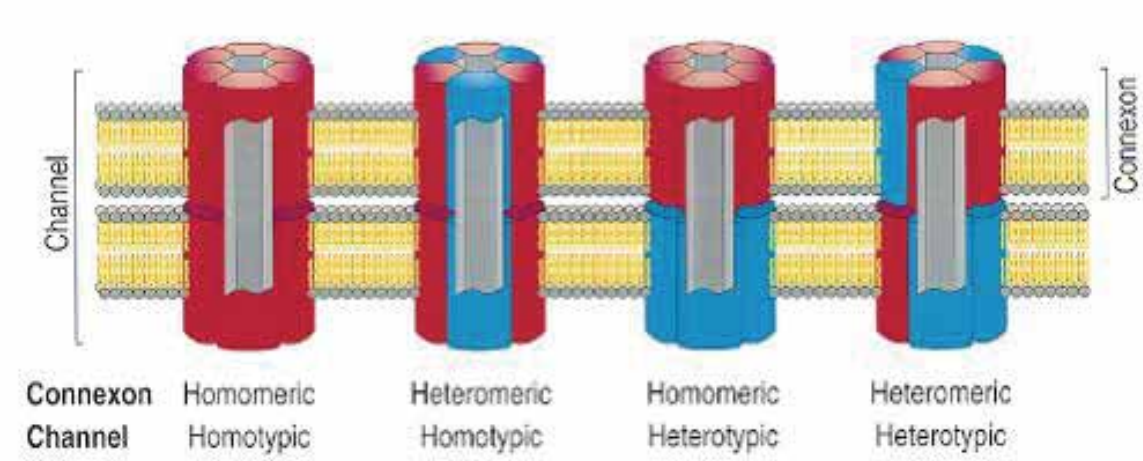

Figure I2-3 **|** Schematic drawing of possible arrangement of Connexons to form Gap Junction channels. Connexons consisting of six connexin subunits (red and blue) are illustrated in various configurations. Connexons may be homomeric (composed of six identical connexins) or heteromeric (composed of more than one species of connexins). Connexons associate end to end to form a double membrane gap junction channel. The channel may be homotypic (if connexons are identical) or heterotypic (if the two connexons are different). (From Kumar & Gilula, 1996)

Distinct electrophysiological and ion selective properties have been shown not only for homotypic gap junction channels made of different connexins but also between homotypic and

heterotypic gap junction channels. The net result of such diversity could provide communication compartments that enable a group of cells to be regulated by changes in the concentration of a specific second messenger or metabolite. Reviewed by [7, 8, 10, 11]

2.3 Hemichannels

At first it was thought that opening of hemichannels would kill cells through loss of metabolites, collapse of ionic gradients and influx of Ca^{2+}, however, recent findings indicate that non-junctional hemichannels can open under both physiological and pathological conditions, and that opening is functional or deleterious depending on the situation [12]. The first evidence of hemichannel opening was when Paul et al [13] found that expressing Cx46 in *Xenopus* oocyte resulted in membrane depolarization and eventual cell death unless the extracellular medium contained high Ca^{2+} levels. Since then, further evidence of hemichannels activity has been found in other connexins [14, 15]. Hemichannel activity has also been related to calcium waves and ATP release, suggesting that astrocytes release ATP through Cx43 hemichannels and that stimulates purinergic receptors in surrounding astrocytes, which would raise intracellular Ca^{2+} levels of these cells propagating the Ca^{2+} wave [16, 17]. Other evidences for hemichannel functions are studies in which ATP release was reported to correlate with connexin expression [18], and it is blocked by FFA [16], which inhibits both hemichannels and gap junctions, but not by octanol [18], which inhibits intercellular

communication.

Many mechanisms regulating hemichannels open and close state have been described, and they depend on each connexin: phosphorilation state [19], mechanical stimulus [20, 21], extracellular Ca^{2+} levels [22], presence of quinine [16], membrane potential [23] or pH [24].

2.4 Connexin voltage sensitivity

Connexin channels exhibit a complex channel sensitivity, the conductance (G_j) of most of them is sensitive to transjuntional voltage (V_j, the voltage difference between two cell interiors coupled by gap junctions), but many are also sensitive to membrane potential (V_m, a cell absolute inside-outside voltage). It is hypothesized that this dual voltage regulation is due to the existence of two different gates, each of which specifically senses one type of voltage [25]. The G_j of most homotypic connexin channels is typically maximal at V_j=0 (G_{jmax}), and it decreases symmetrically for positive and negative V_j pulses to non-zero conductance values. Transitions between the main open state and the closed state could be either fast or slow. Accordingly, these two gating processes have been termed "fast V_j-gating" and "slow V_j-gating" respectively. Little is know about the mechanisms responsible for slow V_j-gating but there are evidences that the C-terminal domain is involved in the fast V_j gating, as it is abolished when this domain is truncated [26] or fused to a large molecule like GFP [27], and it is recovered when truncated connexins are coexpressed with C-terminals domains

[28]. It is hypothesized that the fast V_j gating can be explained by the "ball-and-chain" model, where the displacement of the C-terminal domain toward the inner mouth of the channel pore would physically close the pore, a model that had already been proposed for the closing state triggered by pH [29], Insulin and IGFs [30]. Nanometric data using AFM also support this model [31].

Connexins sensitive to V_m have also a slow V_m-gating mechanism. This mechanism would regulate electrical coupling when V_j=0, specially in excitable cells. The slow V_m-gating has been also related to the C-terminal domain, but to the residues close to the fourth transmembrane domain [32]. These findings suggest that slow V_m-gating is mediated by an outwardly directed movement of the voltage sensor, which would lead to conformational changes that close the pore.

2.5 Connexin 32

Cx32 gene (GJβ1) follows the general structure of connexin genes with two main exons and the complete coding sequence in the second exon but with variants. There are two different spliced transcripts of Cx32 in humans and three in mouse. Human Cx32 has three exons (1, 1B & 2), and mouse Cx32 contains four exons (1, 1A, 1B & 2) that are alternatively spliced. In liver and pancreas promoter P1 (8Kb upstream the start codon) is used and the transcript is processed to remove a large intron, in nerve cells promoter P2 is used and the intron to be removed is smaller. Cx32 coding sequence is shared by both mRNAs (*Figure I2-4*).

Cx32 expression is regulated by ubiquitous transcription factors and also by cell-type transcriptions factors as HNF-1 in the liver, Mist1 in the pancreas and Sox10 and EGR2/Krox20 in Schwann cells [7]

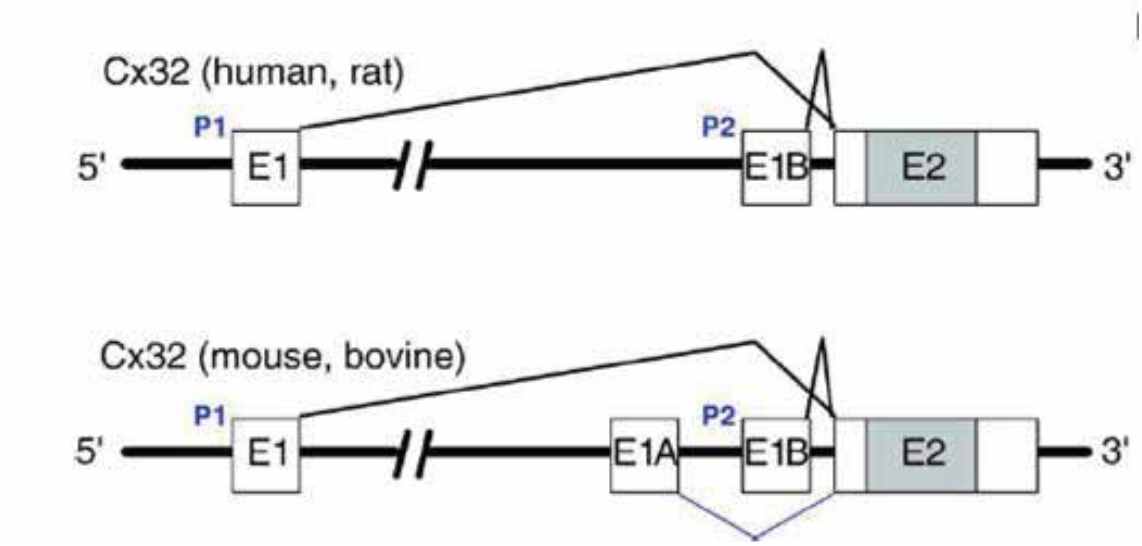

Figure I2- 4 **|** Structure and splice patterns of the human, rat, mouse, and bovine Cx32 genes. Exon (E) sequences are shown as boxes, whereas the solid grey parts represent coding sequences. (from Oyamada et al., 2005)

Cx32 was the first ever cloned connexin and was named Cx32 according to the expected weight (32 KDa). It is a highly conserved protein as human Cx32 is 98% identical to rat and mouse Cx32 [33,34]. Cx32 form not only homomeric hemichannels but can also form heteromeric hemichannels with Cx26 and heterotypic gap junctions with Cx26 and Cx30 [35]. Though Cx32 is most abundantly in liver it is also expressed in kidney, guts, lungs, spleen, stomach, pancreas, uterus, testis, brain and peripheral nerves.

Electrophysiological studies reported that Cx32 hemichannels are activated by membrane depolarization [36], that these hemichannels have 90pS conductance, with substates of 18pS,

and extracellular calcium modulates them [22]. It has been described that Cx32 hemichannels open with increasing intracellular Ca^{2+} and that they can be closed with gap junction blockers and with specific peptides such as ^{32}gap27, which binds to 110-122 residues of the second extracellular loop, and ^{32}gap24, which binds to the intracellular loop [37].

Cx32 is the principal oligodendrocytic connexin and was the first connexin described in oligodendrocytes, were it is expressed in the large myelin fibres. [9]. Cx32 is also the principal connexin in Schwann cells [38] where it is expressed in paranodal zones and in Schmidt-Lanterman incisures of the myelin sheath (of peripheral nerves) [39]. Cx32 would form reflexive gap junctions in the myelin sheath that would bypass the communication through various myelin layers that separate adaxonal and abaxonal cytoplasm [40] facilitating intracellular redistribution of K^+ and restoring the extracellular concentration back to basal levels, allowing renewed axonal propagation of action potentials. (*Figure I2-5*) [9].

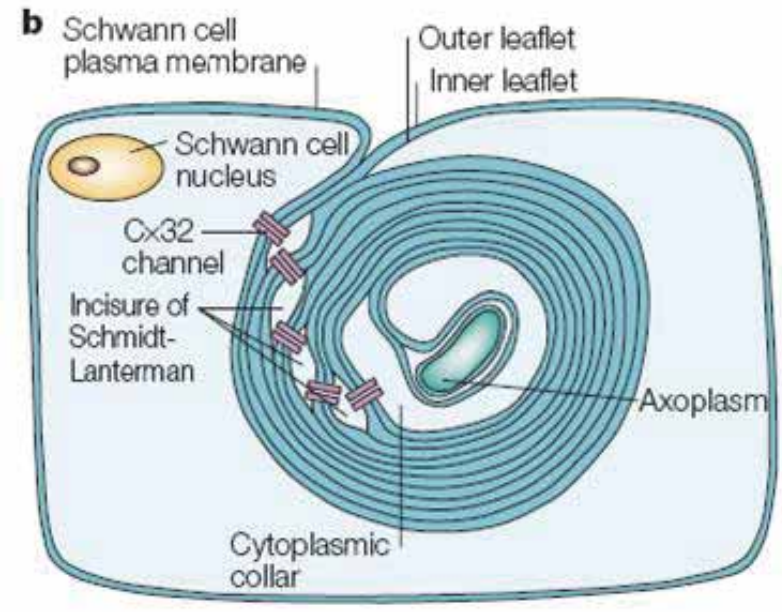

Figure I2-5 | Scheme of a Schwann cell showing the reflexive gap junctions formed by Cx32, which establish a bypass across the cytoplasm between the periaxonal and the perinuclear area. (From Goodenough & Paul, 2003).

2.6 hCx32 & CMTX

More than 270 different mutations on the human Cx32 gene (GJB1) have been described to cause CMTX (http://www.molgene.ua.ac.be/CMTMutations/Datasource/mutbygene.cfm). These mutations affect all regions of hCx32 and lead to defects in hCx32 trafficking, interactions with other proteins and hemichannel or gap junction function. Here we have focused on 5 mutation described in CMTX patients and that have been generated and used in this work (*Figure I2-6*):

- **S26L**: this mutation localized in the first transmembrane domain results in a reduction in the pore diameter from 7Å to less than 3Å [41, 42]
- **P87A**: This proline in position 87 (in the second transmembrane domain) is highly conserved, and it has been related with voltage gating. This mutation may produce pore alterations that affect the permeability properties [41]
- **Del111-16**: This deletion of part of the intracellular loop alters the recovery from pH gating [42, 43]
- **D178Y**: A point mutation of the second extracellular loop related to Ca^{2+} detection [22]
- **R220St**: This mutations eliminates the last part of the C-terminus, abolishing the interactions with other proteins [42, 43]

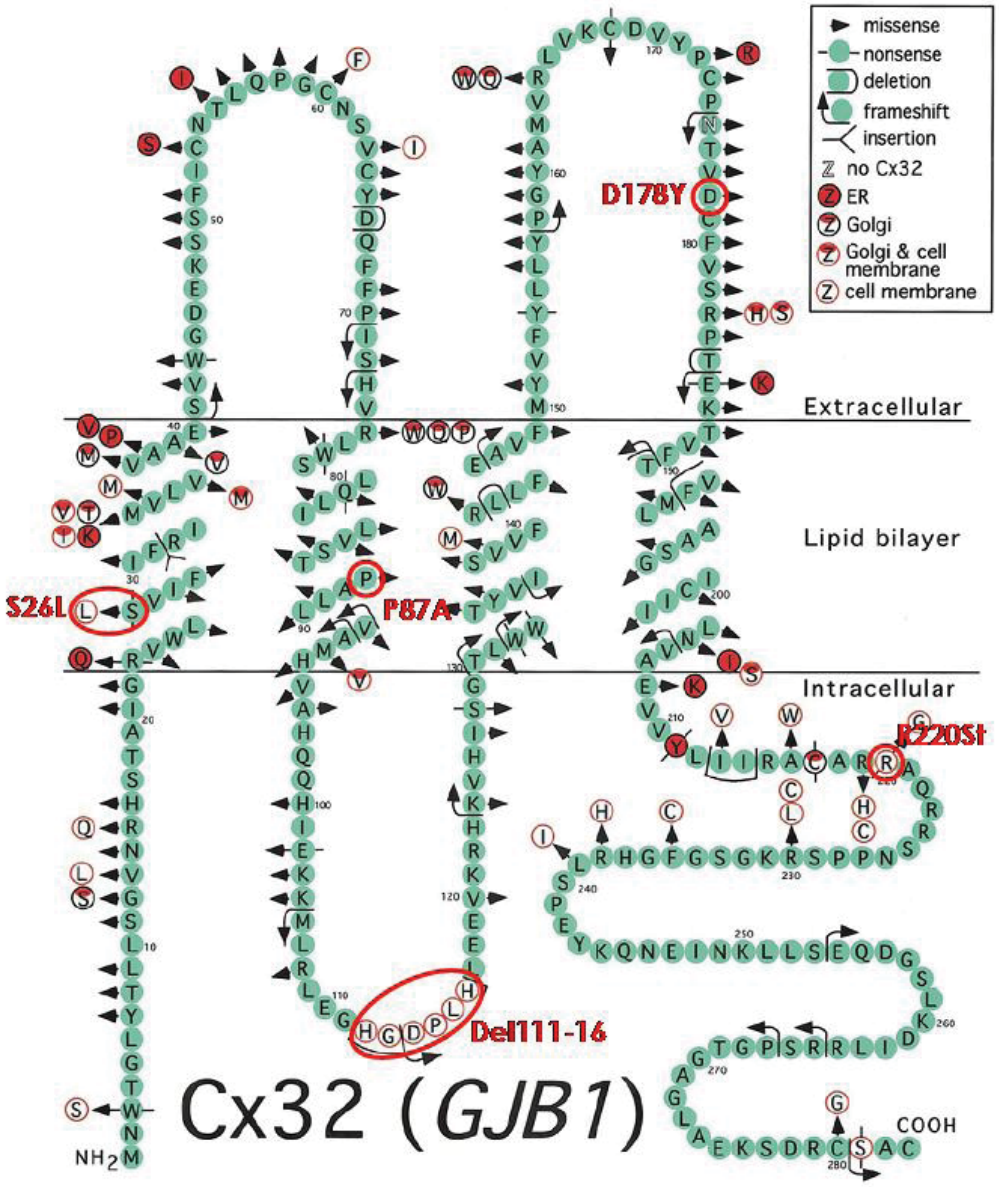

Figure I2-6 **|** Structure of the human Cx32 protein showing some known mutations leading to CMTX disease. Mutations generated in our laboratory are marked in red. (Image from Yume et at., 2002)

Physiological consequences of dysfunctional Cx32 could be compensated in oligodendrocytes in the CNS, as most CMTX patients do not have clinical CNS manifestations. However, subclinical evidences of dysfunctions are common, and few mutations have been described to lead to clinical CNS dysfunction [44, 45].

Moreover, there are few mutations related to CMTX that do not directly affect GJB1 gene (hCx32 gene) but other closely related proteins like the transcription factors Sox10 & EGR2/Knox20. These transcription factors bind to the P2 promoter of Cx32 gene activating its expression in Schwann cells. Mutations on Sox10 and EGR2/Knox20 [46] and on P2 promoter [47] eliminating the binding site to Sox10 have been described in some patients with CMTX1.

2.7 Connexin 32 knock-out mice

Although the first data from Cx32-null mice suggested no peripheral neuropathy in those mice [48] and that the only affectation of these mice was on the liver, where Cx32 is mostly expressed [49,50], later studies revealed a late-onset demyelinating peripheral neuropathy on mice older than 3 months which is comparable to human CMTX [51]. This neuropathology is characterized by unusually thin myelin sheaths, cellular onion-bulb formations, induced Schwann cell proliferation and enlarged periaxonal collars, but the conduction velocity is only slightly decreased [52]. This progressive peripheral demyelination starts at 3 months of age and motor fibres are more affected than sensory fibres [51]. A strong evidence that this peripheral demyelinization is due to the lack of Cx32 in Schwann cells and not in other cell types was given by Scherer et al, by expressing human Cx32 in Cx32 null-mice under the MPZ promoter, specific for Schwann cells. Those mice did not develop a demyelienation neuropathy [53].

Many other studies have been done with Cx32 null-mice revealing new characteristics as alteration in the distribution of proteins such as potassium channels Kv1.1 [54], increased expression of GFAP [55], increased presence of oligodendrocyte progenitors [56] and affectations on the CNS [57].

2.8 Connexin 29

The presence of Cx29 has been described in brain, spinal cord and Schwann cells in peripheral nerves of mice, but not in other tissues, suggesting that it can be a neural connexin [58,59]. In brain Cx29 is expressed in olygodendrocytes, specifically in internodal and juxtaparanodal regions of small myelin sheaths [9]. In Schwann cells, Cx29 is expressed in the innermost aspects of the myelin sheath, paranodes, juxtaparanodes and Schmidt-Lanterman incisures (where colocalizes with Cx32 and could form heteromeric gap junctions channels) [59,60]. When a transgenic mouse with Cx29 gene replaced by the LacZ reporter gene was generated, new information about Cx29 location and function was available. Those mice showed that Cx29 is localized effectively, where it had been described before, but also in other cell types and tissues such as Bergmann glia cells, adrenal gland, enteric nervous system and the cochlea. However, Cx29-null mice showed no alterations in peripheral and central nerves or in mechanical transduction and cochlear amplification [61].

2.9 Connexin 43

Cx43 hemichannels have a 15 Å pore size, are anion selective

and have a 100 pS unitary conductance [62]. Cx43 is a widely expressed connexin, its presence has been described in astrocytes [12], leptomeningeal and ependymal cells, vascular and gastrointestinal [63] smooth muscle cells, endothelial cells, olfactory epithelium [64], Kupffer cells, ovary and neural progenitor cells (for reviews see [62, 65]). Additionally, Cx43 is the main cardiac connexin, where it is expressed in ventricular myocardium, and the heart (which also express Cx40 and Cx45) is the location where it has been mostly studied [66, 67]. Cardiac connexins are responsible for the propagation of the action potential from cell to cell through the cardiac atrioventricular conduction system, during the heart beat. The electrical continuity of this action potential involves overlapping distributions of Cx40 and Cx43 in the heart [67]. Cx43 expression in the heart has been related to infarct size and it has been described to have a cardioprotective role by ischemic preconditioning [68, 69].

Cx43 in the peripheral nervous system has been described in sciatic nerve, in Schwann cells primary cell cultures, in immortalized Schwann cell line T93 and in Schwanomas [70, 71]. It has been described an up-regulation of Cx43 in Schwann cells stimulated with mitogens [70] and also an increase of Cx43 expression in endoneural fibroblasts after an injury [72], however, the role of Cx43 in the PNS remains unclear.

2.10 *Xenopus laevis* connexins

Until now, four different connexins have been described in

Xenopus laevis: Cx43 [73], Cx38 [74], Cx30 [75] and Cx41 [76]. But of these four only one is expressed in oocytes (that's why is called a maternal connexin), where it is expressed from the first developmental embryonic stages until neurulation [74,75]. Recently, other maternal connexins have been described (Cx31 and Cx43.3) which would be inactive in oocytes and raise its activity on early embrions [77].

2.11 Pannexins

Similarly to the connexin family, another molecular family has been related with gap junction formation: The pannexin/innexin superfamily [78]. Innexins have been described as the gap junctions of invertebrates and, while connexins have been found only in chordates, the pannexin presence has been described both in chordates and invertebrates genomes [79-81]. Although connexins and pannexins have very different primary structures, their topology is similar, with four transmembrane domains and the C and N-terminal intracytoplasmatic domains [79] (*Figure I2-7*).

Up-to-date there are three mammalian pannexins described: pannexin1 (PANX1), which is ubiquitous but disproportionaly present in some tissues like embryonic CNS. PANX2 is brain specific and PANX3 is expressed in osteoblasts and synovial fibroblasts [80, 82]. Both PANX 1 and 2 have been also described in the retina [83].

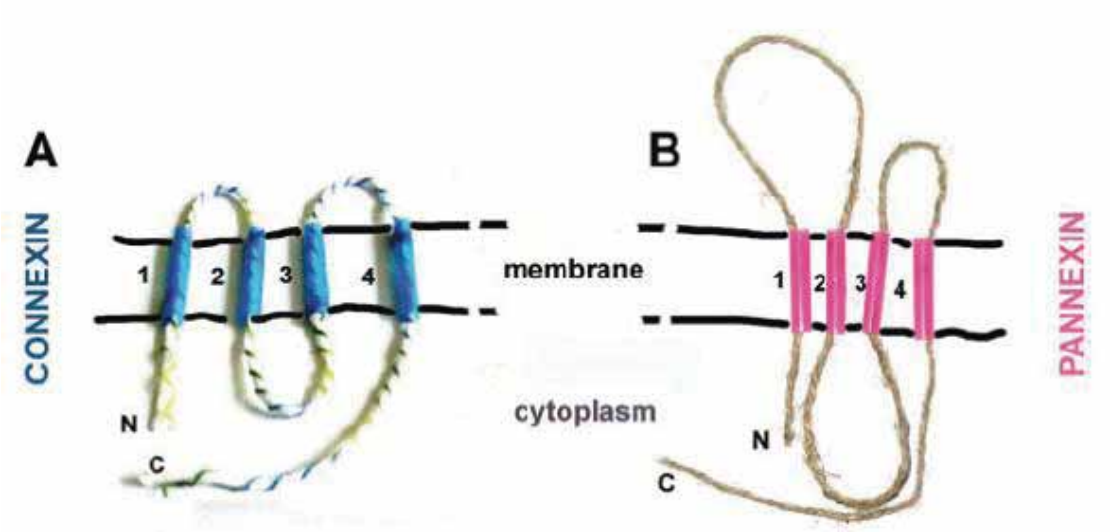

Figure I2-7 **|** The topology of connexins (A) and pannexins (B), with four transmembrane domains and intracellular N and C terminal domains, is the same, yet their sequences are not related. (from Panchin, Y; 2005)

The function of pannexins is still quite unclear, at first it was hypothesized that they would have redundant functions as gap junctions channels together with connexins but, although it has been described that pannexins can form gap junction channels in experiments with paired oocytes [82], nowadays there is no evidence that pannexins form gap junctions *in vivo*. Other authors suggest the idea that during evolution, pannexins retained the hemichannels (pannexons) functions while connexins overtook the gap junction role [84]. To support this idea it has been proposed that PANX1 supports the release of ATP in erythrocytes [85] and taste buds [86], and that it is also responsible for the ion fluxes dysregulation produced during neuronal ischemia that lead to neuronal death [87]. Recent studies have also related PNX1 with the large pore pathway described for $P2X_7$ purinergic receptors in macrophages, which appears later than the ion channel selective current for small cations (as Ca^{2+}) that

would be generated by the receptor itself, after an inflammatory stimuli [88, 89]. There are also experimental evidence that suggest that pannexins could also work in synergy with metabotropic P2Y purinergic receptors to support the ATP induced ATP release [90, 91].

3. SNARE proteins

3.1 SNARE proteins & Exocitosis

Regulated neurotransmitter release is restricted to active zones, where synaptic vesicles dock and undergo a priming reaction that prepares them for exocytosis when a Ca^{2+} influx occurs in response to an action potential. Many proteins have been identified to take part in this process but the central components of the exocytic apparatus are SNARE proteins (SNAREs), the proteins that are responsible for executing membrane fusion by forming a tight complex (SNARE complex) that brings the vesicle and plasma membrane together and facilitates the fusion (reviewed by Rizo & Südhof [92], *Figure I3-1*).

SNARE proteins include synaptobrevin/VAMP-2 (v-SNARE), syntaxin and SNAP25 (t-SNAREs). According to the SNARE hypothesis, SNARE proteins expressed in transport vesicles (v-SNARE) and those expressed in the plasma membrane (target membrane, t-SNARE) recognize each other in opposed membranes and form the SNARE complex, which is extremely stable [93], and will lead to membrane fusion [94].

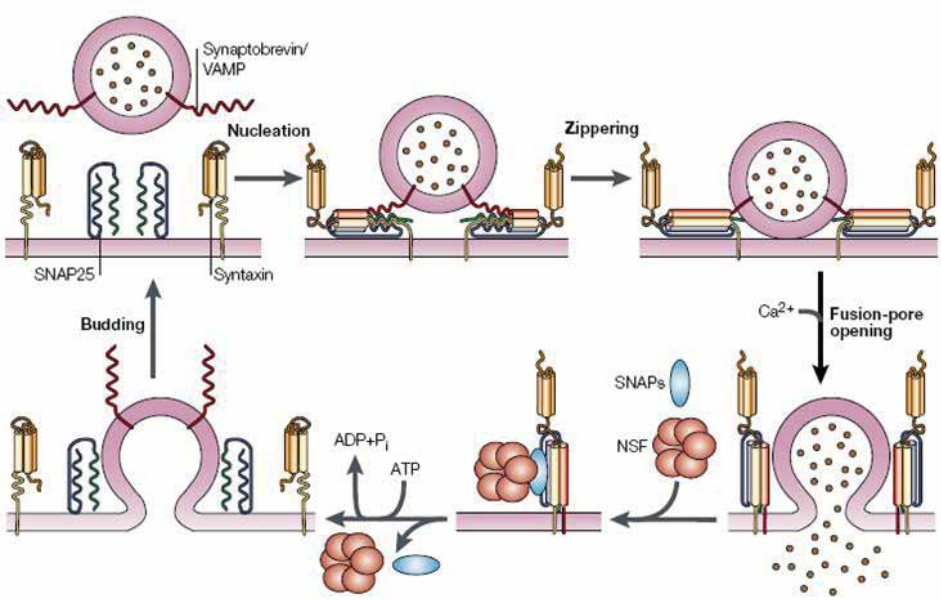

Figure I3-1 **|** Cycle of assembly and disassembly of the SNARE complex in synaptic vesicle exocytosis. Syntaxin in a closed conformation needs to open to initiate core-complex assembly (nucleation). 'Zippering' of the four-helix bundle towards the carboxyl terminus brings the synaptic vesicle and plasma membranes towards each other, which might lead to membrane fusion. After fusion, NSF and soluble NSF-attachment proteins (SNAPs) disassemble the *cis*-core complexes that remain on the same membrane to recycle them for another round of fusion. (from Rizo & Südhof, 2002)

3.1 Syntaxin 1A

Syntaxin 1A is a 35 kDa protein consisting of a single C-terminal transmembrane domain, an adjacent SNARE motif to interact with SNARE partners, and an intracellular N-terminal domain (Habc). The SNARE motif and the Habc domain are separated by a 40 aminoacid linker region [95] (*Figure I3-2*).

S1A null-mice have normal basic synaptic transmission but impaired long-term potentiation and consolidation of conditioned fear memory, suggesting that syntaxin 1A is important for synaptic plasticity [96].

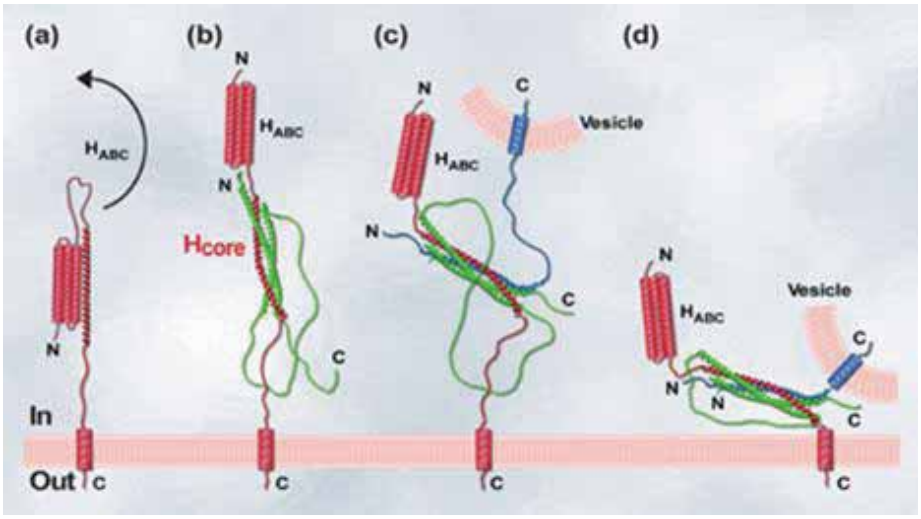

Figure I3-2 **|** Different conformational states of the SNARE protein syntaxin. (a) The N-terminal Habc domain interacts with the H3 domain to fold into a closed conformation unable to bind to SNAP 25 or synaptobrevin. (b) The formation of the tertiary SNARE complex appears to be proceeded by a binary interaction of syntaxin and SNAP 25. (c,d) The tertiary SNARE complex (Hcore) is composed of four parallel helices: the syntaxin H3 domain, one coiled-coil domain from synaptobrevin and two from SNAP 25. Colour code: syntaxin 1, red; synaptobrevin, blue; SNAP 25, green. From *Trends in Cell Biology, Vol. 13 No.4 April 2003*

As well as its role in the SNARE complex machinery, S1A has been described to interact with and regulate several other membrane proteins such as L-type [97, 98], N-type [99, 100] and R-type [98] calcium channels, Kv2.1 potassium channel [101], BK_{Ca} calcium activated potassium channels [102], ENaC epithelial sodium channels [103] and CFTR cystic fibrosis transmembrane conductance regulator [104]. Moreover, studies in our lab showed a functional interaction of S1A with Xenopus Cx38 Hemichannels (unpublished data).

4. ATP release

4.1 ATP release mechanisms

ATP release mechanisms have been widely studied during the last decade and it is accepted that ATP can act as a signalling molecule or neurotransmitter, released by excitable cells. Subsequently, other evidences support the hypothesis that non excitable cells can also release ATP in response to different stimuli such as mechanical stimuli [16], stress [105], hypotoncity [106-108], distension [109], high $InsP_3$ concentration [110] or low extracellular Ca^{2+} concentration [111].

The proposed mechanisms that would allow this ATP release are diverse and require different organelles and proteins [112], including exocytosis, CD39, connexin hemichannels, CFTR or anionic channels.

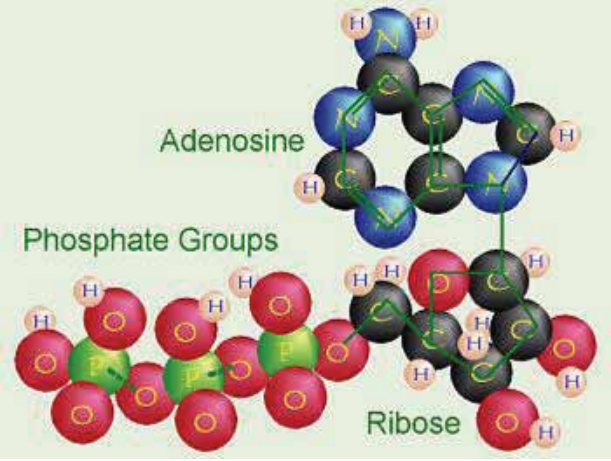

Figure I4-1 **|** Scheme of an ATP^{-4} molecule, displaying one adenosine, one ribose and three phosphate groups.

ATP is co-secreted with classic neurotransmitters in PNS and CNS neurons. Other cells, like chromaffin cells, platelets, mastocytes and cells from pancreatic acini [113] release neurotransmitters, ATP and other messengers through exocytosis of synaptic vesicles, chromaffin granules or dense granules [113-115].

Some studies support the idea that ABC binding cassette

protein family (members of this family are CFTR and P glycoprotein) function as ionic channels and allow ATP release [116-119], but other support the contrary [120-122]. So the controversy is still open.

On the other hand, many studies support the role of anionic channels in ATP^{-4} release. For example, anion channels blockers inhibit ATP release by hypotonicity in a prostate cancer cell line [123], volume-regulated anion channels (VRAC) release ATP in a bovine aortic epithelia cell line [124] and a mammary cells from mice primary cultures or a cell line also release ATP under hypotonic stimulus [125].

CD39 has also been described to be implicated in the release of ATP when expressed in *Xenopus* oocytes and in response to hyperpolarizing pulses [126]. Moreover, CD39 expression on *Xenopus* oocytes enhance the currents generated during ATP release, suggesting that it could also be implicated in its release as well as ATP degradation, as originally described [127].

Once the ATP has been released and done its function it must be inactivated. It is usually done by enzymatic hydrolysis, which generates adenosine and phosphate groups. There are different enzymatic families that can extracellularly hydrolyse ATP: E-NTPDases family, E-NPP family, alkaline phospatase and ecto-5'-nucleotidase.

4.1.1 ATP release through connexins

ATP release regulated by gap junctions was suggested for the first time by Cotrina et al [18]. This work showed an ATP

release potentiation on cell lines transfected with connexins, and this potentiation correlated with Ca^{2+} signalling.

ATP release is an important component of the propagation of calcium waves in astrocytes [128, 129] and osteoblasts [130]. It has been described in astrocytes that this ATP release could be mediated by Cx43 hemichannels [16]. ATP released by this connexin would activate P2 purinergic receptors of surrounding cells activating $InsP_3$ synthesis and raising intracellular Ca^{2+} concentration, which would generate an unknown signal that would open connexin, ATP would be released and the cycle would start again propagating the calcium wave [131] (*Figure I4-2*).

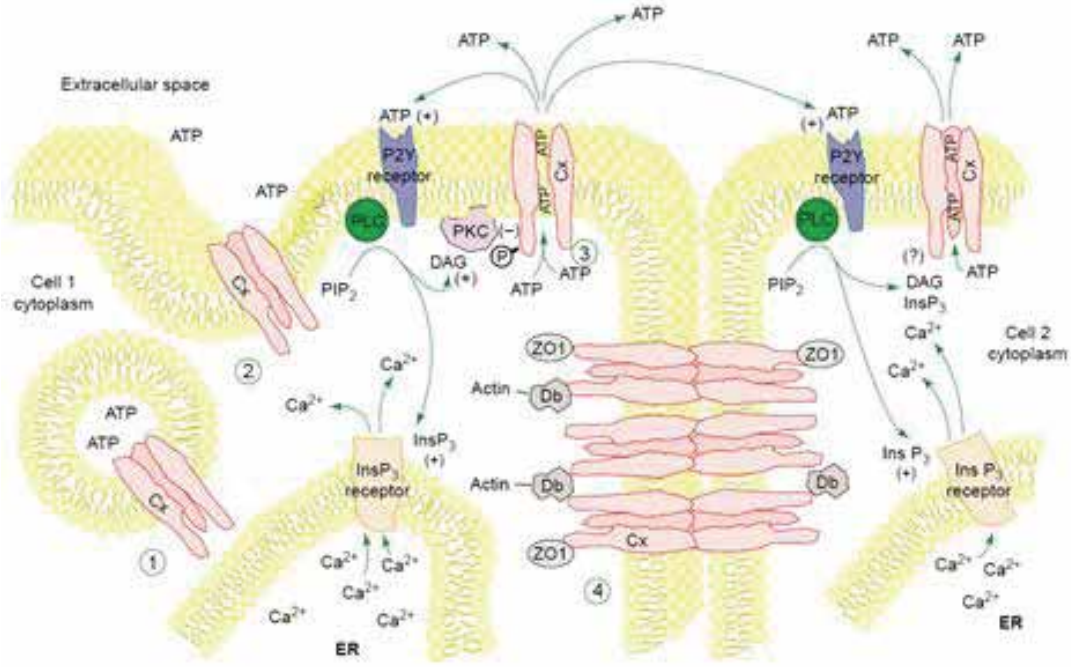

***Figure I4-2* | ATP release through hemichannels & calcium waves propagation.** A stimulus (e.g. shear stress) activates the phospholipase C (PLC), InsP3 synthesis and intracellular calcium mobilization. Hemichannels open and ATP is released. ATP binding to P2Y receptors from adjacent cells propagates the calcium wave (From de Stout et al., 2004)

This model of calcium wave propagation is supported by other evidences that show that exogenous expression of

connexins enhances ATP release [18], and that ATP release induced by low extracellular calcium is inhibited by hemichannels blockers.

Other works, however, support the idea of two different pathways for ATP release [132], each one triggered by different stimuli, or even are against the role of connexins in calcium wave propagation, as gap junction blocker also inhibits $P2X_7$ receptors. Accordingly, this receptor, and not Cx43 hemichannels, would involved in the release of ATP amplifying calcium waves in astrocytes [133].

Besides these studies, evidences of possible ATP release through hemichannels have been described in a wide range of cells like osteoblasts under mechanical stimulation [134], bovine corneal epithelial cells also after a mechanical stimulus [135], pigmentary epithelia of the retina [136], mammals cochlea [137] and *Xenopus laevis* oocytes [138].

4.2 ATP as extracellular signal

ATP (adenosine triphosphate) is formed by one adenine, one ribose and three phosphate groups (*Figure I4-1*). ATP is the central molecule for chemical energy storage; it is necessary for many essential cellular activities as molecular biosynthesis and metabolite and protein phosphorylation, and it also acts as an enzyme cofactor and has a role on active transport of ions and molecules.

But ATP can also act as a neurotransmitter. This hypothesis was raised for the first time from Pamela Holton studies back in

1959 [139], when her studies demonstrated the release of ATP when sensorial nerves were stimulated. But it was Geoffrey Burnstock who, in 1972, postulated ATP as the principal neurotransmitter in non-adrenergic, non-cholinergic neurons present in smooth muscle, giving birth to the purinergic hypothesis [140, 141].

After these first studies, the role of ATP as a neurotransmitter has been proven in CNS [142-144], PNS [145] and autonomous nervous system [140, 146].

On the other hand, ATP is considered a mediator in other signalling pathways, ATP signalling role has been described in epithelial cells [147], platelets [148] and cell lines [149] among others.

4.3 ATP receptors: Purinergic receptors

ATP and its metabolite, adenosine, are specifically recognized by purinergic receptors and there are two main types of purinergic receptors, P1 and P2 receptors[150]. P1 receptors have a higher affinity for adenosine than for ATP and modulate adenyl ciclase activity; P2 receptors have higher affinity for ATP and are related to phospholipase C activity and intracellular Ca^{2+} concentration.

Among the P2 purinergic receptors, with a higher affinity to ATP, there are two main families of receptors: P2X and P2Y. P2X are ionotropic receptors while P2Y receptors are metabotropic receptors linked to G proteins [151].

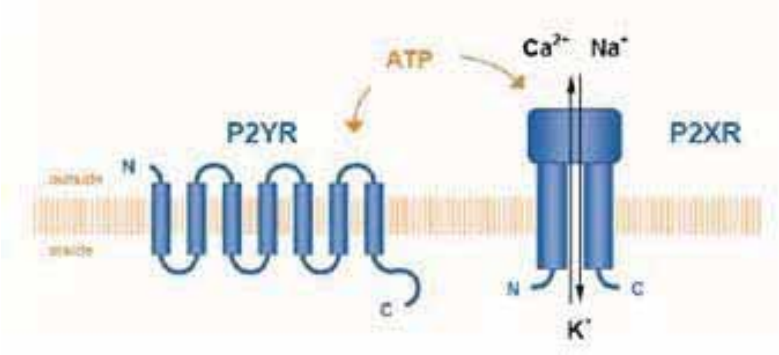

Figure I4-3 **|** Schematic view of a G-Protein coupled P2Y receptor (the structure is much like that of other GPCRs) and an ionotropic P2X receptor (It is thought that ATP binds in the extracellular domain, although a binding site has not been mapped). The physiological ligand for both receptors is ATP and its metabolites. (taken From: http://www.acris-antibodies.com/focus_review/focusreview0006-purinergic.php).

There are seven different P2X receptors cloned up-to-date ($P2X_{1-7}$). These receptors are cationic channels formed by 3 or 4 homomeric or heteromeric subunits [152]. Each subunit is formed by two transmembrane domains, a large extracellular loop and intracellular C and N-terminals (*Figure I4-3*). Each P2X receptor is expressed in a wide variety of tissues and organs; in peripheral nervous system many different P2X receptors are expressed with different distribution. $P2X_1$ [153], $P2X_2$ [154], $P2X_3$ [155] and $P2X_4$ [156] are expressed in spinal cord and $P2X_7$ is expressed in Schwann cells [157].

P2Y receptors on the other hand, have seven transmembrane domains with extracellular C-terminus and cytoplasmatic N-terminus (*Figure I4-3*). All P2X receptors specifically bind ATP but different P2Y receptors show different affinities for ATP, ADP, UTP and UDP [158]. Up-to-date there are eight different P2Y receptors cloned ($P2Y_{1,2,4,6,11,12,13,14}$). While in CNS P2Y receptors are located over the synaptic buttons, no important roles in

peripheral nervous system (PNS) have been described for these receptors, which have been related to platelets aggregation, haematopoiesis and secretion triggering in the respiratory system.

5. Peripheral glia

5.1 Schwann cells

The nervous system is built from two major kinds of cells: neurons and glia cells. Glia cells, among other functions, are responsible for the formation of myelin sheaths around axons allowing the fast conduction of action potentials, and for maintaining appropriate concentrations of ions and neurotransmitters in neuron surroundings [159]. In the PNS glia cells are Schwann cells, enteric glial cells and satellite cells but the most abundant and studied among them are Schwann cells.

In the nineteenth century, while investigating the nervous system, Theodore Schwann, the cofounder of the cell theory, discovered that certain cells are wrapped around axons of the peripheral nervous system. What Schwann discovered then is now termed "Schwann cells". Schwann cells develop from the neural crest, a population of cells that migrates away from the dorsal aspect of the neural tube [160, 161] and generates melanocytes, smooth muscle, connective tissue and neurons and glia of the PNS. The generation of Schwann cells requires a first differentiation to a Schwann cell precursor that forms immature Schwann cells. This population gives rise to myelinating and

non-myelinating Schwann cells populations [162](*Figure I5-1*). This last step is reversible and, in case of injury, Schwann cells are able to dedifferentiate, proliferate again and become myelinating or non-myelinating depending on the axonal signals, which gives a good chance of regrowing to injured PNS axons.

Non-myelinating Schwann cells form Remark bundles, which means that a single Schwann cell wraps around multiple small, unmyelinated axons, separating them with a thin layer of cytoplasm (*Figure I5-1*).

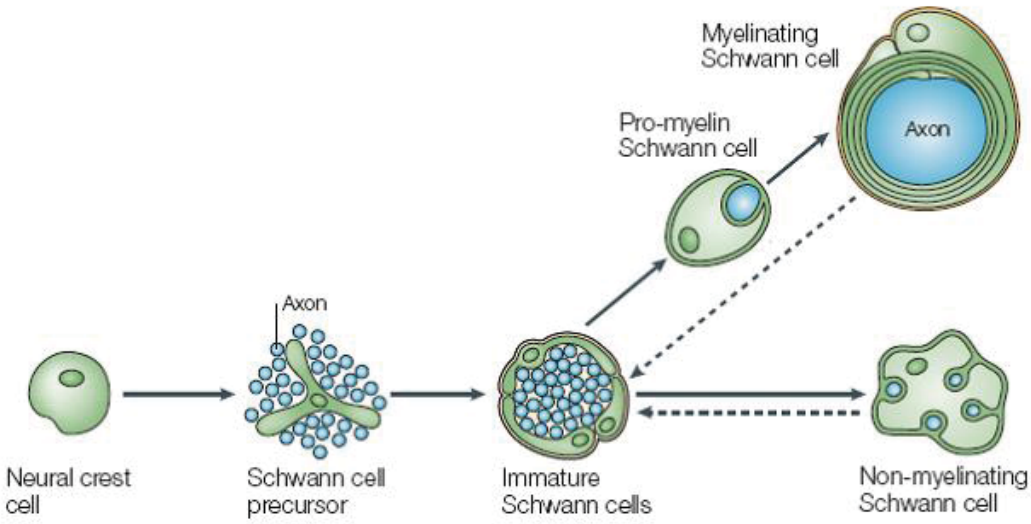

***Figure R5-1* | The Schwann cell lineage.** Schematic illustration of the main cell types and developmental transitions involved in Schwann cell development. Dashed arrows indicate the reversibility of the final, largely postnatal transition during which mature myelinating and nonmyelinating cells are generated. The embryonic phase of Schwann cell development involves three transient cell populations. First, migrating neural crest cells. Second, Schwann cell precursors (SCPs). Third, immature Schwann cells. All immature Schwann cells are considered to have the same developmental potential, and their fate is determined by the axons with which they associate. Myelination occurs only in Schwann cells that by chance envelop large diameter axons; Schwann cells that ensheath small diameter axons progress to become mature non-myelinating cells. (From Jessen & Mirsky, 2005)

Myelinating Schwann cells ensheath axons bigger than 1µm

in diameter in peripheral nerves, each Schwann cell forming myelin around one single axon [163]. The myelin sheath is basically a multilamellar spiral of specialized membrane around the axon (*Figure I5-1*). Its presence makes possible the saltatory nerve conduction, which means that the machinery responsible for action potential propagation is concentrated at regular, discontinuous sites along the axon: the nodes of Ranvier, the only regions (less than 1µm in length) in the axon without myelin sheath.

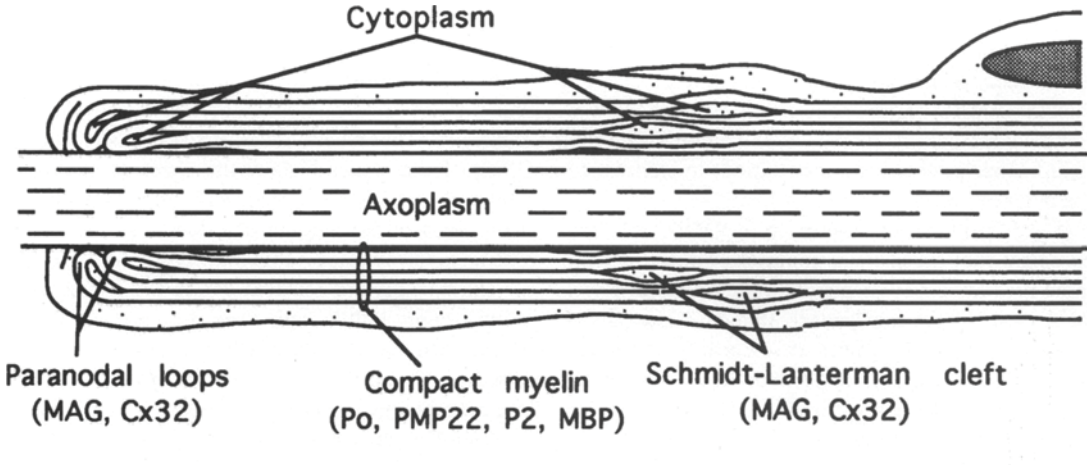

Figure I5-2 **|** Schematic longitudinal section through a single myelinated axon showing the distribution of some of the peripheral nerve myelin proteins, MAG, Po, PMP22, P2, MBPs and Cx32 and their association with the major domains of compact and noncompact myelin. (From Snipes & Suter, 1995).

The myelin sheath itself can be divided in two domains: compact and non-compact myelin. Compact myelin represents most of the myelin sheath and is composed of lipids, especially cholesterol and sphingolipids. The main compact myelin proteins are protein zero (P_0), peripheral myelin protein 22kDa (PMP22) and myelin basic protein (MBP) [164]. Non-compact myelin is rich in Cx32 and found in paranodes (the borders of the myelin sheath close to the nodes of Ranvier) and in Schmidt-Lanterman

incisures (funnel-shaped interruptions in the compact myelin) (*Figures I5-1 &2*). Most of the cytoplasm and the nuclei of Schwann cells are external to the myelin sheath. (Revised by Arroyo et al [165]).

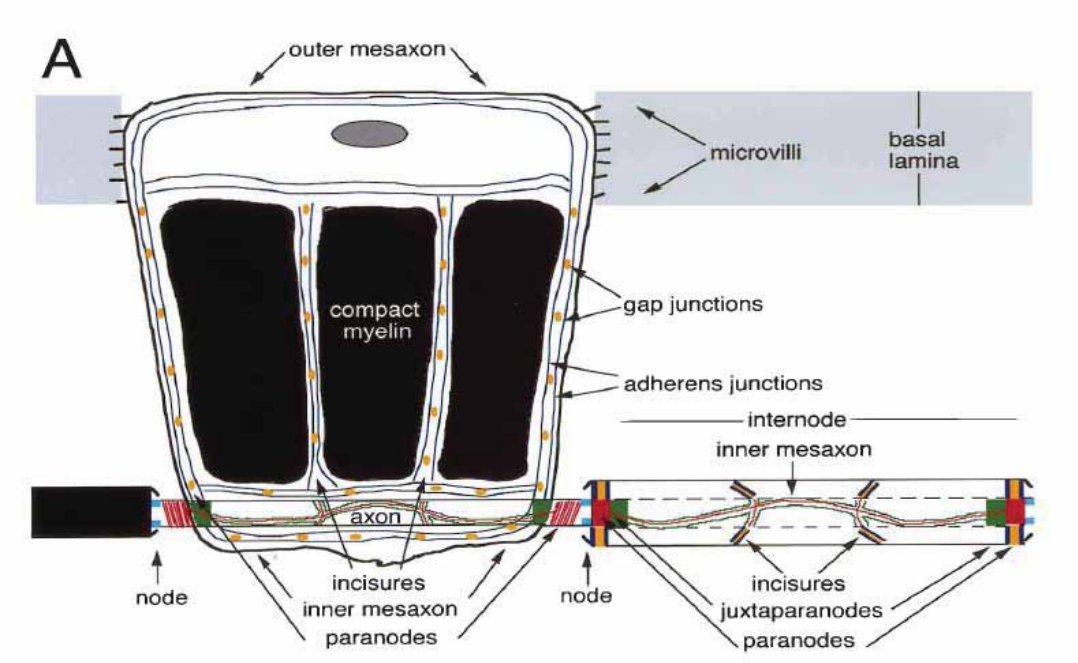

***Figure I5-2* | Schematic view of a myelinated axon in the PNS**. One myelinating Schwann cell has been unrolled revealing the regions that form non-compact myelin, the incisures and paranodes. Adherens junctions are depicted as two continuous (*purple*) lines; these form a circumferential belt and are also found in incisures. Gap junctions are depicted as (*orange*) ovals; these are found between the rows of adherens junctions. The nodal, paranodal, and juxtaparanodal regions of the axonal membrane are colored *blue*, *red*, and *green*, respectively. (From Arroyo & Scherer, 2000).

Already in 1928 Ramón y Cajal deduced that nodes, paranodes, and incisures contained different molecular components (*Figure I5-3*). In the axolemma of the nodes of Ranvier, voltage-gated Na^+ channels are highly concentrated [166] and the main isoform expressed is Sca8/PN4 ($Na_v1.6$). Also in nodal axolemma an isoform of Na^+/K^+-ATPase is expressed [167]. Together, the high concentration of Na+ channels and Na+/K+

ATPase is in keeping with the physiological function of the nodal membrane. On the other hand, the paranodal axolemma express contactin associated protein (Caspr) [168, 169], and the juxtaparanodal axolemma (a region extending 10-15μm from the paranode) express an homologue of Caspr, Caspr2 [170]; and delayed rectifying K^+ channels [171], specifically $K_v1.1$, $K_v1.2$ and their associated unit β2 [172, 173] . Both Caspr2 and $K_v1.1/K_v1.2/β2$ colocalize in the juxtaparanodes [170]. $K_v1.1/K_v1.2/β2$ channels are though to have an important function, dampening the excitability of myelinated fibres, as $K_v1.1$ null-mice have epilepsy [174], as well as marked temperature sensitivity in neuromuscular transmission [175] (*Figure I5-4*).

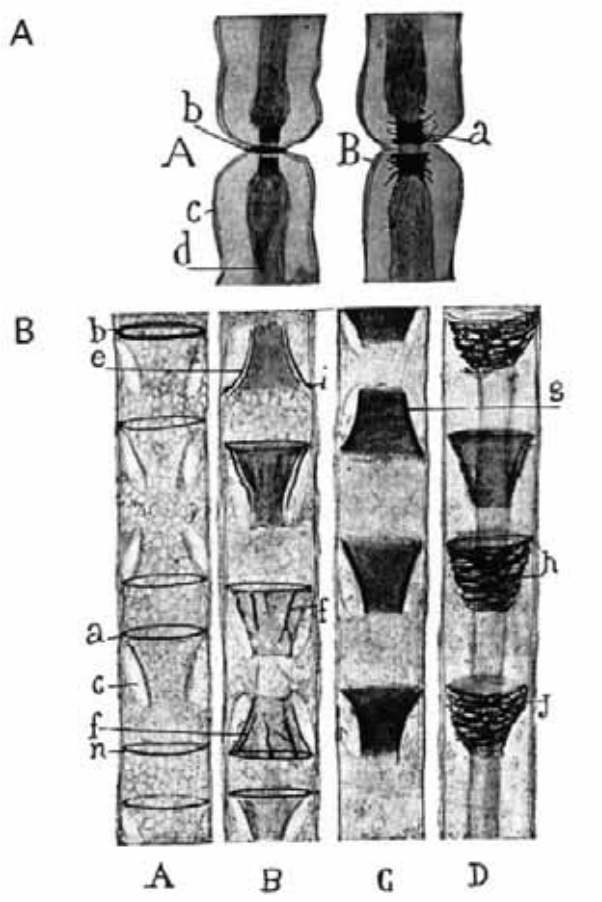

Figure I5-3 **|** Ramon y Cajal's (1928) depiction of the nodal region (**A**) and incisures (**B**) (from Arroyo & Scherer, 2000).

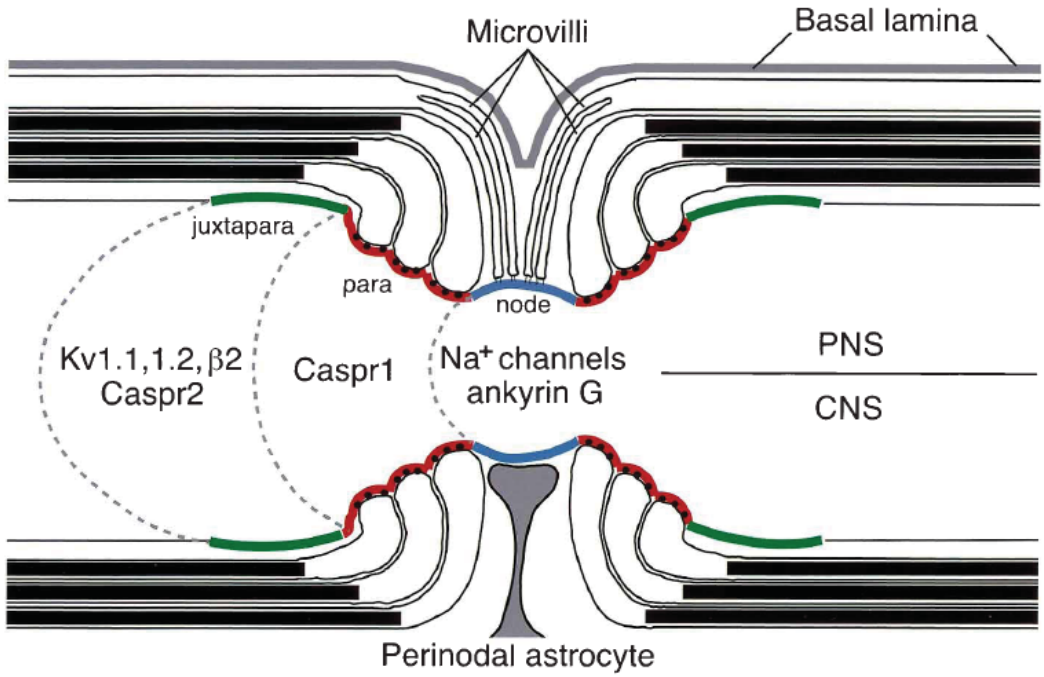

Figure R5-4 **|** Schematic depict on of the node, paranode, and juxtaparanode indicating the expression of different proteins used as markers for the different regions in the PNS and the CNS (from Arroyo & Scherer, 2000).

5.2 Schwann cells & connexins

Cx32 is widely regarded as the primary connexin of Schwann cells where it is abundant at paranodal regions and in Schmidt-Lanterman incisures [39] (in these structures the myelin layers are not compacted). Later it was reported that Cx32 is also expressed between the two outer layers of internodal myelin, throughout the zone of "partially compact myelin" [176].

In 1998, Balice-Gordon et al. observed a radial pathway of small molecular mass dyes diffusion across incisures, from the outer to the inner cytoplasm [40], providing evidence that gap junctions mediate this radial pathway, which represents a much shorter pathway for small molecular diffusion that could be up to 3 million times faster than through the cytoplasm [40]. Cx32 role in

this radial pathway is widely accepted nowadays [14]. Disruption of this radial pathway was proposed as the mechanism in which mutations in Cx32 cause CMTX, but as this pathway is not disrupted in Cx32-null mice [40] it has been suggested that there should be functional gap junctions in the myelin sheath formed by another connexin/s. This was supported by single-channel analysis of paired Schwann cells which suggested that the two cells were coupled by gap junctions with two different channels size which could reflect the expression of two different connexins [177].

Cx29 is a mice and rat connexin, which corresponds to human Cx30.2 [58]. It was reported that Cx29 is also expressed in Schwann cells, where its expression first appears when neural crest cells generate Schwann cells precursors, while Cx32 is not expressed until the onset of myelination occurs [178]. In adulthood, expression of Cx29 decline to lower levels than Cx32. In adult sciatic nerve, Cx29 is localized in the innermost aspects of the myelin sheath, the juxtaparanode, and in the inner mesaxon [59]. Both Cx32 and Cx29 are found in the paranodes and in the Schmidt-Lanterman incisures[59]. Cx29 displays a striking coincidence with Kv1.2 K+ channels, which are localized in the axonal membrane [59], although it is expressed in the innermost layers of myelin but not in the outer layers [179]. This differential subcellular distribution of Cx29 and Cx32 imply that connexin with different properties are required at different cellular locations, and that there are functional differences in the apical and basal Schwann cell compartments.

Cx43 expression in Schwann cells has also been suggested, first in neural crest cells [178], and later in rat sciatic nerve and cultured Schwann cells [71], with a low intensity immunostaining of Cx43 along the myelin sheath and Schwann cell bodies [70], thus showing a different distribution pattern from Cx32 and Cx29.

After peripheral nerve injury Cx32 expression dramatically decreases, retuning to basal levels at newly formed nodes of Ranvier and Schmidt-Lanterman incisures after 30 days [180], on the other hand Cx46 and Cx43 expression is enhanced in rat sciatic nerve, only returning to basal levels, 12 days after injury [180], which could suggest a role of this connexins during remyelination, as it has recently been reported for Cx43 in spinal cord remyelination in a guinea pig model for experimental allergic encephalomyelitis (EAE) [181].

5.3 Schwann cells and CMTX

The pathologies associated with Schwann cells can be divided into injury response, demyelinating disorders and tumour disorders [161]. Among demyelinating disorders there is Charcot-Marie-Tooth disease, in which mutations of different components like PMP22 [182], P0, periaxin, EGR2/Krox, Sox-10, MTMR2 [183], etc. lead to the different described [184] (see section 1). Mutations on the hCx32 gene, ranging from loss of channels formation to altered permeation properties [42], lead to the X-linked form of Charcot-Marie-Tooth disease (see sections 1.3 and 2.5). The successful transgenic rescue of the Cx32 null-mice phenotype by Schwann cell specific expression of wild type hCx32 in mice has

elegantly demonstrated that the CMTX disease has a Schwann cell origin [53].

5.4 Schwann cells & ATP

All types of glia have membrane receptors for extracellular ATP (purinergic receptors). Schwann cells express $P2X_7$ [157, 185] and $P2Y_2$ receptors [186]. The concentration of ATP required to evoke a response through the $P2X_7$ receptors is in the range of millimolar for maximal activation, concentrations that might be achieved *in vivo* with injury in local cell or axonal lysis. However, it has been hypothesised that normal ATP release from axons into the confined periaxonal space between Schwann cell and axon may lead to local high concentrations [187]. Activation of the $P2X_7$ receptor gives rise to a non-specific cation current, which may lead to the activation of other membrane conductances, through an influx of Ca^{2+}, membrane depolarization or Ca^{2+} dependent changes in gene expression, etc [188].

ATP is co-released with acetylcholine and noradrenalin from secretory vesicles in the PNS. Adult Schwann cells have P2 receptors [157], specifically, myelinating Schwann cells express $P2Y_2$ and non-myelinating Schwann cells express $P2Y_1$ receptors, and its activation triggers changes in intracellular Ca^{2+} in paranodal and inteparanodal regions of Schwann cells [189].

Effects on Schwann cell gene expression, mitotic rate and differentiation have been identified in response to activity-dependent ATP release. ATP released from axons during action potentials transmission arrest maturation of immature Schwann

cells and prevents myelination, this could be a mechanism by which developing nervous system could delay terminal differentiation of Schwann cells until exposure to appropriate axon-derived signals [188, 190, 191].

Not only is ATP released by presynaptic terminals, it can also be released by the postsynaptic membrane and other cells. There is evidence of multiple pathways for ATP release from glial cells besides vesicle release. Cx43, Cx32 and Cx26 connexins have been reported to increase ATP release and intercellular calcium wave propagation [18], suggesting that unpaired gap junctions (hemichannels) could also release ATP.

Schwann cells have been reported to release ATP in response to glutamate, in a concentration dependent manner [192], and UTP [193] (mediated by activation of $P2Y_2$ receptors), and it is released from vesicles as well as through anion transporters across the plasma membrane.

OBJECTIVES

In our laboratory we study connexin hemichannels, ATP release through the plasma membranes and the combination of both: ATP release through connexin hemichannels.

Connexin 32 is expressed in many tissues, among them in the Schwann cells of the peripheral nervous system. Mutations on Cx32 lead to the X-linked from of Charcot-Marie-Tooth disease, but the mechanisms by which this neuropathy is generated remain unclear. In order to know the possible role of ATP in this disease, **we studied the ATP release through Cx32 hemichannels.**

Connexin 32 is expressed in Schwann cells and its hemichannels open in response to hyperpolarizing potentials. Action potentials are a naturally occurring depolarizing event of the axonal plasma membrane, and it affects also the Schwann cell membrane apposed to the axon in the paranodes, where Cx32 is expressed. To reproduce this physiological condition, **we studied the ATP release from Sciatic nerves after electrical stimuli.**

Cx32 is expressed in paranodes and Schmidt-Lanterman incisures. Other two connexins are expressed in Sciatic nerve: Cx29 and Cx43. Cx29 is also expressed in paranodes and Schmidt-Lanterman incisures whereas Cx43 is low expressed along the myelin sheath. To test this expression we **performed immunostainings to localize peripheral nerve connexins.**

Peripheral nerve releases ATP and connexins are expressed in Schwann cells wrapping the nerve axons but, do the Schwann cells release this ATP? To further study this possibility we **studied the ATP release from cultured Schwann cells in response to hypotonicity.**

ATP in Schwann cells could be released through other channels or exocytosis besides Cx32 hemichannels. To elucidate the role that Cx32 hemichannels play in ATP release in response to hypotonicity **we studied ATP release in response to hypotonicity in HeLa wild type and hCx32 stable transfected cells.**

Syntaxin 1A (S1A) has been reported to modulate many ionic channels, and studies in our laboratory revealed that S1A can also inhibit Xenopus oocytes endogenous connexin (Cx38). With this background we wanted to **study the possible modulatory role of S1A upon Cx32 hemichannels and its capacity to release ATP.**

MATERIALS & METHODS

1. Solutions

Ringer solution (NR): 115 mM NaCl 2 mM KCl 1.8 mM $CaCl_2$ 10 mM HEPES pH 7.4 Ringer Mg^{+2}: 115 mM NaCl 2 mM KCl 1.8 mM $CaCl_2$ 10 mM HEPES 1.8 mM $MgCl_2$ pH 7.4 Barth's Solution: 88 mM NaCl 1 mM KCl 0.33 mM $Ca(NO_3)_2$ 0.41 mM $CaCl_2$ 2.40 mM $NaHCO_3$ 0.82 mM $MgSO_4$ 20 mM HEPES (100 U/ml) Penicillin G (100 µg/ml) Streptomycin pH 7.5	TBS buffer (10X) 100mM Tris 1.4M NaCl 1% Tween-20 pH 7.4 Electrophoresis Buffer 192mM Glycine 25mM Tris 1% SDS Sandwich buffer 192mM Glycine 25mM Tris 20%m Methanol Semi-dry buffer 48mM Tris 38mM Glycine 1.3mM SDS 20% Methanol Milk buffer TBS 1x 5% fat free powder milk

PBS buffer 137mM NaCl 2,7mM KCl 2mM NaH_2PO_4 10mM Na_2HPO_4 pH 7.4 (HCl) ECL A solution 100mM Tris pH 8.5 450nM Coumaric acid 2.5mM Luminol ECL B solution 100mM Tris pH 8.5 0.06% H_2O_2 Mammal Physiological buffer 154mM NaCl 5mM KCl 1.25mM $MgCl_2$ 11mM Glucose 5.46mM HEPES 1.8mM $CaCl_2$ pH 7.4 LB agar: LB medium 15 g/ L Bacto agar	Medium Luria-Bertani (LB): 10% Bacto Tryptone 5% Yeast extract 10% NaCl pH 7.0 IF blocking solution PBS 1x plus: 20% FBS or NGS 0.2% X-100 Triton 0.2% gelatine IF incubating solution PBS 1x 1% FBS or NGS 0.2% X-100 Triton 0.2% gelatin Alkaline Solution 1 500mM D(+)Glucose 25mM Tris 10mM EDTA Alkaline Solution 2 0.2M NaOH 1% SDS Alkaline Solution 3 3M KAc 5M AcA

TBF I solution	Isotonic solution
30mM KAc	140 mM NaCl
100mM RbCl	5 mM KCl
10mM $CaCl_2$	1 mM $CaCl_2$
50mM $MnCl_2$	10 mM $MgCl_2$
15% Glycerol	10mM HEPES
(0.22µm filtered)	pH 7.4 (NaOH)
	(0.22µm filtered)
TBF II Solution	
10mM NaMOPS	Na^+ free solution
75mM $CaCl_2$	5 mM KCl
10mM RbCl	1 mM $CaCl_2$
15% glycerol	10 mM $MgCl_2$
(0.22µm filtered)	10mM HEPES
	pH 7.4 (NaOH)
	(0.22µm filtered)

2. Injection material for *Xenopus* oocytes

2.1 Cx38 Antisense obtention

An antisense nucleotide for the Cx38 mRNA (ASCx38) 5'-GCTTTAGTAATTCCCATCCTGCCATGTTTC-3' [194] was sintetized by Invitrogen-Life Technologies S.A. (Barcelona). This oligonucleotide was resuspended with pure water and injected (50nl, 2 mg ml^{-1}) into the *Xenopus* oocytes 24-48h before experiments, to abolish the endogenous Cx38 expression.

2.2 Cx32 & S1A cRNA production

Dr. Luis Barrio from the "Ramón y Cajal" Hospital, Madrid, Spain, kindly provided the plasmid containing the hCx32 cDNA. This hCx32 cDNA was cloned in a vector (pBxG) derived from the commercial vector PBluescript KSII (Stratagene), inserted in a Stu I restriction site, surrounded by *Xenopus Laevis* β-globin gene fragments which enhance the translation in the oocytes. In addition, the hCx32 cDNA coding sequence is orientated to be transcribed by the T7 polymerase (*Figure M2-1*).

Syntaxin 1A sequence inserted in the pGEM-T easy vector was obtained in the laboratory, and it was also inserted to be transcribed using the T7 polymerase.

To obtain the cRNA from the cDNA we followed the instructions of the mCAP RNA Capping kit (Stratagene, protocol #200350). This protocol starts with 10µg hCx32 or S1A cDNA containing plasmid, which was liniarized using Xho I for hCx32 and PstI for S1A. Transcription was performed using T7

polymerase. All the protocol was performed according the Stratagene manual and the cRNA obtained was resuspended in 15µl DEPC treated water. The volume of 1µl was used to quantify the resulting cRNA (using a Genequant II, Pharmacia Biotech) and 2µl were tested on a 1% Agarose gel to check the size and possible degradation. The cRNA obtained was stored at -80°C until used.

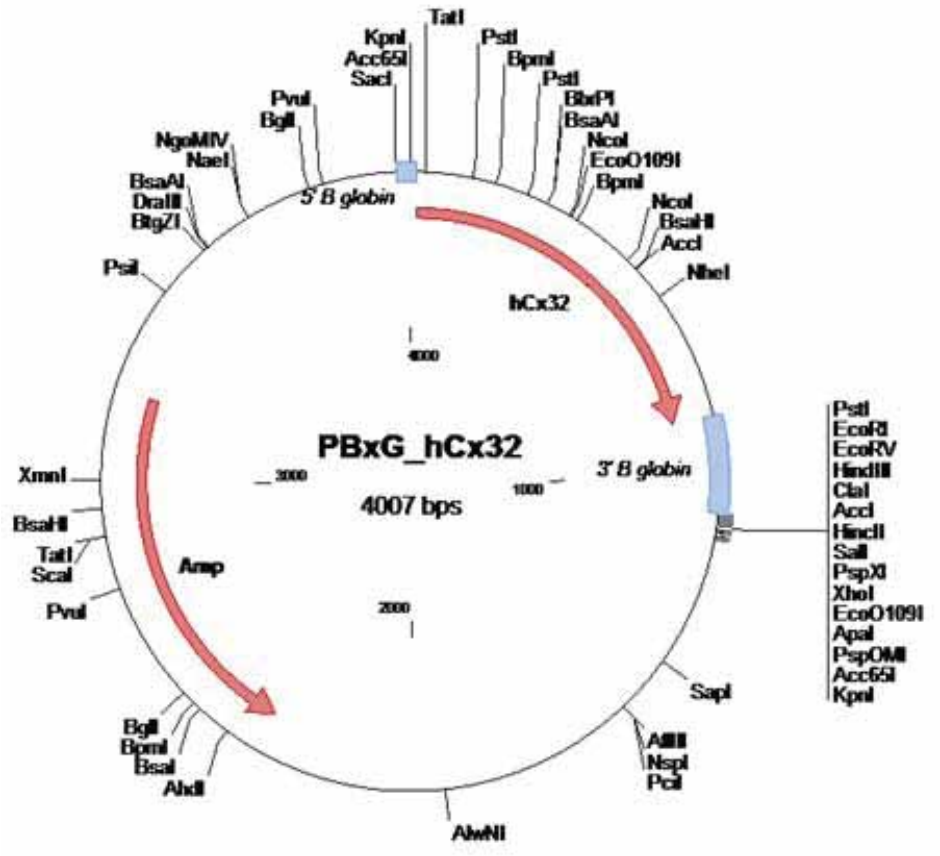

Figure M2-1 **|** Scheme of the pBxG plasmid derived from the pBluescript KSII (Stratagene) and containing the *Xenopus Laevis* β-globin gene fragments and the hCx32 gene sequence.

3. Working with Xenopus oocyte model

3.1 Obtaining and keeping *Xenopus laevis* oocytes

Xenopus laevis female individuals were kept at the animal

facilities of the University of Barcelona, Campus of Bellvitge, Barcelona, Spain. Each specimen was maintained separately in 2% NaCl water and feed three times per week with grinded beef heart meat.

To extract oocytes, *Xenopus laevis* females were anaesthetized by immersion in a 0.3% 3-aminobenzoic acid ethyl ester (Sigma) solution in water. A small incision was performed on the abdominal muscles, first through the skin and afterwards through the muscles, in order to reach the ovary. A few ovarian bags were extracted and placed on a Petri dish filled with sterile Barth's solution. The incisuion was then sewed with 0.2 mm sterile silk yarn, first the muscle and afterwards the skin; avoiding any oocyte or air bag between the muscle and the skin. The animal was left to rest for at least three months before new surgery. Each individual was operated no more than four times. Protocol for animal manipulation and oocyte extraction were certified and approved by the ethical committee for animal research according to the laws of the EU and the Catalan Government.

Once in the Petri dish, the phase V and VI oocytes were manually separated under a magnifier lenses (Sz-40, Olympus), using a pair of watch tweezers (World precision instruments, num.55) and the rest of ovarian tissue was removed. These developmental phases of the oocytes were optically distinguishable, as cells are very big. Selected oocytes were maintained in Petri dishes with Barth's medium at 18°C. Medium was changed daily and dead oocytes were removed. With this

protocol we had a 90-95% oocyte survival.

3.2 Injecting cRNA in *Xenopus laevis* oocytes

Injection micropipettes were pulled from glass capillaries (4878 World precision instruments, Inc; EUA) using a two step pull protocol performed by a puller (P-97, Sutter Instruments Co; EUA). Once pulled, micropipettes tips were broken under a magnifier to reach a 5-15µm diameter, the desired size for microinjection. Micropipettes were sterilized 4h at 200°C.

For the cRNA injection, all material and injection place had to be sterile. Micropipettes were half filled with sterile mineral oil (Sigma, M-5904) to avoid the direct contact of the sample with the nanoinjector plunger. Micropipettes were placed on the nanoinjector (WPI, A203XVZ), which was fixed with a micromanipulator (Narshigue, MMN-3R, Japan). A drop of sample was placed on a cap of an eppendorf tube and then the micropipette tip contacted the drop with the help of a micromanipulator and was filled with the sample solution using the nanoinjector commands. Mature oocytes were placed on a parafilm surface with 1mm holes; oocytes were placed on those holes and kept humid during injection protocol. Each oocyte was injected on the vegetal pole, near the equator and far from the nucleus, 50 nl of sample (cRNA solution, 1-2 mg/ml)/oocyte. All the procedure was repeated with every oocyte until the sample was exhausted. Injected oocytes were then placed on Petri dishes with fresh Barth's medium supplemented with penicillin/Streptomycin for 48-72 hours (changing the medium

every 12-24 hours) before electrophysiological experiments were performed.

3.3 Collagenase treatment

Before using them for electrophysiological experiments, the follicular layer oh the oocytes had to be removed, as it is too thick for the microelectrodes to pierce oocytes without breaking, and because it contains ionic channels and gap junctions that can interfere with the oocytes plasma membrane channels during recordings.

To remove this layer oocytes were placed on a glass tube with Ringer solution containing 0.5 mg/ml collagenase 1A (Sigma) and left at room temperature for 30-45 minutes (until the follicular layer was visible on the tube) on a rotatory shaker, at 10 rpm. The incubation was stopped by washing four times with fresh Ringer solution. Finally, oocytes were placed again on Petri dishes with fresh Barth's medium and left on the incubator at 15°C until electrophysiological records were performed (1-8h). For a less aggressive defolliculation method oocytes were incubated with 0.128mg/ml collagenase 1A in Ringer solution also at RT for 30min shaking at 10 rpm, but these oocytes were used 24h after defolliculation.

4. Two Electrode Voltage Clamp

4.1 Two Electrodes Voltage Clamp

The Two Electrodes Voltage Clamp Technique (TEVC) is

based on two electrodes, one used to monitor the real intracellular potential (the difference of potential between the cytoplasm of an oocyte and the surrounding medium), and the other that inject the necessary current to maintain constant and at a specified value the membrane potential. All this is achieved thanks to a Voltage Clamp amplifier (Gene clamp 500; Axon Instruments, USA). During a TEVC recording, when ionic channels of a voltage clamped oocyte open, the amplifier injects through a microelectrode a current of the same intensity and opposite charge to keep constant the plasmatic membrane potential. This injected current is actually what the amplifier records (*Figure M4-1*).

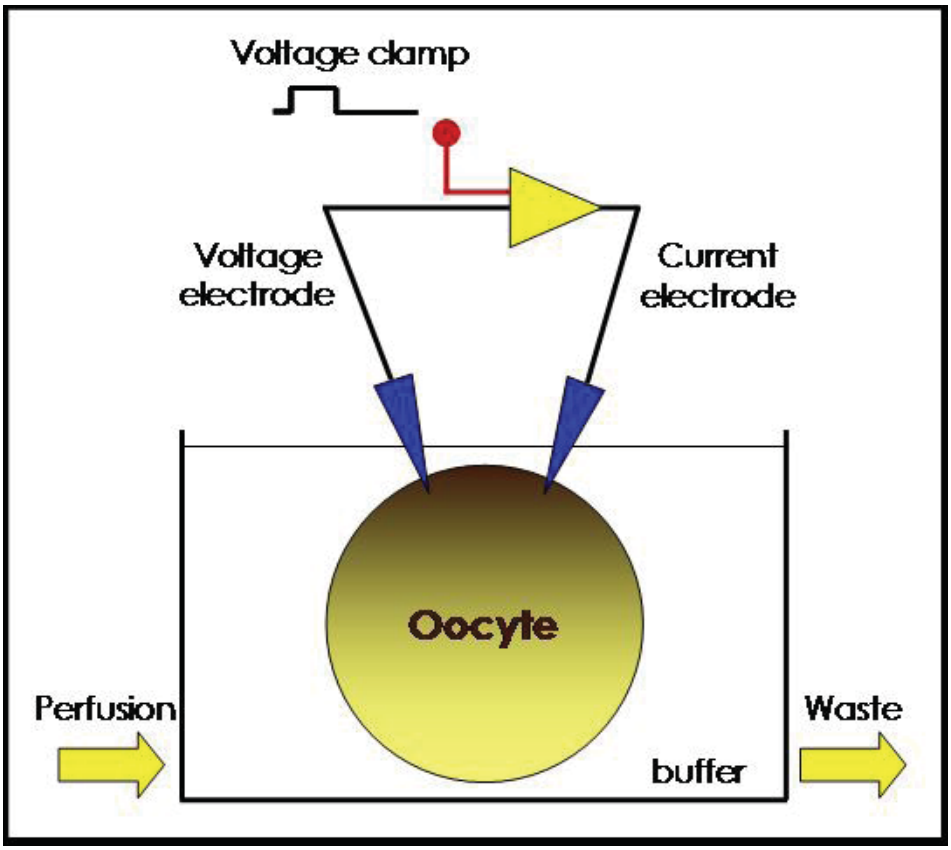

Figure M4-1 **|** Scheme displaying the register chamber and the electrical circuit necessary to clamp the membrane voltage.

4.2 Two Electrode Voltage Clamp *Set up*.

For the TEVC recordings, oocytes were placed on a transparent plastic chamber, with 250 µl of volume capacity and connected to a perfusion system. In this chamber there was a 1-2 mm hole where a single oocyte could be easily placed with a Pasteur pipette. There, oocytes did not move and could be pierced with the two microelectrodes (*Figure M4-2*). Below and above the chamber there was optic fibre, to capture the emitted light from the luciferin-luciferase reaction (see section 5 on materials and methods).

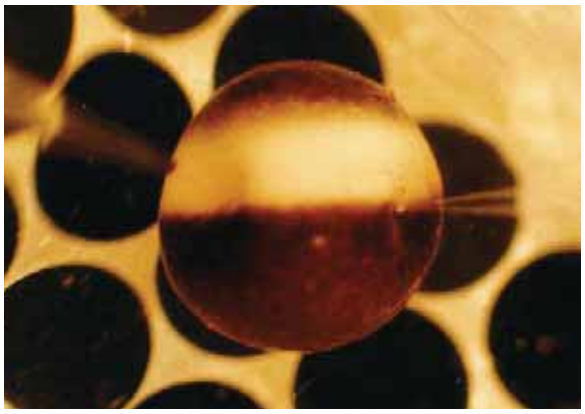

Figure M4-2 **|** Image of an oocyte in the register chamber pierced by the two electrodes, ready for a TEVC recording. Under the oocyte there are small optic fibres to capture emitted light.

The chamber was held under a magnifier (Olympus SZ-CTV), connected to a cold light source (Olympus Highlight 3000). All this was on a vibration isolation table (Technical Manufacturing Corporation, USA), to avoid any vibration that could affect oocytes during recordings. The table was surrounded by an opaque Faraday cage.

The perfusion system had eight 70ml syringes placed at 80cm high to store solutions, each one with an exit by gravity flow at the end. The flow from the syringes reached between 6 and 10 ml/min and was controlled using a BPS-8 valve control

system (ALA Scientific Instruments, USA). Solution flowed to the chamber to bath the oocyte and then drained on the other side of the chamber. All waste solution was collected in double Kitasato system, which was connected to the central vacuum system.

Oocytes were pierced with two intracellular microelectrodes, each one placed on a preamplifier holder, connected to an amplifier (Gene clamp 500; Axon Instruments, USA), which was connected to a computer through an interface card (BNC-2090, National Instruments, USA). Information was processes using Whole cell Analysis software (winWCP) by Prof. J. Dempster (Strathclyde University, Scotland, UK). On the other hand, signals were simultaneously visualized on an Oscilloscope (TDS 420A, Tektronix, USA) (*Figure M4-3*)

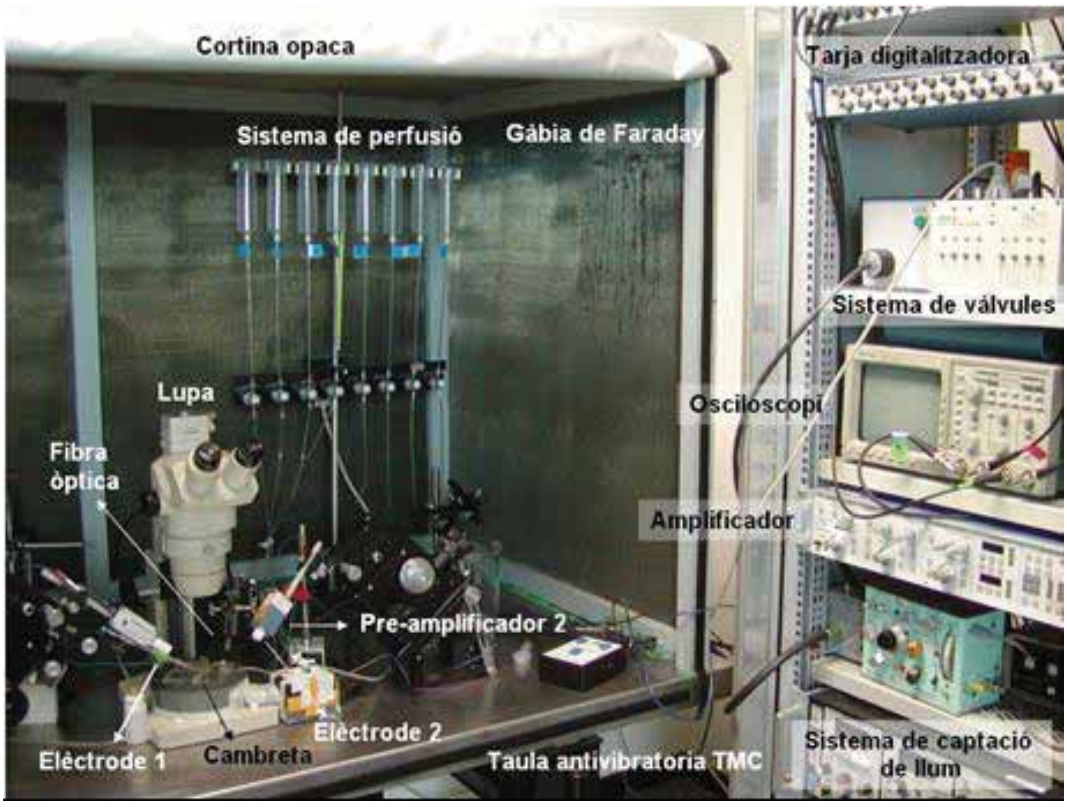

Figure M4-2 **|** Image of the TEVC set up.

4.3 Getting ready for TEVC recordings

First, microelectrodes used for the recordings were made using GC120TF-7.5 glass capillaries (Harvard Apparatus, UK) and pulled using a two step program in a P-97 puller (Stutter Instruments Co; USA). Microelectrodes had to have a resistance between 0.5 and 1 MΩ. Afterwards microelectrodes were filled with a 3M KCl solution and placed on a holder (Axon instruments, USA) with a 0.25 mm chloride silver wire connected to the holder itself and contacting the KCl solution. The holders with the microelectrodes were then placed on preamplifiers or HS-2A headstages (Axon instruments, USA) connected to the amplifier. Preamplifiers, with holders and microelectrodes, were fixed on micromanipulators (Narishigue, Japan) that allowed a fine control to pierce oocytes. The bath chamber had a reference Ag-AgCl pellet connected to the ground.

4.4 Two electrode Voltage Clamp recordings

Once an oocyte was placed in the chamber that was filled with ringer solution and both microelectrodes were placed on holders and fixed on the preamplifiers, microelectrodes tips were submerged in Ringer and offset set to zero. The oocyte on the chamber was then gently pierced with both microelectrodes (which formed approximately a 90° angle between them). When the two electrodes were inside the oocyte the real membrane potential was displayed on the amplifier and only oocytes with lesser than -20mV potential were used for recordings, as higher potential indicated an unhealthy plasmatic membrane.

When a healthy oocyte was clamped the amplifier mode was switched to voltage clamp and membrane potential was fixed to -40mV. Oocyte membrane resistance was calculated before starting by calculating the difference between the currents recorded when the membrane potential was -60mV and -40mV, and then using Ohms law. Oocytes with resistance smaller than 0.1MΩ were discarded. Oocytes with resistance greater than 0.1MΩ were used for the recordings. Oocytes plasma membrane was clamped at -40mV and depolarized by clamping the potential at -80mV for 30 seconds before returning to the basal potential (-40mV). Currents generated applying that protocol were afterwards analyzed. This protocol was applied to oocytes injected with different samples (AsCx83, Cx32 and S1A) and recorded currents compared and analysed.

5. TEVC & ATP release measurements

5.1 Using Luciferin-Luciferase reaction to detect ATP

One of the most widely used and accepted assays to detect ATP is the Luciferin-Luciferase luminescent reaction [195]. This method can detect direct and continuously ATP levels on a solution or sample. It is based on the luciferin capacity to, in presence of luciferase (an enzyme obtained from the American firefly, *Photinus pyralis*) and ATP, to become oxiluciferin and emit light (*Figure M5-1*). Luminescence can be easily detected and quantified using photomultipliers. This is a very sensitive method and can detect in the range between femto and

micromolar ATP concentrations.

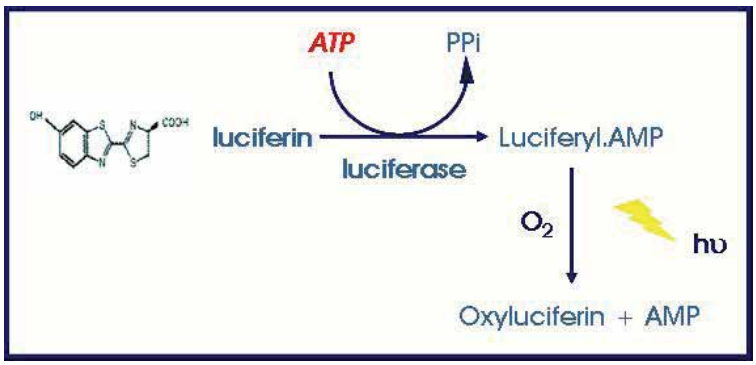

Figure M5-1 | Luciferin-Luciferase reaction

5.2 Preparing Luciferin and Luciferase solutions

To purify Luciferase, 250 mg of Firefly lantern extract (Sigma, FLE250) were diluted in 2.5 ml of ultrapure water and centrifuged for 2 minutes at 12000 rpm (eppendorf 5417R centrifuge), at 4°C. The supernatant was gel filtered on a disposable chromatography column (10 ml, Econo-pac 10DG BioRad, UK) previously equilibrated with working solution. Eluted luciferase was collected and aliquoted on eppendorfs (100µ/eppendorf). Aliquots were stored at -20°C until used.

10 mg of Luciferin (Sigma, L-9504) was diluted in 1.5ml ultrapure water and pH was adjusted to pH 7.4 with NaOH. Aliquots of 100µl were stored at -20°C until used.

Before use, 30 µl of luciferin solution were added to a 100 µl luciferase aliquot, and this luciferin/luciferase mix was used to detect ATP. The luciferin/luciferase reaction is pH sensitive (needs neutral pH values) and needs the presence of Mg^{2+} ions as a cofactor.

5.3 Simultaneous TEVC recordings and ATP release measurements.

To detect ATP release due to voltage changes of the membrane of a single oocyte, an oocyte was placed on the recording chamber filled with Ringer Mg^{2+} solution and 15 µl of luciferin/luciferase mix solution. A 1 mm diameter optic fibre was placed right above the oocyte. There was also optic fibre under the oocyte. The set up was covered with an opaque curtain and the light was switch off. The TEVC recordings were then performed as previously described while, at the same time, any signal of light produced by ATP presence was detected by optic fibres, which were connected to a photomultiplier (P16, Grass Medical Instruments, USA) and filtered in a Bessel (Frequency devices, USA). A known amount of ATP was injected to the recording chamber, near the oocyte, after the voltage pulse, to validate and calibrate the luminescent reaction. The signal was sent to a PC using the same interface and Whole Cell Analysis software (winWCP) used to register currents and voltage [126]. The ATP released was analyzed by deconvolution by Dr. Rafel Puchal, Dep. Of Nuclear medicine, Hospital Universitari de Bellvitge, Hospitalet de Llobregat, Spain; using Sigmaplot 10 software (Systat Software Inc, Richmond, CA, USA) as described before [196].

6. Western blot analysis

6.1 Using *Xenopus laevis* oocytes as samples

After each recording, oocytes were individually stored in eppendorfs at -20°C. Oocytes with significative recordings were

thawed and homogenized with 15-30 µl homogenizing buffer containing 0.1 M NaCl, 1% X-100 triton, 1 mM PMSF, 20 mM Tris-HCl (pH 7.6). Just before use 10 mg/ml Leupeptin, 10 mg/ml Aprotinin, 0.5 mM EGTA and 0.5 mM EDTA were added. The mixture was homogenized by pipetting up and down and left on ice for 15 minutes. Afterwards samples were centrifuged 5 minutes, at 10,000g, 4°C. Supernatants (solubilized membrane and cytoplasm proteins) were transferred to new eppendorfs.

6.2 Using HeLa cells homogenates as samples

To obtain protein homogenates from HeLa cells grown on 12 wells plates, cells were trypsinized (tryspin from Gibco, 25300-061) and centrifuged for 5 min at 800 rpm (Hermle 2383 centrifuge). Sediments were resuspended with 1 ml of PBS supplemented with protease inhibitors (10 µg/ml Leupeptin, 10 µg/ml Aprotinin, 1 mM EDTA, 1 mM PMSF) and were centrifuged twice for 2 min at 900rpm. Pellets were rinsed with PBS plus protease inhibitors. After the second centrifugation, pellets were resupended in 1 ml PBS plus protease inhibitors and were homogenated with repeated aspirations through the pipette. The homogenates were left for 5 min on ice, and finally were centrifuged again for 10 min at 1000g. Pellets were kept and supernatants were transferred to new eppendorf tubes and centrifuged again 30 min at 100,000g. Pellets obtained both before and after these centrifugations were resuspended in 100 µl PBS plus protease inhibitors. Protein concentration was quantified using the BCA method (Pierce protein assay kit) and samples were stored at -20°C until used. Pellets obtained before

the last centrifugation contained the cell nuclei and pellets obtained after the last centrifugation contained all intracellular and plasma membrane proteins.

6.3 General Western Blot protocol

Acrilamide/bisacrilamide gels for electrophoresis were made using a concentration of 12 % for the resolving part and at 4% for stacking portion. Loading buffer was added and samples were boiled for 5 minutes before loading them on a gel and ran for 1 hour and 10 minutes at 200 V and 18 mA (per gel). Proteins were then transferred from acrilamide gels to nitrocellulose membranes either using the wet or semi-dry protocol. For the wet protocol all parts were soaked in sandwich buffer and transference was held at 100 V, for 1 hour. For semi-dry protocol, it was soaked in semi-dry buffer and the transference was done at 20 V, 40 mA per gel, for 45 minutes.

Transferred nitrocellulose membranes were then blocked for 45 minutes with milk buffer. Milk buffer was removed and new milk buffer with primary antibody at the convenient concentration was added for 1 h, at RT or ON, 4°C. The membranes were washed three times with milk buffer before the secondary HRP conjugated antibody diluted in milk buffer was added for 1 hour, at RT. Membranes were then washed three times with milk buffer and twice with TBS. Membranes were developed using the ECL reaction system. This system use HRP conjugated to the secondary antibody to, in conjunction with H_2O_2 and luminol (a chemiluminescent substrate) generate a

light signal that is captured by a film (Kodak). In some experiments the light was not recorded on a film but in a new integrated system for chemiluminiscence detection (Syngene Bio imaging, Gene-Gnome).

Primary antibodies were used at the following dilutions: anti HPC-I (S1A) 1/1000, anti Cx32 (Sigma 106-124) 1/500.

7. Peripheral nerve ATP release imaging

7.1 Mouse and Rat sciatic nerve extraction

Mice (Swiss CD1) were sacrificed by cervical dislocation and rats (Sprague Dawley) were anaesthetized and decapitated, before quickly proceeding to extract sciatic nerves. Animals were cleaned with 70% ethanol and skin around hind limbs was retracted. Muscles were then separated to localize and aseptically remove sciatic nerves from each leg. Nerves were extracted and immediately submerged in PBS (*Figure M7-1*). A sciatic nerve was then fixed on a special chamber for the experiments with physiological buffer.

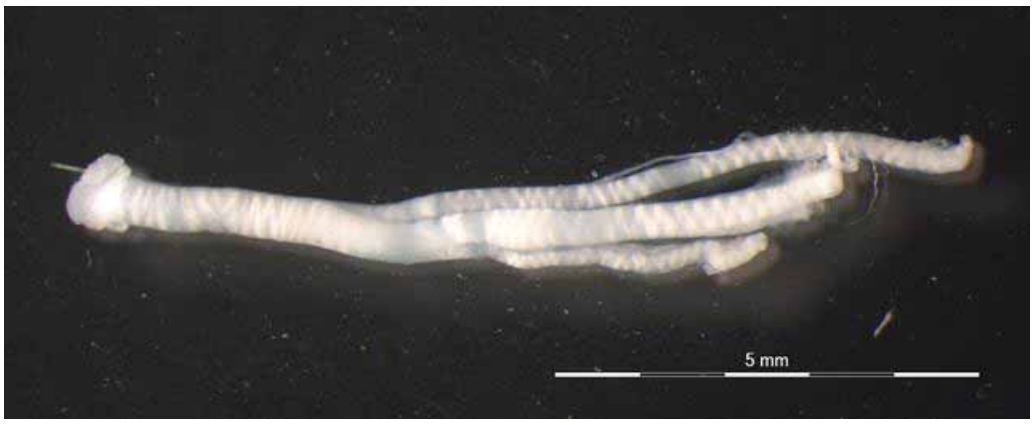

Figure M7-1 **|** Image of an extracted mouse sciatic nerve.

7.2 Sciatic nerve ATP release imaging

An ORCA II cooled camera (Hamamatsu, Japan) was connected to a Microscope (IX-50, Olympus) placed on a vibration isolation table (Technical Manufacturing Corporation, USA). The camera was connected to a computer, via a temperature controller, from where the camera was controlled using Aquacosmos software (Hamamatsu, Japan). Next to the microscope there was a suction electrode connected to a stimulator (S88, Grass Medical Instruments, USA).

The chamber with a sciatic nerve was placed on the plate of the microscope and the stimulation suction electrode was connected to one nerve end. A mixture of luciferin-luciferase was added to the physiological buffer, and left for 10-30 minutes to avoid unspecific light. Expositions between 10-30 minutes were taken with the Orca II camera with and without electric stimulation with the suction electrode and using the whole nerve and teased sciatic nerves. Images were processed with Aquacosmos (Hamamatsu) and Photoshop (Adobe) software.

8. Immunofluorescences

8.1 Sciatic nerve teasings

For these preparations we used Swiss CD1, C57BL6 mice and Knock out C57BL6 mice for Cx32 and Cx29. CD1 mice were taken from the animal device installation from the Campus Bellvitge, Universitat de Barcelona, Spain. All kinds of C57BL6 mice were gently provided by Dr. Klaus Willecke, Institut für

Genetik, Bonn University, Germany.

There were two ways to prepare sciatic nerve teasings for immunofluorescences: The first method is fixing the tissue: Ketolar and Rompun were mixed (4:1) and injected intraperitoneally to mice (500µl/mouse) to anaesthetize them before perfusion. When mice were correctly anaesthetized, they were secured on a surface and dissected to expose the heart. A needle connected to the perfusion system was inserted to the left ventricle, and we the right auricle was cut open to let blood flow. First we washed injecting PBS through the perfusion system and then we switched to 4 or 2% paraformaldehyde. When the animal was fixed we extracted both sciatic nerves (see section 7.1 on materials and methods). Sciatic nerves were placed on a Petri dish with PBS to wash them and then postfixed with 4 or 2% paraformaldehyde until used.

The second method (not fixing) was to sacrifice mice by cervical dislocation and immediately extract sciatic nerves. From that point all samples (fixed or unfixed) were placed on a microscope slide and covered with a drop of PBS. Under a magnifier and using a pair of fine tweezers the connective layers were removed and nerve fibres were gently separated and placed on superfrost microscope slides (Esco, Erie scientific company. USA), trying to get single fibres separated from the others. PBS was aspirated and microscope slides were let dry. Dried samples were stored at -20°C until used.

8.2 Sciatic nerve immunofluorescence

Coverslips were thawed and post-fixed 10 minutes with ice-cold acetone. Coverslips were washed with PBS before being blocked with IF blocking solution for 1 hour, at RT.

Primary antibodies were diluted in IF incubation solution (concentration depending on antibody) and placed on the coverslips for 1h 30 min, at RT or ON at 4°C. Samples were then washed three times with PBS. Secondary, Fluorochrome conjugated (Alexa Fluor® 488 or Alexa Fluor® 546, Molecular probes, A-11034 and A-11035), antibodies diluted in IF incubation solution were then transferred to the coverslips and left for 1h, at RT. Afterwards nuclei were stained with TO-PRO-3 (Molecular Probes, Invitrogen) 1/6000 in PBS for 10 min, at RT. Coverslips were washed three times with PBS and mounted with anti-fading immunofluore mounting medium (ICN Biomedicals, USA). Samples were stored at 4°C for 12-24 hours in darkness conditions until the mounting media was dry. Coverslips were observed using a Leica Confocal microscope, or a Karl Zeiss LSM microscope. Photographs were taken using Leica or Karl Zeiss specific camera and software.

Primary antibodies were used at the following dilutions:

-Antibody against Cx32 106-124 (Sigma, C3595): 1/500

-Antibody against HPC-I (Syntaxin 1) (Sigma, S0664): 1/500-1/1000

-Antibody against syntaxin (abcam): 1/500-1/1000

-Antibody against Cx32 monoclonal (Zymed 13-8200 and 35-8900): 1/300

-Antibody against Cx32 polyclonal (Zymed 71-0600)

-Antibody against Cx29 (Zymed, 34-4200): 1/100

-Antibody against Cx43 polyclonal: 1/500

-Antibody against Cx43 monoclonal: 1/100-1/200

-Antibody against $Na_v1.6$ (Sigma, S0438): 1/100

8.3 Immunofluorescence on cells

Cells (cultured Schwann cells or HeLa cells) grown on coverslips were rinsed twice with PBS and fixed with ice cold ethanol for 10 min. Afterwards, coverslips were washed again twice with ethanol and blocked with a PBS solution containing 5% NGS, 5% BSA and 0.1% Triton X-100, 1h at RT. After that the blocking solution was removed and fresh blocking solution with primary antibodies was added for 1h 30 min at RT or ON at 4°C. Coverslips were then washed three times with PBS for 10 min and incubated with secondary antibody diluted in blocking solution. Coverslips were washed again in PBS three times for 10 min, rinsed with ultrapure water and dried before mounted with permafluor mounting media (Immunotech, Beckman coulter company) and stored at 4°C in darkness conditions, at least for 24 h, before observed on LSM or fluorescence microscope.

Primary antibodies were used at the following dilutions:

-Antibody against Cx29 (Zymed, 34-4200): 1/100

-Antibody against Cx32 monoclonal (Zymed 13-8200 and 35-8900): 1/300

-Antibody against Cx43 polyclonal: 1/500

-Antibody against Cx43 monoclonal: 1/100-1/200

9 Cx32 Constructs

9.1 hCx32 mutant generation by PCR

Starting with the hCx32 inserted in pBxG used to obtain cRNA to inject oocytes, and following a two step PCR strategy we generated the desired following hCx32 mutant sequences: WT, S26L, P87A, Del111-16, D178Y and R220St.

We designed the primers to introduce the mutations we wanted as well as a new restriction site to have a preliminar and quick identification method for each construct (*table 1*).

PRIMER	SEQUENCE	ENZIME
Cx32_all_for	5' CGG**GGTACC**GGGACAAC 3	Acc65I
Cx32_all_rev	3' CGCTGCTCGGCCTGC**TGA**TGC**CGCCGGCG**TAAGAATA 5'	NotI
Cx32_S26L_for	5' CGAGTATGGCT**ACTAGT**CATCTTC 3'	SpeI
Cx32_S26L_rev	3' GCTCATACCGA**TGATCA**GTAGAAG 5'	SpeI
Cx32_P87A_for	5' CTAGTTTCCA**CAGCTG**CTCTCCTC 3'	PvuII
Cx32_P87A_rev	3' GATCAAAGGT**GTCGAC**GAGAGGAG	PvuII
Cx32_Del111-16_for	5' CGGCTTGA**AGGCCT**GGAGGAGGTGAAGAGGCAC 3'	StuI
Cx32_Del111-16_rev	3' CTTTTACGATGCCGAACT**TCCGGA**CCTCCTCCAC 5'	StuI
Cx32_D178Y_for	5' CCCAACACAG**TGTACT**GCTTCGTG 3'	TatI
Cx32_D178Y_rev	3' GGGTTGTGTC**ACATGA**CGAAGCAC 5'	TatI
Cx32_R220St_for	5' GCCTGTGCCCGCT**AGTACT**AGCGCCGC 3'	ScaI
Cx32_R220St_rev	3' CGGACACGGGCGA**TCATGA**TCGCGGCG 5'	ScaI

Table 1 **|** Table displaying all the designed primers to generate the hCx32 constructs containing the mutations and a new restriction site enzyme.

This first set of primers was used for the first PCR. For the second PCR, the general carboxyl and amino terminal primers (all_for and all_rev) were used together with the first PCR products as templates to generate the final constructs (*table 2*). Due to the primers design all constructs will have the same Carboxyl and amino terminal ends, which can be cut with the

restriction enzymes Acc65I (C-terminus) and Not I (N-terminus).

PCRs	WT	S26L	P87A	Del111-16	D178Y	R220Sl
Ia	X	All_for S26L_rev	All_for P87A_rev	All_for Del111-16_rev	All_for D178Y_rev	All_for R220Sl_rev
Ib	X	S26L_for All_rev	P87A_for All_rev	Del111-16_for All_rev	D178Y_for All_rev	R220Sl_for All_rev
II	All_For All_rev	All_For All_rev	All_For All_rev	All_For All_rev	All_For All_rev	All_For All_rev

Table 2 **|** Table with the PCR performed to obtain hCx32 sequences with the desired mutations. Red: first set of PCRs. Blue: second set of PCRs performed with the indicated primers and the products of the first PCRs.

Once the PCRs were performed the products were electrophoresed in an 0.8% agarose gel and DNA bands with the expected size were cut off and purified using a DNA purification Kit for Agarose embedded DNA (Bioclean, Biotools), and finally DNA was resuspended in 20µl of ultrapure water.

9.2 Clone Cx32 mutants in pBSK.

The commercial vector pBSKII (stratagene, *Figure M9-1*) was digested with Acc65I and Not I to generate sticky end to insert the constructs. After this digestion an agarose gel was run and the band containing the vector was cut out and purified using the same kit as described before. In order to avoid self religation of empty vector the ends were dephosphorilated using SAP enzyme. Briefly, the digested vector was incubated in SAP enzyme for 45min, the enzyme was inactivated with 15min at 65°C.

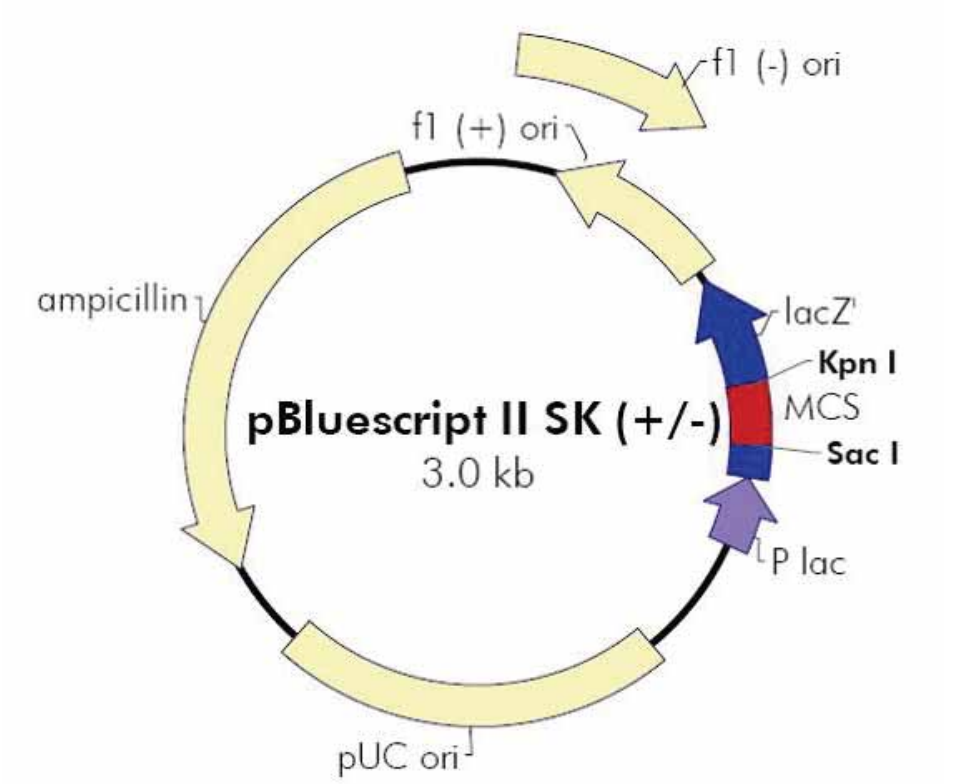

Figure M9-1 **|** The comercial vector pBSKII from Stratagene. MCS: Multiple cloning site, the NotI and Acc65I restriction site used are located in this region.

Once the vector was ready to bind the inserts, ligations were performed. Each insert was mixed with digested and dephosphorilated pBSK vector in two different ratios vector:insert (1:7 and 1:10), and left for more than 2 hours at RT in presence of ligase enzyme. Afterwards, ligation products were transformed into competent *E.coli*. Briefly, each ligation was added into one competent bacteria aliquot on ice for 30min and heat shocked for 45 s at 65°C. After that, aliquots were placed on ice again for 2min before fresh LB medium was added. Bacteria were then incubated at 37°C with continuous shacking for 30 min-1h and seeded on LB 50µg/ml ampicillin supplemented Agar plates. Plates were left ON at 37°C.

9.3 MiniPREPs for hCx32 constructs.

From each hCx32 mutation a variable number of transformed colonies grown on LB ampicillin plates were picked and further grown in 3 ml LB ampicillin ON at 37°C. 1.5 ml of grown cultures were centrifuged and pellets were resuspended with 100 µl of alkaline solution 1 supplemented with 1 µl/ml RNAse 2000 (New England Biolabs, UK). After 2 min at RT, 200 µl of alkaline solution 2 was added, all was mixed and left for 2 min more at RT. Finally 150 µl alkaline solution 3 was added and mixed and centrifuged for 10 min at 12,000 rpm (eppendorf 5417R centrifuge). Supernatants were transferred to new eppendorf tubes containing 500 µl of absolute ethanol. After mixing, samples were centrifuged again for 6 min at 12,500 rpm. Pellets were washed with 70% ethanol air dried. Dried pellets were resuspended with 50-100 µl of ultrapure water. MiniPREPs were stored at 20°C until used.

To check if vectors had an insert, miniPREPs were digested with Pst I restriction enzyme and ran in a 0.8% agarose gel. Those positive clones were further tested by digestion with the specific restriction enzymes for the newly generated restriction sites of each mutant. The best clone for each mutation and for hCx32WT insert was selected to perform the MidiPREPS.

9.4 MidiPREPs to obtain hCx32 constructs in pBSK.

The best MiniPREP clone for each construct was selected and grown further in 50 ml LB ampicillin ON at 37°C. Grown cultures were transfered to falcons and centrifuged 5 min at 8,500rpm

(Beckman J2-HS centrifuge). From that point the instructions for the Jet Star Kit, the novel plasmid purification system (Genomed, USA) were followed. The final pellet was resuspended with 100 µl of ultrapure water. Each MidiPrep was digested with the corresponding restriction enzymes, checked by electrophoresis on 0.8% agarose gels and sequenced (Agowa, Germany). MidiPREPs were stored at -20°C when not in use.

9.5 Bacterial glycerol stocks of hCx32 constructs.

The selected colonies were stored in glycerol after checking the correct sequence of respective plasmids. To do that, new LB ampicillin cultures of bacteria containing the appropriated plasmids were grown ON at 37°C. 850 µl of each culture and 150 µl of glycerol were mixed in an eppendorf tube and immediately frozen in liquid Nitrogen. Eppendorfs containing glycerol stocks were then stored at -80°C.

9.6 Cloning the hCx32 mutations and wt in pMJgreen vector.

To clone all the hCx32 constructs (wt, S26L, P87A, Del111-16, D178Y and R200St) in a new pMJgreen plasmid (*Figure M9-2*) for eukaryotic expression, all MidiPREPs of PBSK constructs with the different hCx32 inserts and a MidiPREP of the empty pMJgreen vector were digested with Acc65I and NotI restriction enzymes.

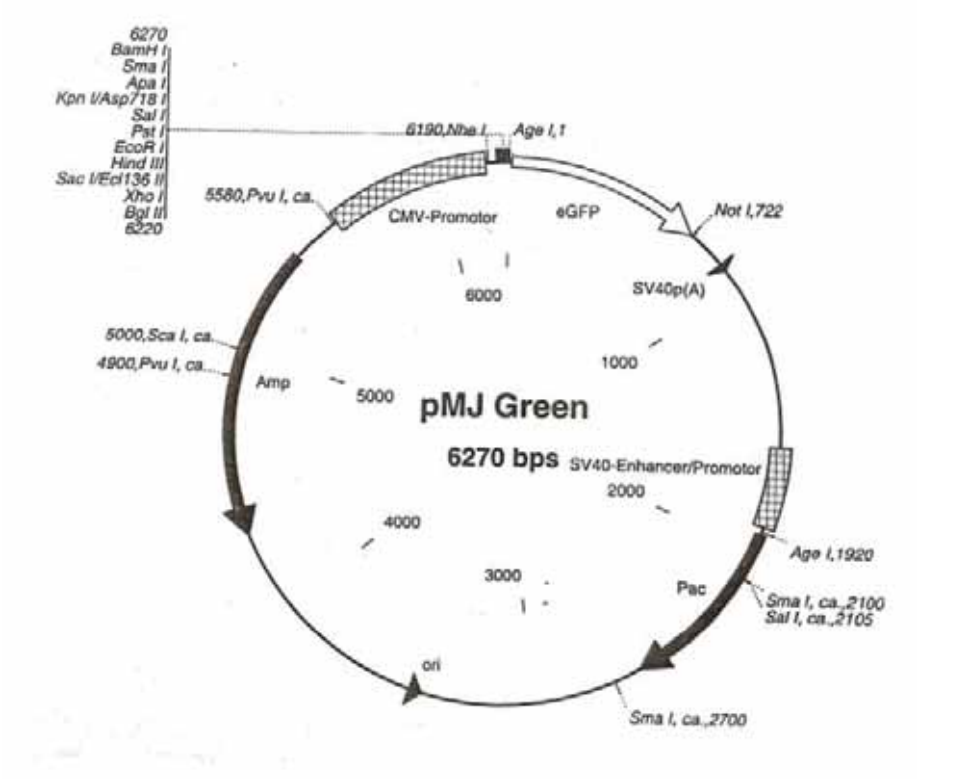

***Figure M9-2* | Restriction map of the pMJgreen vector.** It contains the human CMV promoter for eukaryotic expression and the green fluorescent protein (GFP) sequence, to easy identify transfected cells. In our case we removed this sequence and had no GFP expression when hCx32 constructs were inserted.

After this digestion, inserts were liberated from the pBSK vector and pMJgreen was liniarized with the right sticky ends for an easy ligation with the inserts. Then, pMJgreen was also treated with SAP enzyme as described before and ligation of the hCx32 inserts with pMJgreen vector was also performed as described above. Ligation products were transformed into *E.coli* competent bacteria and seeded on LB ampicillin agar plates. clones obtained were processed as described before. First Mini PREPs were performed, and after checking the sequence of each clone with restriction enzymes, the best clone was used to make MidiPREPs of each hCx32 construct in the new vector pMJgreen. Those Midis were also checked by enzymatic restriction and

those clones with expected digestion fragments were sequenced. Midis were stored at -20°C and glycerol stocks were also made (see section 9.5) and stored at -80°C.

9.7 Cloning the hCx32 mutations and wt in PBxG vector

To clone all the hCx32 constructs (wt, S26L, P87A, Del111-16, D178Y and R200St) in the pBxG plasmid (*Figure M9-3*) to express them in *Xenopus* oocytes, a similar the procedure to clone them in pMJgreen was used with some variations. First, empty pBxG vector was liniarized using StuI restriction enzyme and treated with SAP enzyme.

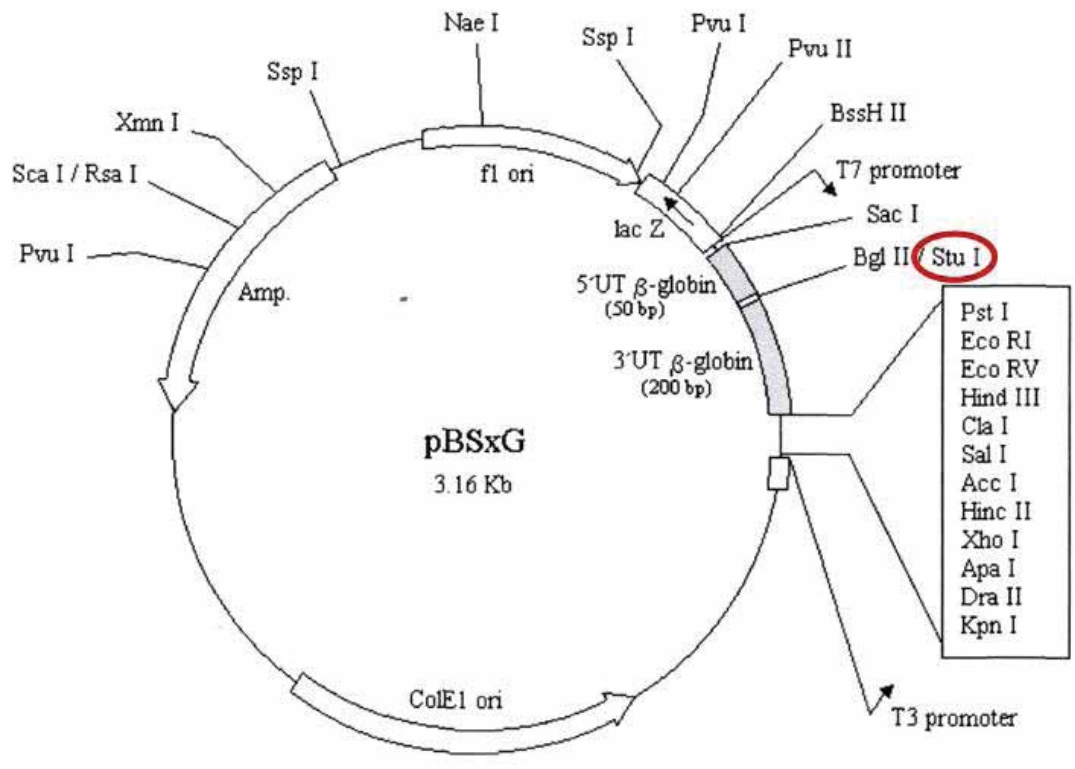

***Figure M9-3* | Restriction map of the pBxG vector.** It contains the *Xenopus* β-globin sequence to enhance the translation of inserted proteins in *Xenopus* oocytes and the T7 and T3 promoter for *in vitro* transcription. The signalled StuI restriction site was used to insert our constructs, in the right orientation to be transcripted by T7 polymerase.

At the same time, all constructs inserted in pBSK were digested with Acc65I and NotI. As StuI is a blunt cutter, once inserts were digested the sticky ends were blunted with Klenow enzyme, which adds nucleotides to single strand DNA ends. Ligations were performed as described above and the inserts ligated to the new vector were transformed into *E.coli* competent bacteria. MiniPREPs from the resulting clones were performed also as described above and were digested first with PstI to check the insert presence and also the direction of insertion. Insert and vector ends were blunt constructs and had two possible insertion directions. We were only interested on one direction, the one that allowed us to use the T7 polymerase to transcribe them into cRNA (to inject them into *Xenopus* oocytes), so only clones with the correct direction were digested further to test the different mutations. As shown before, the best clones were chosen to perform MidiPREPs and glycerol stocks.

9.8 Competent bacteria

To obtain *E.coli* bacteria in a competent state a new *E.coli* aliquot was thaw and seeded in a LB agar plate ON at 37°C. Two clones were picked up and grown further on 2 ml LB media each, ON at 37°C. 200 µl of a grown culture were transferred to an Erlenmeyer containing 100 ml of 20 mM $MgSO_4$ in LB media. Bacteria were allowed to grow at 37°C until the culture optic density was between 0.4 and 0.6 (about 4h). From this moment on all steps were performed at 4°C. Bacteria were centrifuged at 5,000rpm, for 5 min. The pellet was resuspended with 10 ml ice

cold TBF I and kept on ice for 10 min. Then it was centrifuged again at 5,000rpm for 5 min, resuspended with 2 ml cold TBF II and kept on ice for 20 min. Finally, the new competent bacteria were aliquoted in eppendorf tubes (100 µl/ aliquot) and quickly frozen in liquid Nitrogen. Aliquots were stored at -80°C until used.

10. Stable transfections in HeLa cells

To obtain a stable transfection for hCx32WT, hCx32S26L and hCx32P87A, first, 5.8µg DNA of each construct (on pMJgreen vector) were liniarized by digesting with Sca I. This procedure was identical for the three different constructs of hCx32.

For this transfection HeLa cells were used. HeLa cells can divide an unlimited number of times in a laboratory cell culture plate and proliferate abnormally rapidly, even compared to other cancer cells. Moreover, they naturally have a very low connexin expression.

HeLa cells, grown in 10 cm diameter culture plates up to 50-80% confluence, were transfected using Lipofectamine 2000 (invitrogen, 11668-027) and following the instruction manual. After 48-72 hours of transfection, cells were splitted and resuspended in a selective medium (normal HeLa medium supplemented with 0.5 µg/ ml puromycin). Cells were diluted at 1:3, 1:5, 1:10 and 1:20 and seeded on new 10 cm diameter culture plates with selective media. Selective media was changed every 48-72 hours and clones were allowed to grow. Clones

were picked up and placed on 48 well plates (1 clone per well). Each clone was splitted from one 48 well plate to two 24 wells plates (one with coverslip). The presence of hCx32 on cells on coverslips was tested by immunofluorescence. Two clones with high expression of hCx32 were selected for each construct and split to wells from a 12 wells plate, then to a well from a 6 well plate and finally to a 10 cm diameter culture plate. An aliquot of each clone was frozen and stored in liquid nitrogen.

11. Cell culture

11.1 HeLa cells culture.

HeLa cell line was kindly provided by Dr. Klaus Willecke, from *Rheinische Friedrich-Wilhelms-Universität Bonn*, Institut für Genetik, Bonn, Germany. For more information about this cell line see section 10 on materials and methods.

HeLa cell line cultures are easy to maintain and grow. Cells were splitted every 3 or 4 days and maintained using DEMEM media (Sigma, D-6046) supplemented with 10% FBS (Biological Industries, 04007-1A) and 1% Penicillin/Streptomycin (Sigma, P-0781).

11.2 Scwhann cell primary culture

Schwann cell primary cultures were grown using a modification of Brokes method [197], which is based on culturing Schwann cells from adult peripheral nerve. We did our cultures according to Dr. Conxi Lázaro group, from the department of

Genetics, Hospital Duran i Reynals - IDIBELL, Barcelona, Spain [198, 199]. The method is based on Schwann cell cultures from human schwannomas, adapted to Mice sciatic nerve Schwann cells from Swiss CD1, male mice (20 g body weight).

11.2.1 Extraction & Pre-incubation.

Mice Schwann cells for primary cultures were obtained from sciatic nerves. Sciatic nerves from each limb of 12 mice were extracted as described before (7.1 on materials and methods) and placed on Petri dishes with basal growth media for Schwann cells (DEMEM supplemented with 10% FBS and 1% penicillin/Streptomycin, DMEM was commercially enriched with glucose/glutamine/pyruvate, GIBCO, 41966-029), and pre-incubated on a incubator at 37°C, 10% CO_2 for 3 to 5 days. During this period of time, the plates were not removed from the incubator to check the cell growth. The best results are obtained when the preparations are not submitted to any vibration or gentle movement.

11.2.2 Coating culture plates.

Before plating, cell culture plates have to be coated. With this aim, 0.1 mg/ml poly-L-Lisine (Sigma, P-1524) solution was prepared from a stock solution (10 mg/ml) in PBS and filtered with 0.45 µm pore filter (Millex HA SLHA033SS, Millipore). Poly-l-lisine concentration was raised to 1 mg/ml if cells had to be seeded on cleaned glass circular coverslips. The poly-L-Lisine solution was placed on 12 wells from a 24 wells plates, covering

the entire bottom, and was left for 1 hour at RT. Poli-L-Lisine was recovered and wells were washed twice with PBS before adding a 4 µg/ml of laminin solution. Laminin stock solution was diluted in PBS to 4 µg/ml and also filtered with a 0.45 µm pore filter before placing it on the culture wells. Laminin was left on culture wells for 4 hours, at RT or ON, at 4°C. After that, laminin was recovered and wells were washed twice with PBS and left with PBS at 4°C until the time to plate cells. Coating only lasts for a few days.

11.2.3 Digestion & plating.

Media from Petri dishes containing pre-incubating sciatic nerves was removed and nerves were disaggregated with sterile scalpel blades. Once properly disaggregated 1 ml basal growth media containing enzymes 0.8-1U Dispase I (Roche 210-455 or Sigma, D-4818) and 160 U Collagenase 1A (Sigma, C-0130) was added and left for 1 hour in the incubator (37°C, 10% CO_2). Tissue was further disrupted with suction through a glass Pasteur pipette and placed it in a centrifuge tube. After 5 min, 1,500 rpm centrifugation (Hermle Z383) the supernatant was discarded and the Pellet was resuspended with complete GFM media (Basal Growth media supplemented with 0.5 µM Forskolin (Sigma, F-6886), 0.5 mM IBMX (Sigma, I-7018), 2.5 µg/ml Insulin (Sigma, I-5500) and 10 nM Herregulin β (R&D systems, 396-HB)), and placed in coated culture wells. Plates with seeded cultures were placed on the incubator at 37°C, 10% CO_2.

11.2.4 Schwann cell maintenance.

Schwann cell medium had to be changed according to a certain cycle which implied two "pulses" of 24 hours with Forskolin each week and the rest of the time the media was only enriched with growth factors and IBMX. New cultures were plated preferentially on Monday or Thursday as they are seeded in GFM media. The cycle goes as described in *table 3*:

Monday	Tuesday	Wednesday	Thursday	Friday	Saturday	Sunday
GFM	**GFM-F_o**	X	**GFM**	**GFM-F_o**	X	X

Table 3 **|** schedule for Schwann cells medium changes. The cells were supplemented with forskolin for 24 hours twice a week, every Monday and Thursday.

11.2.5 Harvesting Schwann cells

Once grown, Schwann cells were split only once, to obtain a higher amount of cells. Splitting them more than once lead them to stagnate and finally to cell death.

Schwann cells were splitted similarly to other cell line. Cells were treated with typsin (Sigma) for 1-1.5 minutes and centrifuged 5 min at 800 rpm. Pellets were resuspended with fresh complete GFM media and plated on new coated wells.

11.2.6 Freeze Schwann cells or sciatic nerves for Schwann cell culture

To freeze Schwann cells they were first trypsinized and centrifuged. (To freeze whole sciatic nerves preincubated with basal growth media they were only centrifuged). Pellets were

resuspended with 1 ml basal growth medium supplemented with 40% FBS and 10% DMSO. All was quickly mixed and placed on an isopropanol surrounded freezing plate. Samples were left at -80°C for 24 hours, and then transferred to liquid nitrogen for a long term storage.

12. Hypotonicity and ATP release assay

12.1 Assays on Schwann cells

For ATP release in response to hypotonicity assay, confluent Schwann cells were grown on 24 well plates. The Medium of these cells was changed to isotonic buffer 4 hours prior to experiments. Just before experiments, this solution was removed and 250 µl of fresh isotonic buffer were added. Luciferin and luciferase were mixed (100 µl luciferase + 30 µl luciferin) and 40 µl of the mixture were added to each well containing cells. Plates were then inserted into the microplate reader (Fluostar Optima, BMG) and the following program was runned: Luminiscence was read every 4 seconds, with a total number of 75 readings per well (5 minutes/well). At second 40, 250 µl of either isotonic, 280-290 mosm (controls) or Na^+ free solution, 27 mosm (hypotonic shock) were injected. To quantify the amount of ATP released the same protocol was performed, and known amounts of ATP were injected to wells containing the concentration of luciferin-luciferase used in cell containing wells. The resulting regression straight line was used to interpolate the results obtained in cell containing wells.

To obtain ATP fmols/10^4 cells the number of cells per well had to be calculated. To do that, five different microscope fields were photographed and cells were counted using Image J (NIH, USA). The mean value obtained on each well was used to calculate the total number of cells per well, using known areas from microscope field (at 200x) and surface of wells (from 12 and 42 wells plates).

12.2 Assays on HeLa cells

HeLa cells were grown on 12 or 24 well plates until 70-90% confluence. At that point, the media was removed and cells were washed with PBS and left in the incubator at 37°C, 5% CO_2 for 4 h with isotonic buffer (280-290 mosm). Just before experiments this solution was removed and 250 µl of fresh isotonic buffer were added. Luciferin and luciferase were mixed (100 µl luciferase + 30 µl luciferin) and 40 µl of mixture were added to each well containing cells. Plates were inserted to the plate reader machine and the same program used for Schwann cells was runned. ATP controls were also obtained the same way.

Total number of cells per well were calculated as for Schwann cells (see 12.1 in this section).

12.2.1 Assays on HeLa cells transfected with S1A

HeLa cells were grown on 12 wells culture plates until 50-70% confluence and transfected with S1A (in pDsred plasmid, inserted after the CMV promoter, *Figure M12-1*) following the lipofectamine 2000 commercial protocol (Invitrogen, 11668-027).

Briefly, 0,8 µg S1A DNA/well and 2 µl/well Lipofectamine were separately mixed with OptiMEM (Gibco, 31985) to a final volume of 50 µl/well and left for 5 minutes at RT. Both solutions were mixed and left again for 25 minutes at RT before placing 100 µl/well for transfection. After 4-6 hours the media was changed to normal media again and left ON in the incubator at 37°C, 5%CO_2. The next day assays were performed as described above.

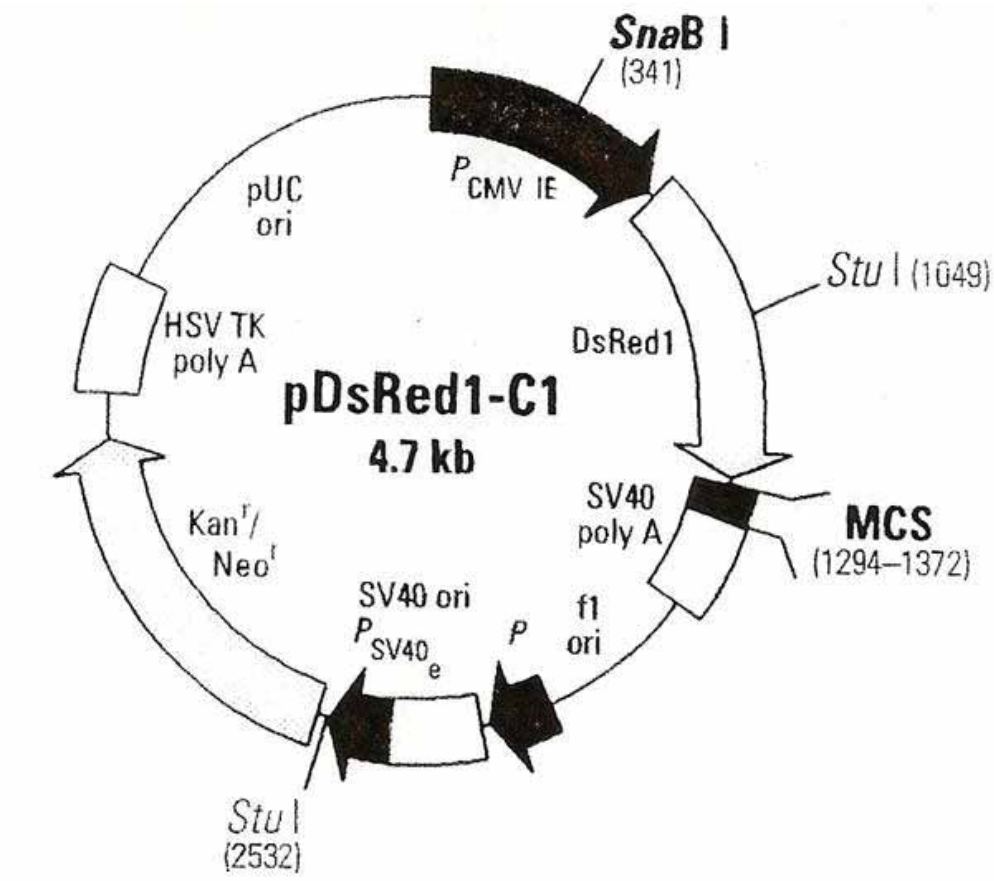

Figure M12-1 **| Restriction map of the pDsRed1 vector.** It contains the CMV promoter for eukaryotic protein expression, the pDsRed sequence that codifies for a red fluorescent protein, and afterwards a multiple cloning site (MCS) to clone the desired sequence (in this case the syntaxin 1A sequence) and obtain a fusion protein with the red protein, that is easy to identify using a fluorescence microscope.

12.2.2 Assays on HeLa cells treated with Brefeldin A

These assays were performed similarly to those described in the section 12.2 on materials and methods with the difference that the isotonic buffer added to the cultures 4 h before the hypotonic shock contained 5 μM Brefeldin A, a drug that disrupts the Golgi apparatus and blocks exocytosis.

RESULTS

1. Cx32, Syntaxin 1A & ATP RELEASE

1.1 hCx32 and S1A cRNA obtention. TEVC: Cx32 hemichannels & ATP release

1.1.1 hCx32 and S1A cRNA obtention

In order to express foreign proteins in *Xenopus laevis* oocytes we have first obtained the cRNA to express these proteins (hCx32 and S1A). The hCx32 cDNA sequence cloned in the Xenopus pBxG plasmid for Xenopus oocyte improved expression was obtained from Dr. Luis C. Barrio, Hospital Ramón y Cajal, Madrid, Spain. S1A cDNA sequence inserted in pGEM t-easy vector had previously been obtained in our laboratory. Using the molecular biology techniques described in materials and methods section (section 2.2) cRNA for these proteins was transcribed from the cDNA. The cRNA of hCx32 was about 1000 bp long and the cRNA of S1A was about 2000 bp.

cRNAs were injected into *Xenopus* oocytes 48-72h prior to electrophysiological recordings together with the antisense oligonucleotide for Cx38 (ASCx38) to abolish the possible currents generated by the endogenous *Xenopus* connexin.

1.1.2 TEVC recordings and ATP release through Cx32

In order to study the activity of hCx32 hemichannels expressed in *Xenopus* oocytes after a depolarizing stimulus, we have used the Two Electrode Voltage Clamp technique as described in section 4 in materials and methods. We applied a voltage protocol designed to depolarize the plasma membrane for 30s [22]. The resting membrane potential of oocytes was fixed

at -40mV. We switched up to +80mV for 30s and then went back to -40mV. In oocytes injected with hCx32, while the plasma membrane was depolarized there was an outward current with an increasing amplitude respect time, at 30 s the mean amplitude was of 1041.35±81.81 nA, n=135. When voltage went back to resting potential we recorded a transient tail current, with an amplitude of -387.1±46.32 nA, n=68.

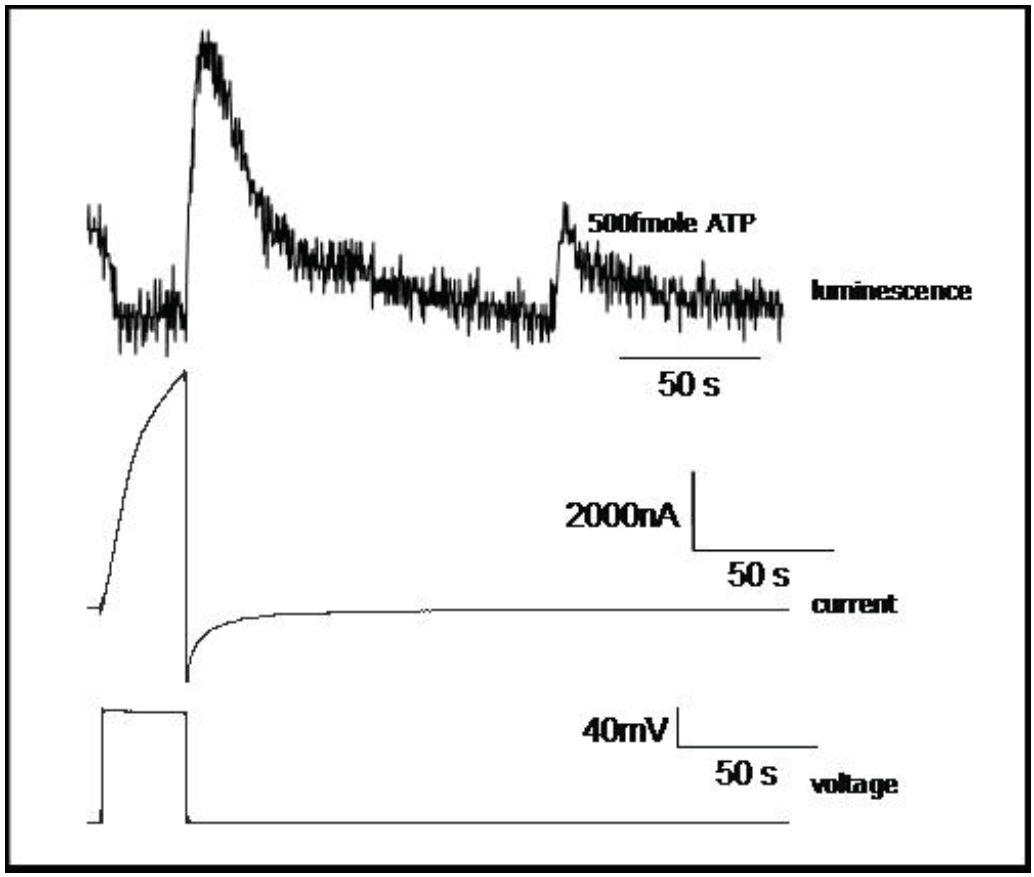

Figure R1-1 **| Cx32 expression and ATP release.** Oocytes injected with cRNA **Cx32** and **AsCx38.** While applying a depolarizing pulse from -40mV up to +80 mV a slow activation outward current is generated but no ATP release is detected. However, when the oocyte is repolarized a tail current is activated, which is associated with the release of ATP from the oocyte. An addition of 500 fmole of ATP is shown and reveals the efficiency of the luminescent reaction.

During the resting conditions and in the depolarizing phase no significant increase of light (produced by release of ATP) was

recorded. However, during the time of activation of the tail current, a peak of light was recorded, indicating the release of ATP. The amount of ATP released was 274.97±88.55 fmole, n=16 (*Figure R1-1*).

When the oocytes were bathed with the ringer solution with luciferin-luciferase, we recorded an image of the release of ATP in a single oocyte, after being stimulated with a depolarization pulse. The light was spread evenly over all the surface of the oocyte, indicating that the sites of release were distributed homogenously on the plasma membrane and no significant differences between the animal and vegetal poles were observed (*Figure R1-2*).

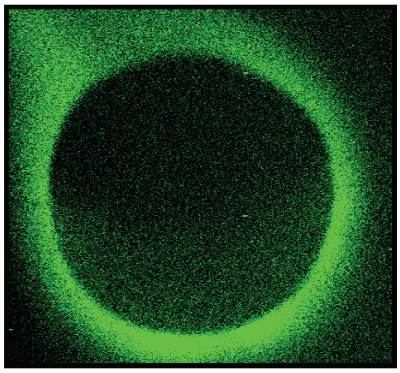

Figure R1-2 **|** An image of luciferin-luciferase luminescence due to the ATP release from a single oocyte. The light was captured with a cooled Hamamatsu camera and modified with Aquacosmos software.

To relate recorded tail currents due to hCx32 activation and ATP release, the areas from the tail currents and ATP release were analyzed. ATP release was quantified calculating the area of the recorded ATP related to the area of the exogenous (and known) amount of ATP that was added after each TEVC record. There is a lineal relation between the electric charge supported by the tail current and the amount of ATP released. So the bigger charge related with the tail current, corresponds to a greater amount of ATP released. (*Figure R1-3*)

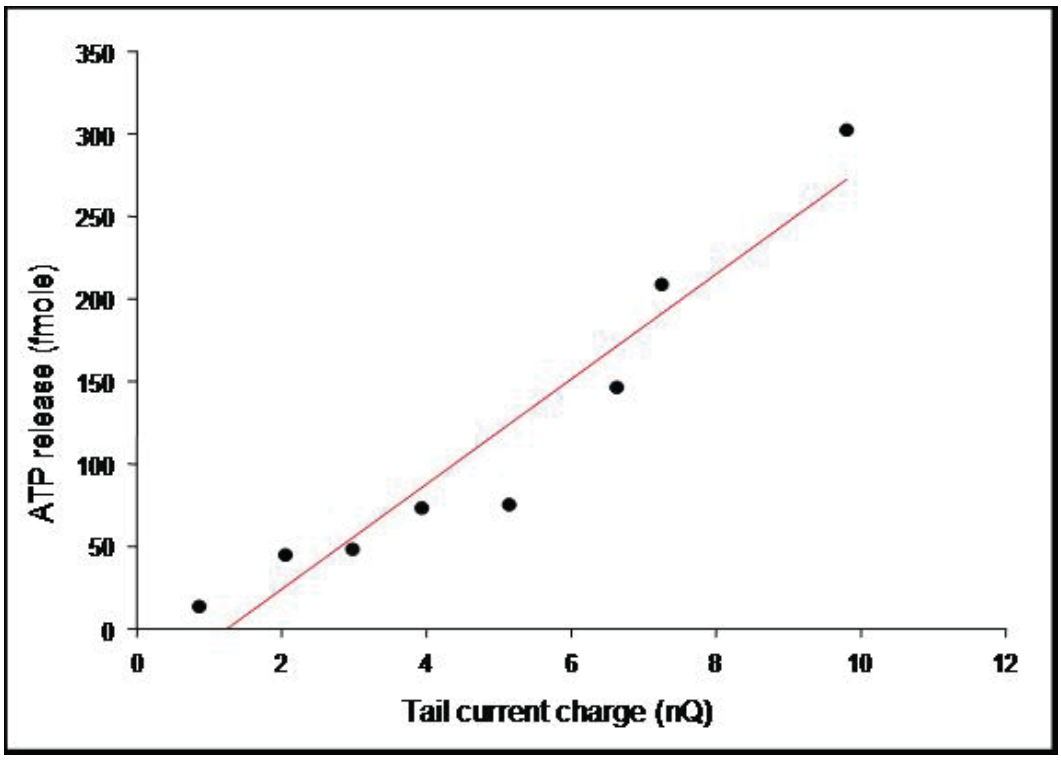

***Figure R1-3* | ATP vs. Tail Current correlation.** Currents recorded on hCX32 expressing oocytes were related to the ATP release value from each register. The greater the recorded current, the greater the ATP release. Thus ATP release, and the tail current, depends of the amplitude of current generated by Cx32 hemichannels. r^2=0.96.

Moreover, deconvoluting the light signal, we observed that the time course of the tail current and the time course of ATP release are synchronized and coincident (*Figure R1-4*). The deonconvolution was performed by Dr. Rafel Puchal, Dep. of Nuclear medicine, Hospital Universitari de Bellvitge, Hospitalet de Llobregat, Spain, as described in materials and methods (section 5.3)

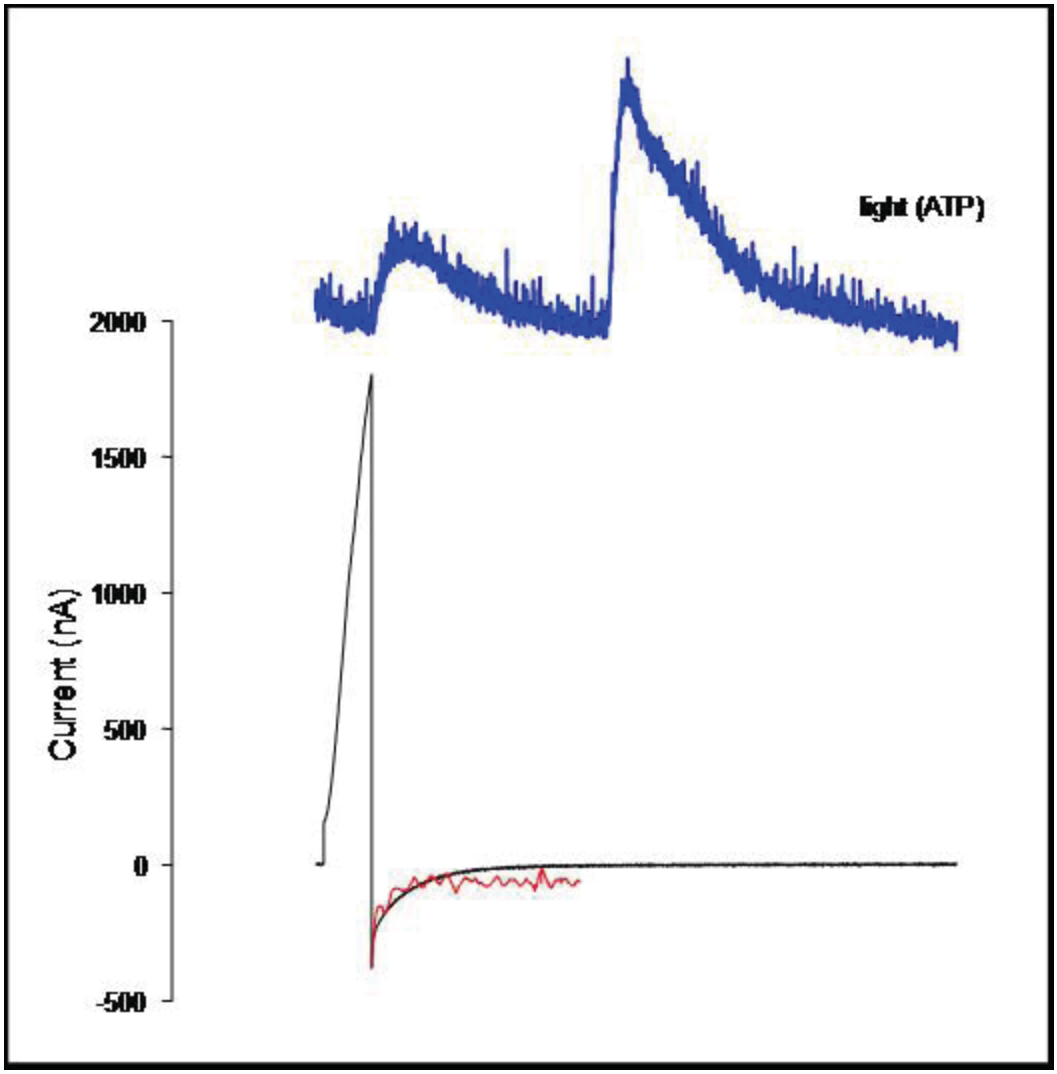

Figure R1-4 **|** Deconvoluted image of the light signal (red line), notice that the time course of the tail current and the ATP released are coincident.

When we applied the same voltage protocol to oocytes injected only with ASCx38 we did not detect any significant outward current in response to depolarization, neither could we detect any tail current during the repolarizing phase, and no ATP release was detected. So ATP was released through hCx32 hemichannels expressed on the plasma membrane of *Xenopus* oocytes. (*Figure R1-5*).

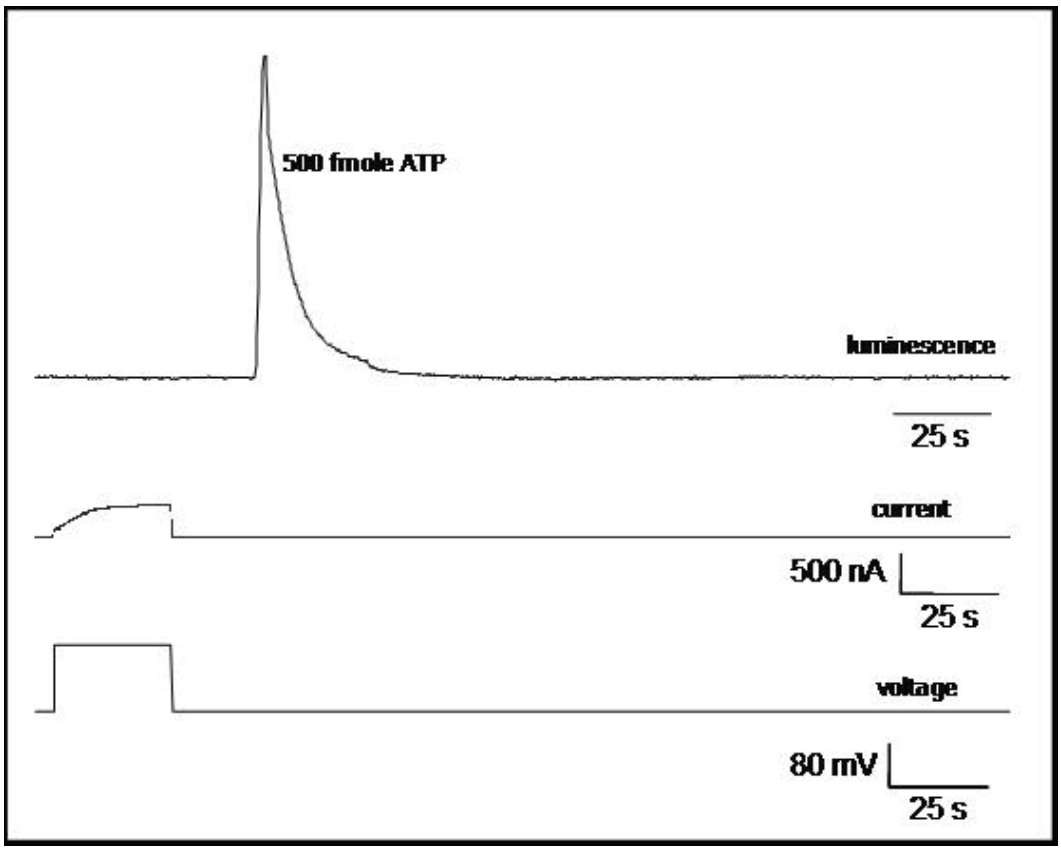

***Figure R1-5* | AsCx38 injected oocyte.** Ionic currents supported by *Xenopus* endogenous Cx38 were abolished injecting antisense oligonucleotide (AsCx38). ATP release was neither detected during stimulation nor afterwards. In order to test the Luciferin-Luciferase reaction 500 fmoles of ATP were added as a standart after the stimulation.

1.2 Effect of S1A on Cx32 dependent ionic currents and ATP release

1.2.1. S1A interferes with Cx32 supported ionic currents and ATP release.

The same experiments as described before were repeated injecting hCx32 and S1A cRNA as well as ASCx38 to *Xenopus* oocytes. The same depolarizing protocol was applied to those oocytes, and ATP release was monitored the same way. The results show us also an unspecific outward current and a tail

current related to ATP release, but the currents and, specially the ATP release, were lower than in oocytes injected only with hCx32 cRNA (*Figure R1-6*).

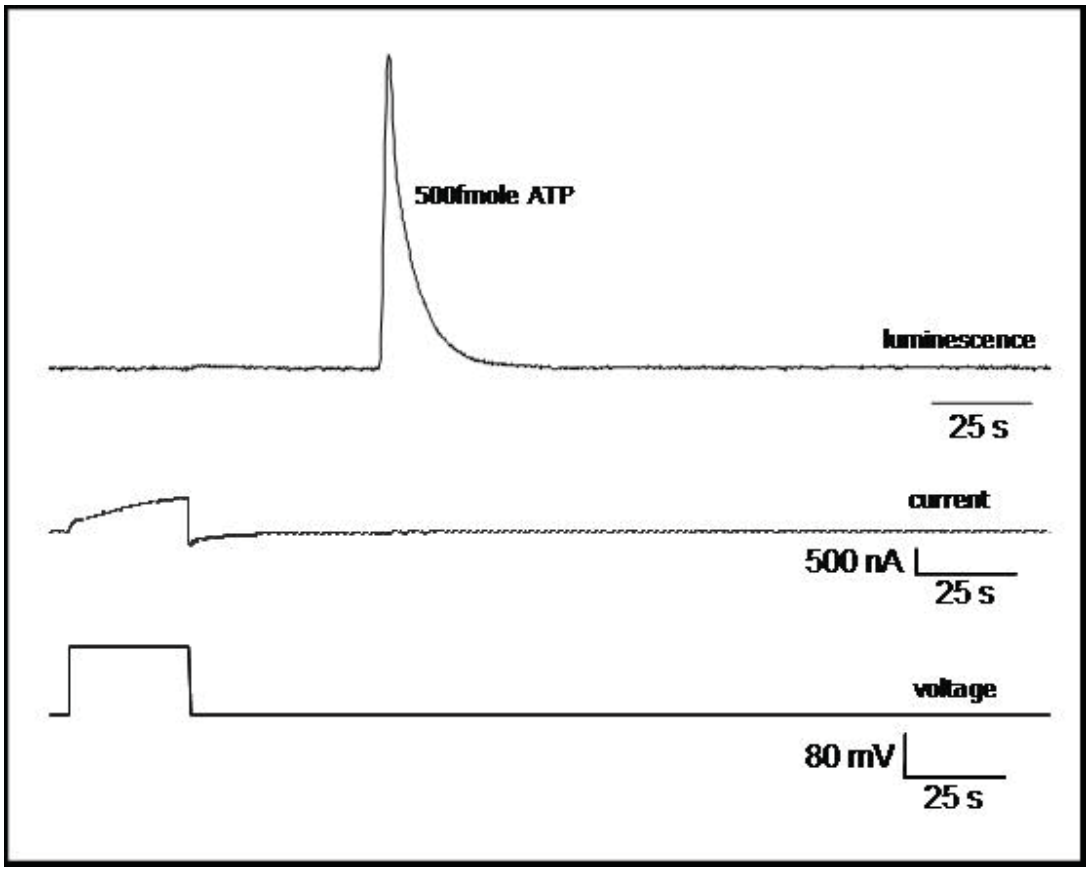

***Figure R1-6* | ATP release from Cx32 and S1A expressing oocytes.** Oocytes injected with Cx32 & S1A cRNA and AsCx38. After the depolarizing pulse both currents and ATP release were inhibited. Again, 500 fmole of exogenous ATP show the luminescent reaction sensitivity. The ATP released was lower than on hCx32 injected oocytes

We analyzed all recordings (n=100) and when were compared to those taken from oocytes injected only with hCx32 we could see partial inhibitions both on currents and on ATP release. Outward currents from oocytes expressing hCx32 and S1A at the same time were 15% lower than currents from hCx32 injected oocytes (*Figure 1-7*). All oocytes were also injected with ASCx38. We used oocytes injected only with ASCx38 as negative

controls.

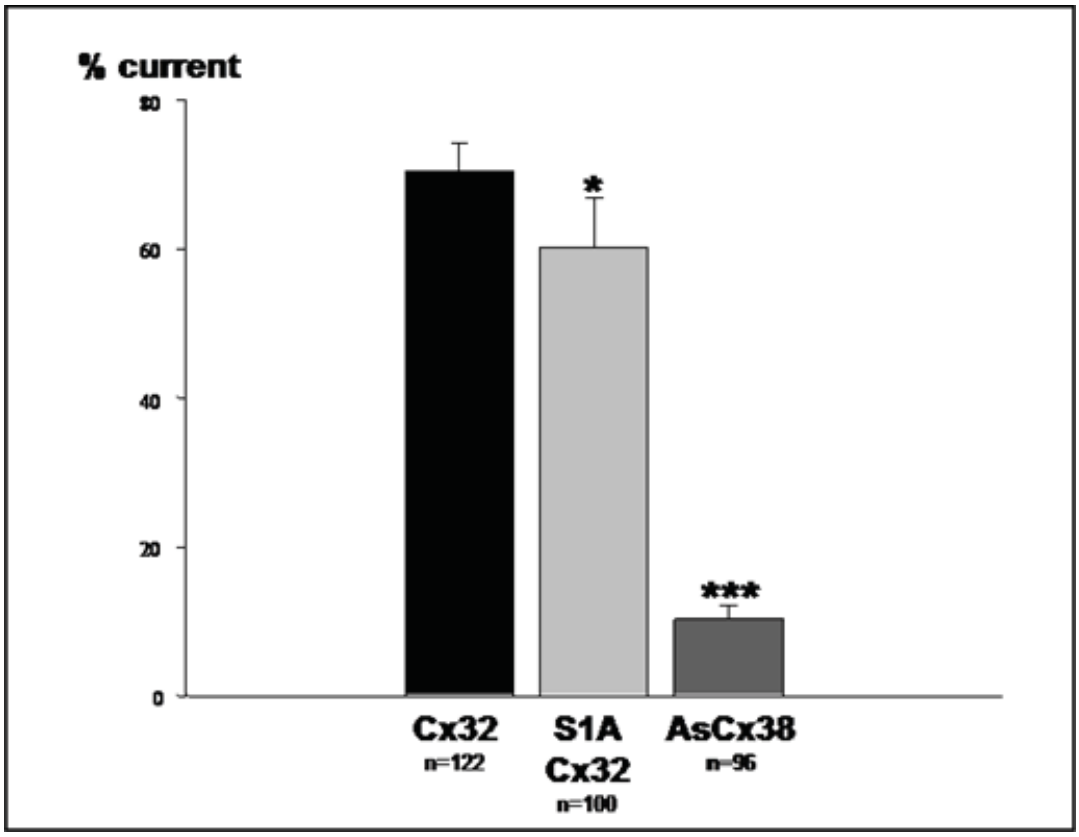

Figure R1-7 **| Histogram of normalized outward currents registered from injected oocytes**. **Cx32**: hCx32 cRNA and AsCx38 injected oocytes; **S1A Cx32**: hCx32, S1A cRNA and AsCx38 injected oocytes; **AsCx38**: AsCx38 injected oocytes. The **Cx32** group exhibited a greater current compared to the control group (**AsCx38**). There was a significant 15% current reduction in **S1A Cx32** group compared to the **Cx32** group. *p<0.05, **p<0.01, ***p<0.005

We had seen a partial inhibition of outward currents of a 15% but when we compared the electric charge from tail currents (related to the ATP release) we saw a 52% inhibition in oocytes injected with hCx32 and S1A compared to those injected only with hCx32 (*Figure R1-8*). Again, all oocytes were also injected with ASCx38 and oocytes injected only with ASCx38 were used as negative controls.

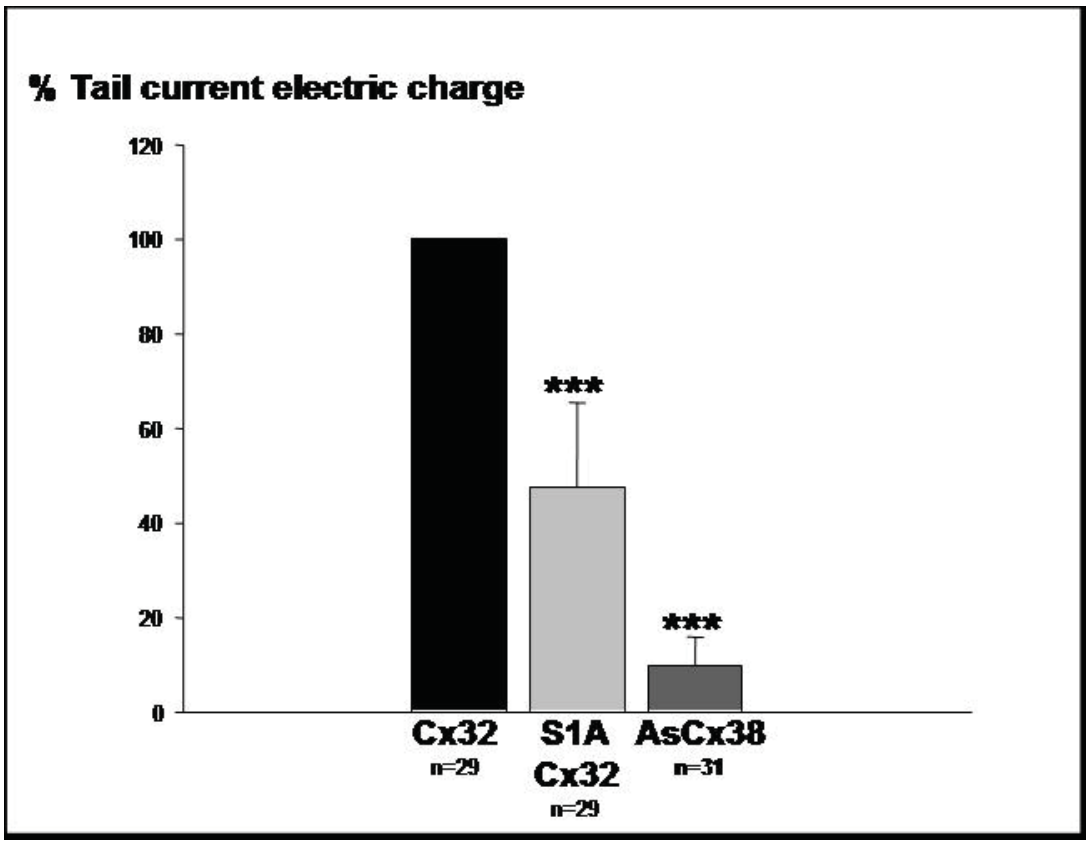

Figure R1-8 **| Histogram of normalized electric charge of tail currents from injected oocytes**. **Cx32**: hCx32 cRNA and AsCx38 injected oocytes; **S1A Cx32**: hCx32, S1A cRNA and AsCx38 injected oocytes; **AsCx38**: AsCx38 injected oocytes. The **Cx32** group exhibited a greater current compared to the control group (**AsCx38**). There was a significant 52% electric charge reduction in **S1A Cx32** group compared to the **Cx32** group. ***p<0.005

The amount of ATP released detected on oocytes injected with S1A and hCx32 was also partially inhibited, we observed about 45% less ATP release compared to hCx32 injected oocytes, as we expected from previous experiments. Again we used ASCx38 injected oocytes as negative controls (*Figure 1-9*).

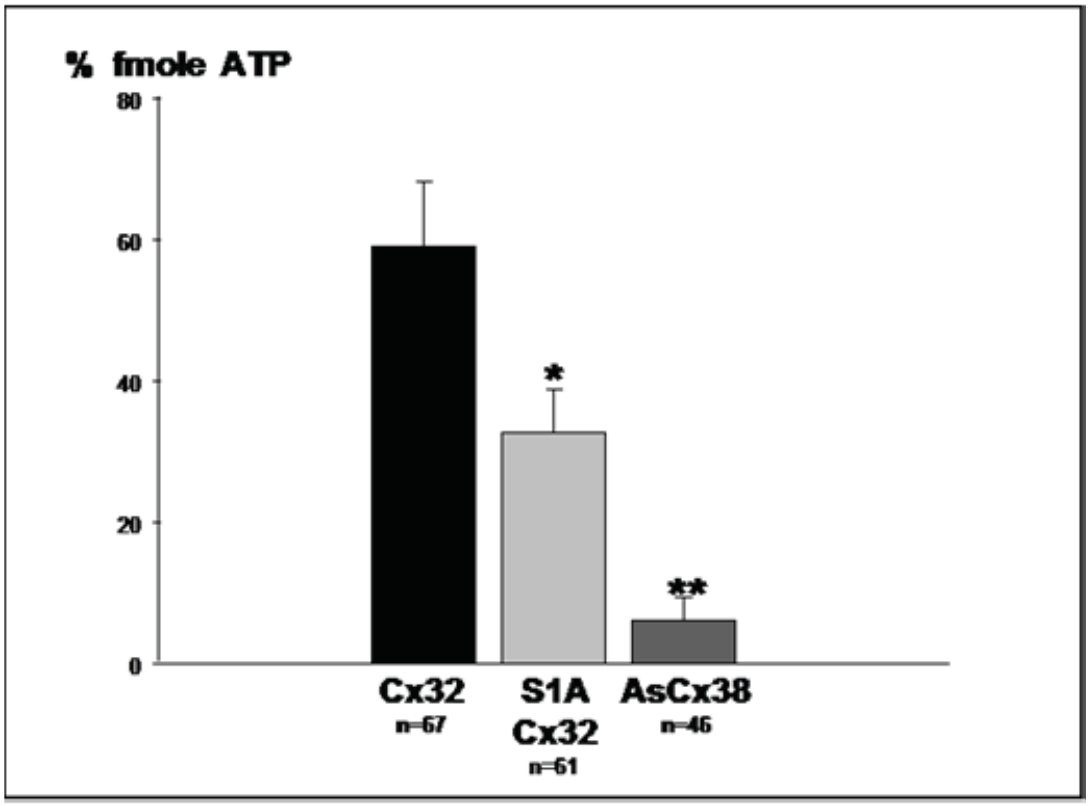

Figure R1-9 **| Histogram of normalized ATP released from injected oocytes**. **Cx32**: hCx32 cRNA and AsCx38 injected oocytes; **S1A Cx32**: hCx32, S1A cRNA and AsCx38 injected oocytes; **AsCx38**: AsCx38 injected oocytes. The **Cx32** group exhibited a greater ATP release compared to the control group (**AsCx38**). There was a significant 45% reduction of the ATP released from the **S1A Cx32** group compared to the **Cx32** group. *p<0.05, **p<0.01, ***p<0.005

So S1A has an inhibitory effect on hCx32 hemichannels, both affecting the unspecific outward currents generated by these hemichannels, and, in a more intense way, the tail currents electric charge and the ATP released through hCx32 hemichannels stimulated by a depolarizing pulse.

Western blots from single oocytes were performed using a specific anti syntaxin 1 antibody (HPC-I, Sigma S0664) to detect the amount of S1A expressed each oocyte and to check and compare the S1A expression level from each Xenopus oocyte batch. In one particular batch we could correlate the expression

of S1A to the intensity of recorded outward currents, and could establish that there was an inverse lineal relation between the amount of S1A detected on the western blot and the current previously recorded for that oocyte. So, the greater the amount of S1A detected, the smaller the recorded outward current (*Figure R1-10*).

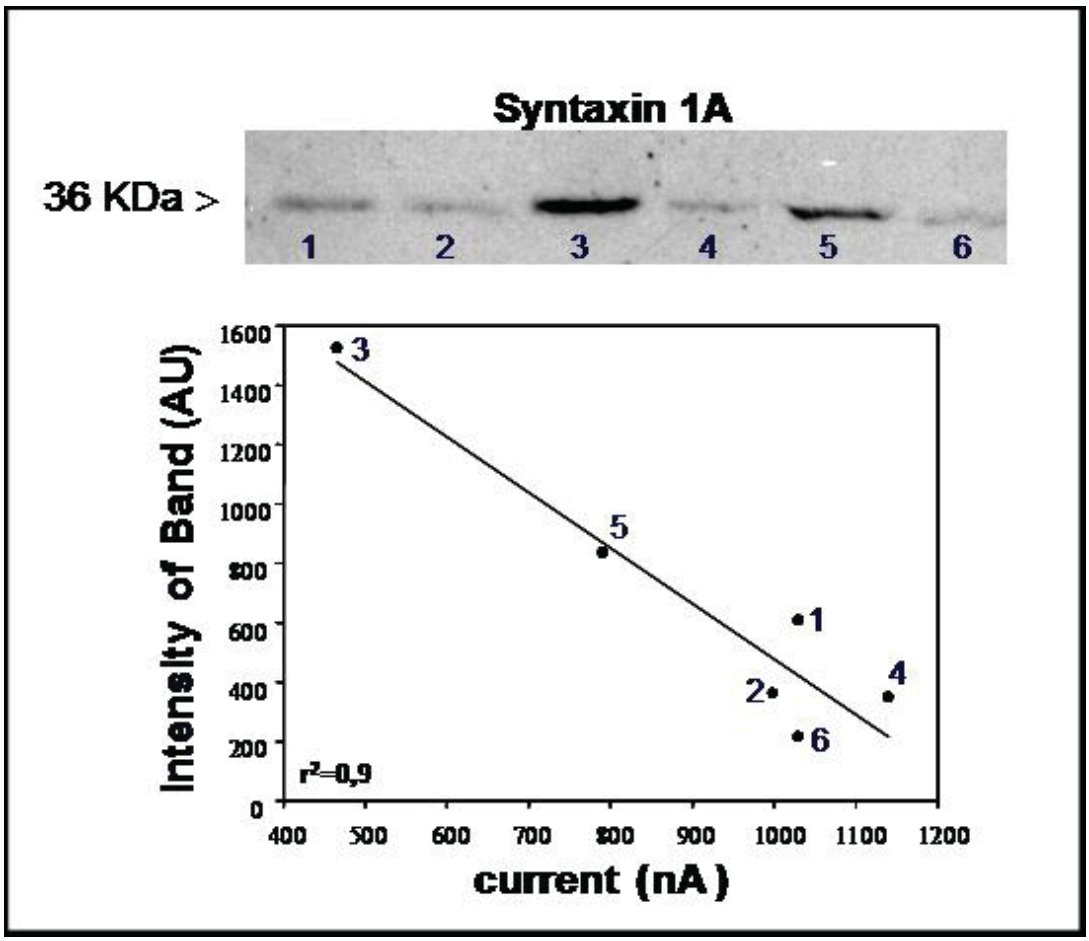

***Figure R1-10* | S1A Western blot and densitometry**. Western blot to detect S1A from one single oocyte (previously injected with hCx32 and S1A and TEVC recorded) per lane. Densitometry values (arbitrary units, AU) were related to recorded currents. An inverted ratio was found.

2. GENERATION OF CONNEXIN 32 MUTANTS AND STABLE TRANSFECTANTS

2.1 hCx32 mutations

Human Cx32 mutations S26L, P87A, Del111-16, D178Y and R220St (see introduction, section 2.5), and the hCx32 wild type construct were generated by PCR and inserted in pBSK (*Figure R2-1*) plasmid first, and subcloned to pBxG and pMJgreen plasmids (for cRNA and posterior expression on *Xenopus* oocytes and eukaryotic expression respectively) as described on materials and methods (section 9).

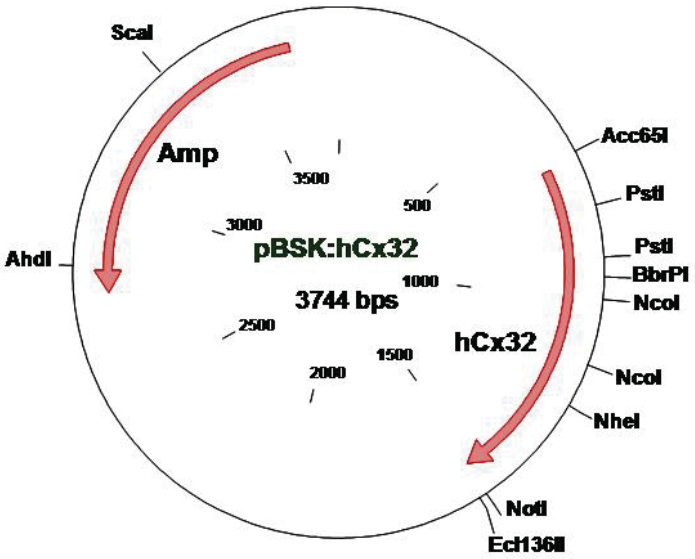

Figure R2-1 | Scheme of pBSK vector containing the hCx32 insert and the ampicillin resistance sequence.

All this part of the work was done at the Prof. Dr. Willecke's laboratory in the Institut für Genetik, Bonn University, Bonn, Germany. First of all, primers to generate these mutations were designed to insert, as well as the mutation desired, a new restriction site for the easy localization and first identification of each mutant. Those new restriction sites were SpeI for S26L, PvuII for P87A, StuI for Del 111-16, TatI for D178Y and BclI for R220St. All these constructs were generated by PCR and

inserted in pBSK vector and subsequently verified by sequencing (Agowa, Germany). After sequencing, correct constructs were subcloned into two new vectors: pBxG for cRNA obtention and *Xenopus* oocyte injection (*Figure R2-2*), and pMJgreen for eukaryotic expression of the proteins under the CMV promoter (*Figure R2-3*).

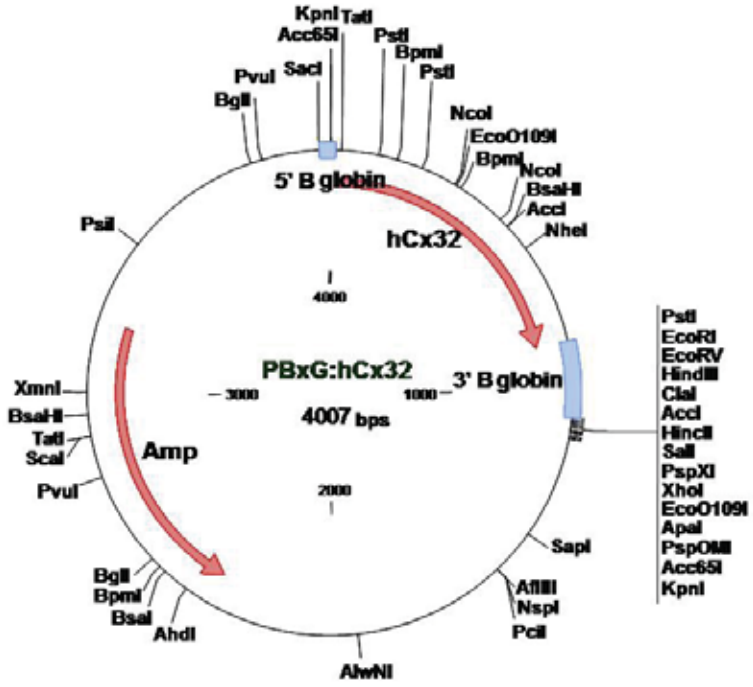

Figure R2-2 **|** Scheme of pBxG vector containing the hCx32 insert between two sequences of Xenopus β-globin to enhance cRNA translation, and the ampicillin resistance sequence.

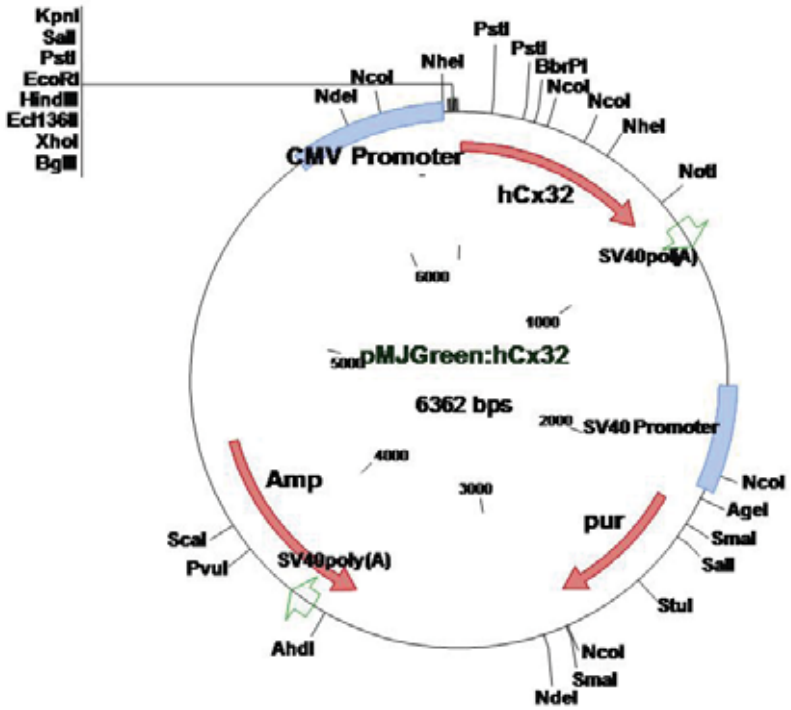

Figure R2-3 **|** Scheme of pMJgreen containing the hCx32 insert after the human CMV promoter. It also contains ampicillin and puromycin resistance sequences.

The MIDI preps for all these constructs were first checked by restriction enzyme digestions (see *Figures R2-4, R2-5, R2-6 and R2-7*), and then by sequencing. All this constructs generated are new tools to investigate hCx32 physiology, both the wild type and of mutants, and can help to know the mechanism by which mutations lead to CMTX disease.

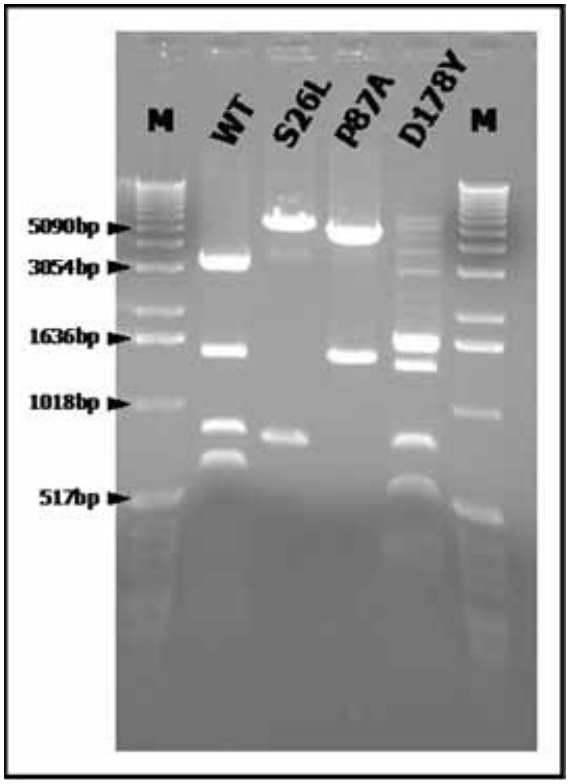

***Figure R2-4* | Agarose electrophoresis gel to check the generated hCx32 mutated sequences in pMJgreen vector**. **M**: Marker, **WT**: hCx32WT, **S26L**: hCx23S26L, **P87A**: hCx32P87A, D178Y: hCx32D178Y. Digestions were performed as follows: WT was digested with Nco I, S26L with SpeI/NotI, P87A with Pvu II and D178Y with TatI. *Expected bands (bp):* **WT**: 3313,1458, 811, 628,152; **S26L**: 5583, 728; **P87A**: 4915, 1450; **D178Y**: 1738, 1581, 1353, 719, 513, 294, 80, 51, 33.

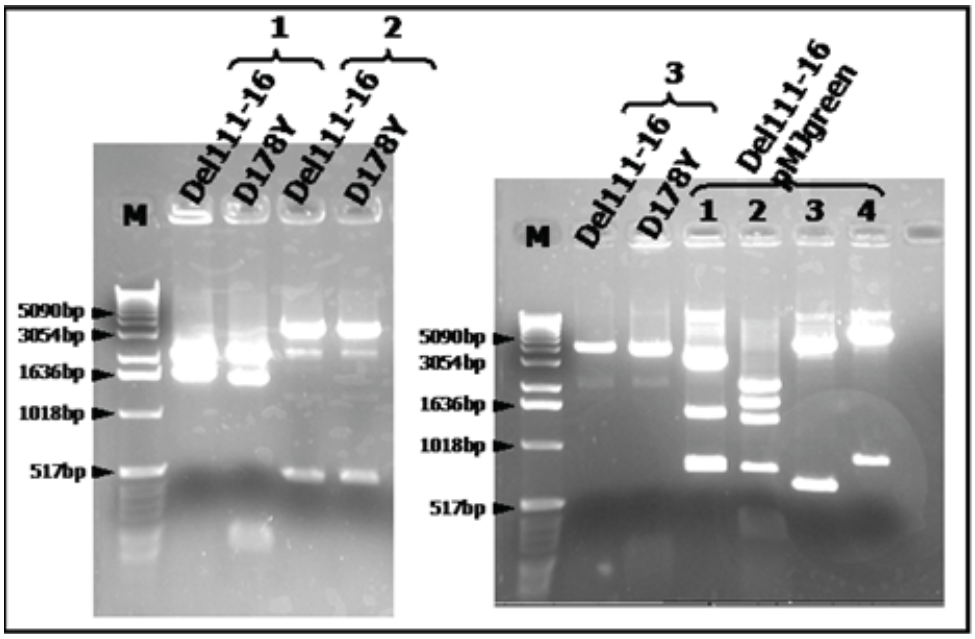

Figure R2-5 **| Agarose electrophoresis gels to check the generated hCx32 mutated sequences in pBxG and pMJgreen vector** (the last four lanes, as indicated). **M**: Marker, **Del111-16**: hCx32Del111-16, **D178Y**: hCx32D178Y. Digestions of constructs inserted in **pBxG** were performed as follows: **1**: Nco I/PvuI, **2**: NheI/ecoRI, **3**: PstI, **4**:NcoI. Digestions of Del111-16 in **pMJgreen** were performed as follows: **1**: NcoI, **2**: TatI, **3**: NheI/PvuI, **4**: Acc65I/NotI. *Expected bands (bp):* **pBxG**, **1**: *del111-16*: 2288, 1701, *D178Y*: 2288, 1549, 152; **2**: *del111-16*: 3510, 479, *D178Y*: 3528, 479; **3**: *del111-16*: 3989, D178Y: 3855, 152; **pMJgreen_Del111-16**, **1**: 3313, 1458, 811, 762; **2**: 2076, 1738, 1353, 719, 294, 80, 51, 33; **3**: 5713, 631; **4**: 5494, 850.

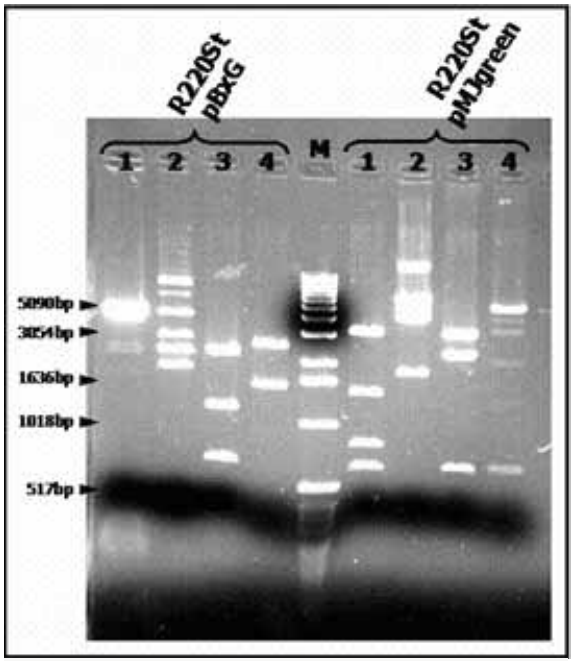

Figure R2-6 **| Agarose electrophoresis gel to check the generated hCx32R220St sequence in pBxG and pMJgreen vector**. **M**: Marker, **R220St**: hCx32R220St. Digestions of R220St inserted in **pBxG** were performed as follows: **1**: Nco I, **2**: ScaI, **3**: TatI, **4**: PvuII. *Expected bands (bp):* **1**: 3855, 152; **2**: 2219, 1788; **3**: 2219, 1146, 642; **4**: 2513, 1494. Digestions of R220St in **pMJgreen** were performed as follows: **1**: NcoI, **2**: ScaI, **3**: PvuI/PvuII, **4**: NheI. Expected bands (bp): **1**: 3313, 1458, 811, 628, 152; **2**: 3524, 2838; **3**: 3996, 2366; **4**: 5713, 649.

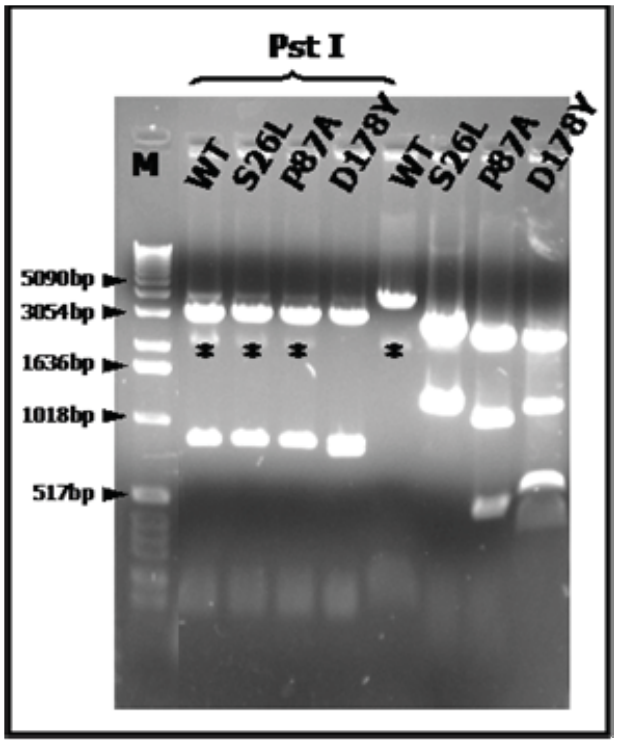

***Figure R2-7* | Agarose electrophoresis gel to check the generated hCx32 mutated sequences in pBxG vector. M**: Marker, **WT**: hCx32WT, **S26L**: hCx23S26L, **P87A**: hCx32P87A, **D178Y**: hCx32D178Y. **PstI**: indicates digestions performed with Pst I to check the insertion. Digestions on the right were performed to check the mutations as follows: **WT** was digested with Nco I, **S26L** with SpeI/ScaI, **P87A** with Pvu II and **D178Y** with tat I. Expected bands (bp): **Pst I** (all lanes): 3068, 820, 119; **WT**: 3855, 152; **S26L**: 2805, 1202; **P87A**: 2513, 1072, 422; **D178Y**: 2438, 1146 513. * corresponds to supercoiled vector bands.

2.2 hCx32 stable transfected HeLa cells

In order to work with cells that express high levels of WT and mutated hCx32, stable transfections were performed as described in material and methods (section 10). We obtained stable transfected HeLa cells with three of the six generated constructs: hCx32 WT, S26L and P87A. Once transfected, clones cultured in glass coverslips were checked by immunofluorescence against Cx32. Clones with high expression of Cx32 in plasma membrane and forming gap junction with adjacent cells for hCx32WT (*Figure R2-8*) or hCx32P87A (*Figure R2-9*) stable transfections were selected.

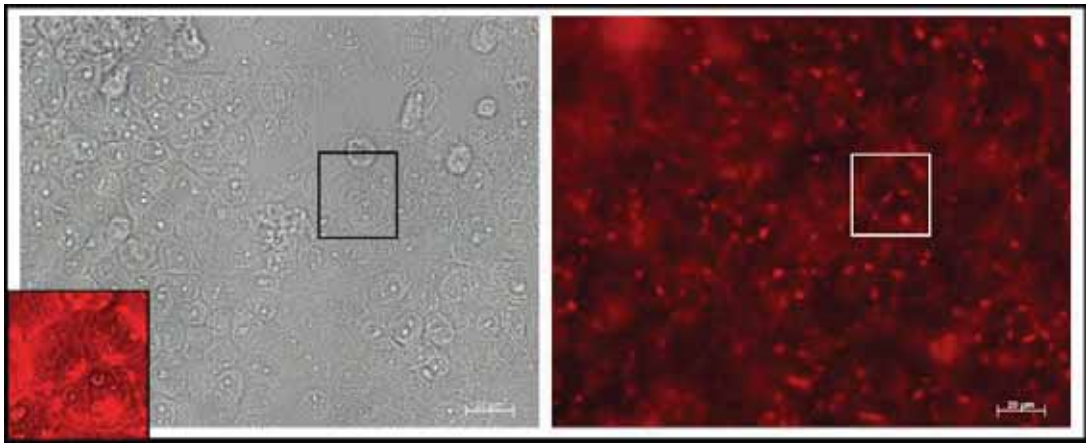

Figure R2-8 **| HeLa hCx32WT stable transfected cells.** Right, phase contrast image of hCx32WT stable transfected HeLa cells. Left, immunofluorescence against Cx32. The image has been taken with a fluorescent microscope, spots of intense fluorescence suggests the establishment of Gap junctions between adjacent cells. Inserted panel: zoom of the image corresponding to the merge of the two marked squares where gap junctions between the cells can be appreciated.

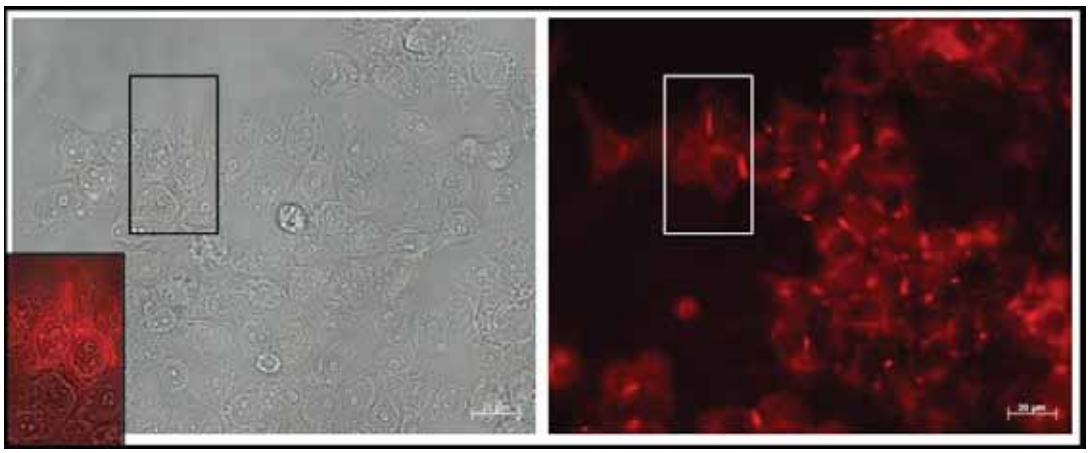

Figure R2-9 **| HeLa hCx32P87A stable transfected cells.** Left, phase contrast image of hCx32P87A stable transfected HeLa cells. Right, immunofluorescence against Cx32. The image has been taken with a fluorescent microscope, Cx32P87A formed Gap junctions are apparent between adjacent cells, although not all cells have the same expression level and some doesn't express any hCx32. Inserted panel: zoom of the image corresponding to the merge of the two marked squares where gap junctions between the cells can be appreciated at the top, and cells that doesn't express hCx32 can be appreciated at the bottom.

On the other hand, for hCx32S26L we could find clones that highly express it but in most of the cells it did not reach the cell plasma membrane, and only few cells were able to form gap

junctions of hCx32S26L in the plasma membrane (*Figure R2-10*), even though it has been described that this mutations is able to reach the plasma membrane and form gap junctions, even when transfected in HeLa cells [42]. To obtain a clonee were all cells express hCx32S26L in the plasma membranes this stable transfectant with a mixed population should be subcloned again and only clones that express the hCx32S26L in the plasma membranes should be selected, discarting the rest that express it but its retained in the cytoplasm. All stable transfectants are an interesting tool to keep on investigating the physiological role of Cx32 and the mutants.

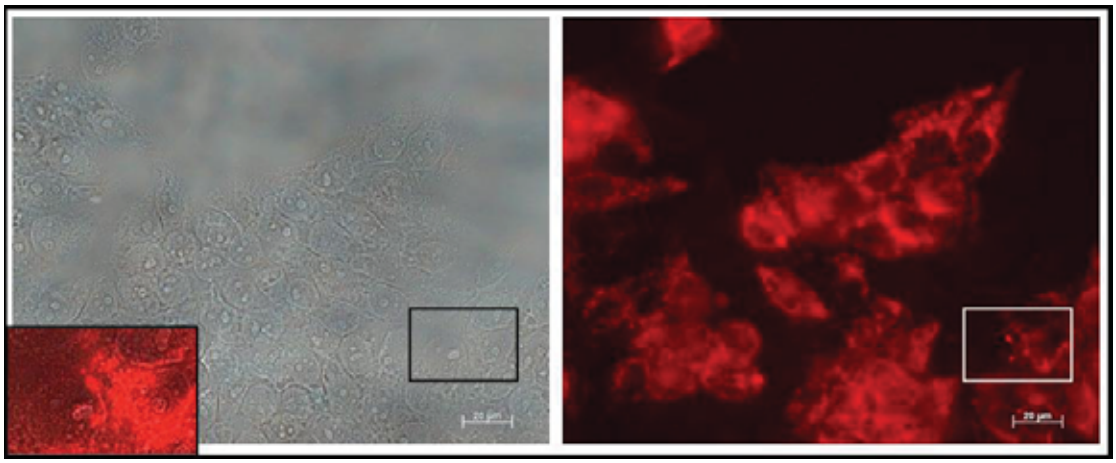

***Figure R2-10* | HeLa hCx32S26L stable transfected cells.** Left, phase contrast image of hCx32S26L stable transfected HeLa cells. Right, immunofluorescence against Cx32. The image has been taken with a fluorescent microscope (not a Confocal microscope), Cx32 formed Gap junctions are not as apparent between adjacent cells and most Cx32S26L expressed is retained in the cytoplasm. Inserted panel: hCxS26L forming gap junctions, so expressed in the plasma membrane

3. SPATIAL DISTRIBUTION OF CONNEXINS IN SCIATIC NERVE AND SCHWANN CELLS

3.1 Mouse Sciatic nerve teasings

Immunofluorescences to detect the presence of Cx32, S1A, Cx29 and Cx43 in teased mice sciatic nerve were performed as described in materials and methods (section 8.2). The first immunofluorescences confirmed the expression of Cx32 in Paranodes and Schmidt-Lanterman incisures as described before [39]. We could see Cx32 immunostaining on these regions both on Swiss CD1 (*Figure R3-1*) and C57BL6 (*Figure R3-2*) mice strands.

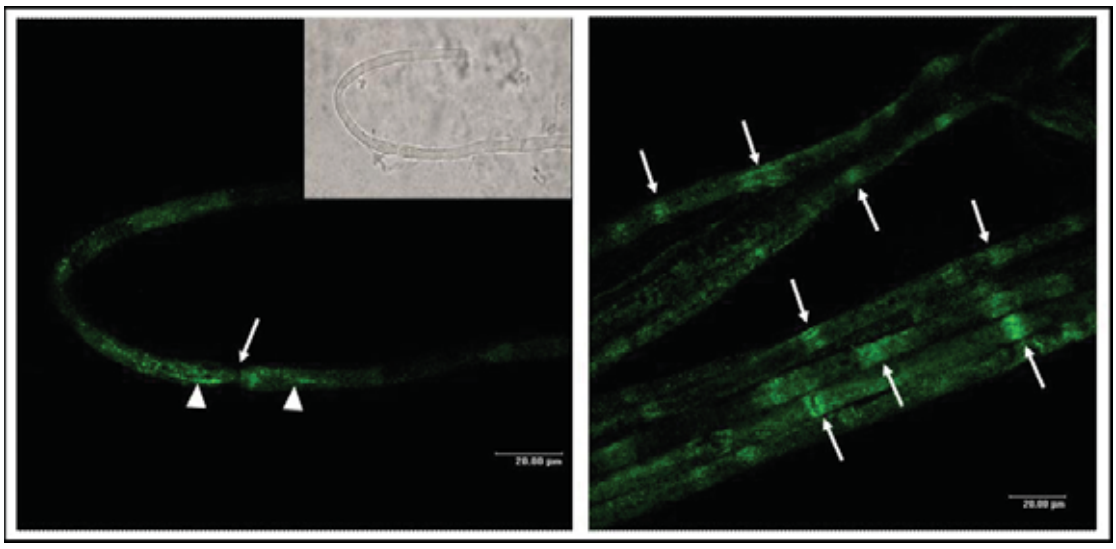

Figure R3-1 **| Immunofluorescence to detect Cx32 in teased mouse sciatic nerve**. Mice strand: Swiss CD1. Cx32 is expressed in paranodes, Schmidt-Lanterman incisures and inner mesaxon of peripheral nerves myelin sheath. Inserted panel: Phase contrast image of the left picture. Arrows: Node of Ranvier, Arrowhead: mesaxon.

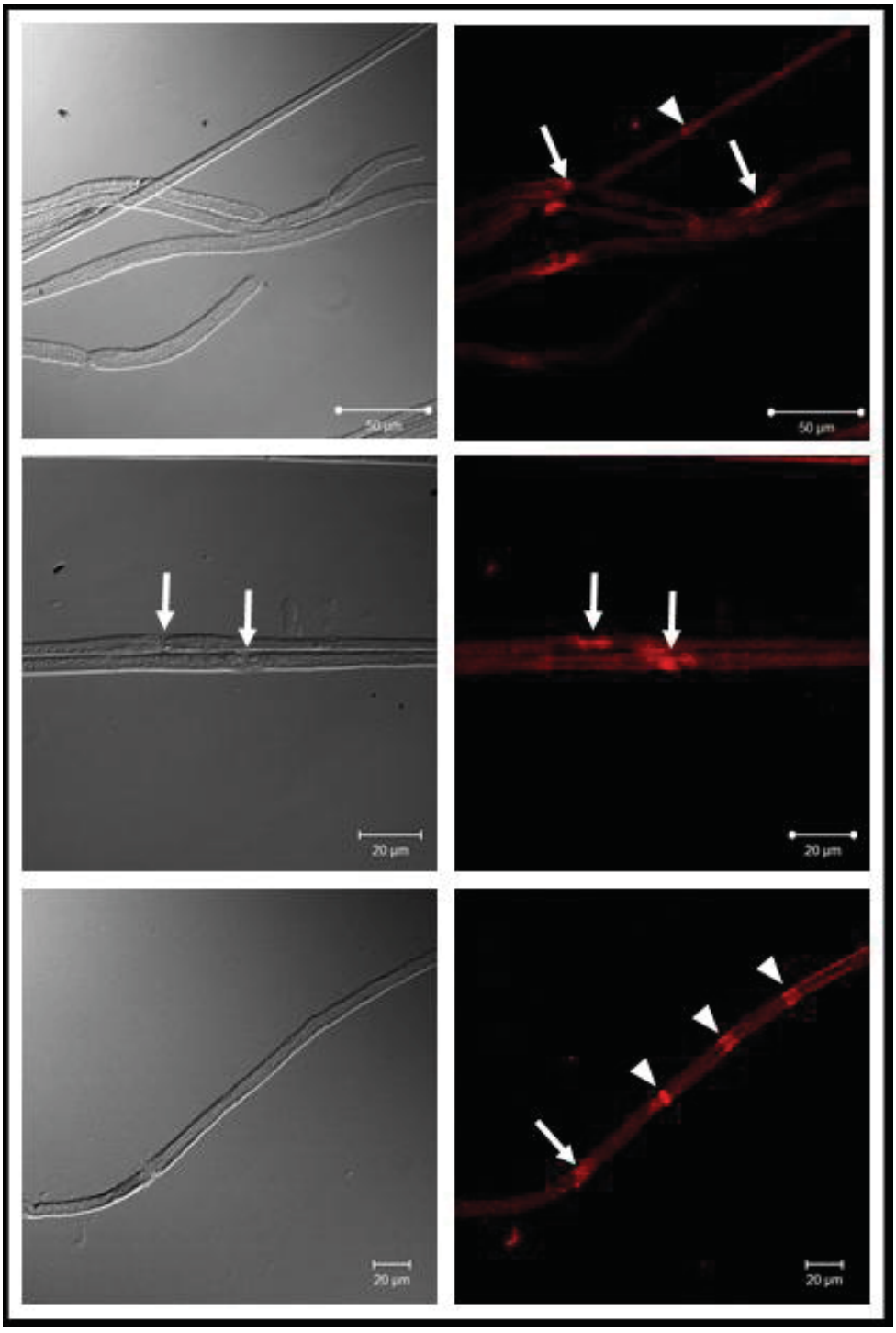

***Figure R3-2* | Immunofluorescence to detect Cx32 in teased mouse sciatic nerve**. Mice strand: C57BL6. Left: Phase contrast images corresponding to the image on their right. Right: Immunofluorescence against Cx32. Cx32 is expressed on paranodes and Schmidt-Lanterman incisures of peripheral nerves myelin sheath. Arrows: Nodes of Ranvier, Arrowheads: Schmidt-Lanterman incisures.

As described in the introduction of this thesis we were interested on the possible interaction of Cx32 and S1A in peripheral nerves. Accordingly, we did an immunostaining to detect S1A in sciatic nerve embedded in paraffin and could see S1A expression in what looks like to be the axons and/or the inner regions of Schwann cells myelin sheath (*Figure R3-3*).

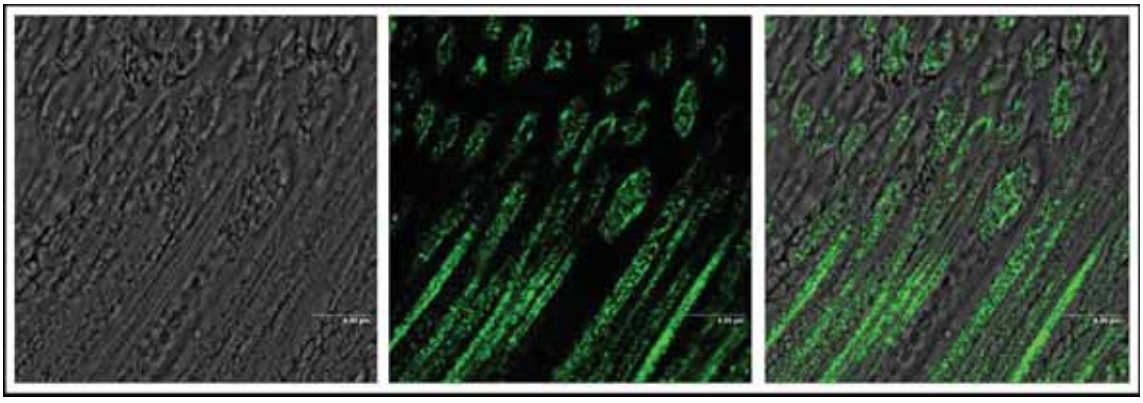

***Figure R3-3* | Immunofluorescence to detect S1A in mouse sciatic nerve**. Image taken from mice sciatic nerve embedded in paraffin. Left: Contrast phase image of mouse sciatic nerve, middle: S1A is expressed on axons of mouse sciatic nerve or in the inner regions of the myelin sheath, right: overlay.

With this result in hand we performed double immunostaining for both proteins. Again, we used teased fibres from mice sciatic nerve and we found Cx32 in paranodes and Schmidt Lanterman incisures, and to a less extent all through the nerve fibres, where we detected also S1A. We could observe a partial immunocolocalization of both plasma membrane proteins in teased mice sciatic nerves in some of our preparations but not in all of them. This colocalization was detected al along the nerve fibres (*Figure R3-4*).

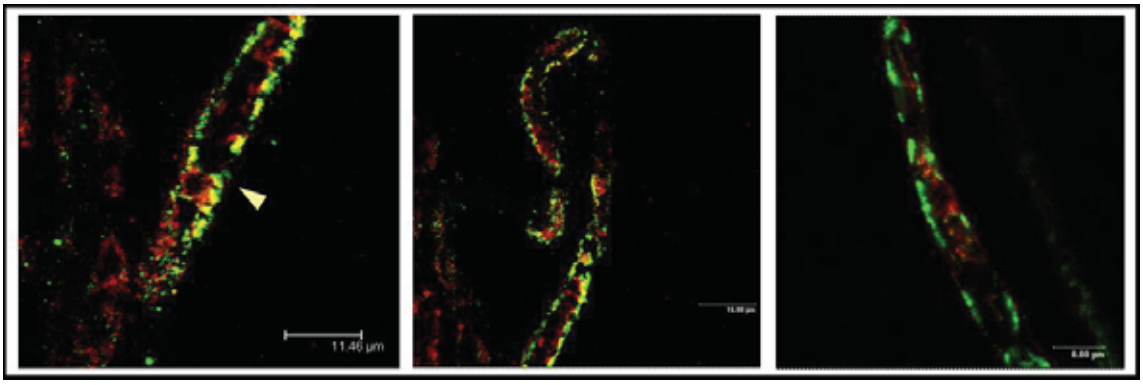

***Figure R3-4* | Immunofluorescence to detect Cx32 and S1A**. Cx32 and S1A show, in some cases, partial colocatization on the paranodes and plasmatic membrane of teased nerve fibres from mouse sciatic nerve (left, center), while in other preparations both molecules do not colocalize at all (right).

We also wanted to know more about localization of the other connexins known to be expressed in Schwann cells: Cx29 and Cx43. We saw immunostaining for Cx29 in the paranodes and in the Schmidt-Lanterman incisures (*Figure R3-5*) as it has been described in the literature [59]. For Cx43, for which there is little data about its localization or role in the peripheral nervous system, we did also immunolocalizations and we detected this connexin also in some of paranodes but not in all of them (*Figure R3-6*).

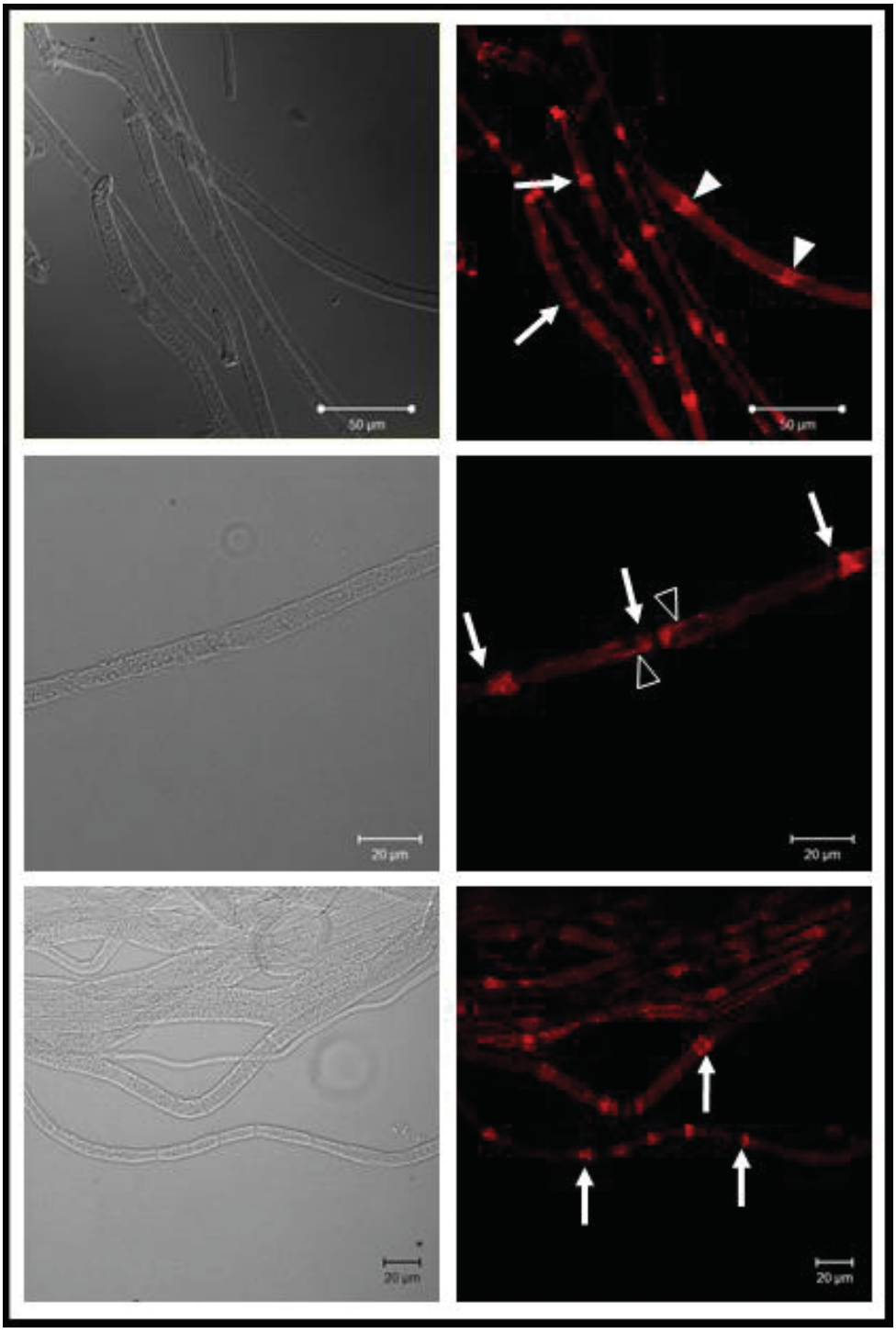

Figure R3-5 **| Immunofluorescence to detect Cx29 in teased mouse sciatic nerve. Mice strand: C57BL6. Left**: Phase contrast images corresponding to the image on their right. Right: Immunofluorescence against Cx29. Cx29 is expressed on paranodes and Schmidt-Lanterman incisures of peripheral nerves myelin sheath. Arrows: Nodes of Ranvier, Arrowheads: Schmidt-Lanterman incisures, empty arrowheads: inner mesaxon.

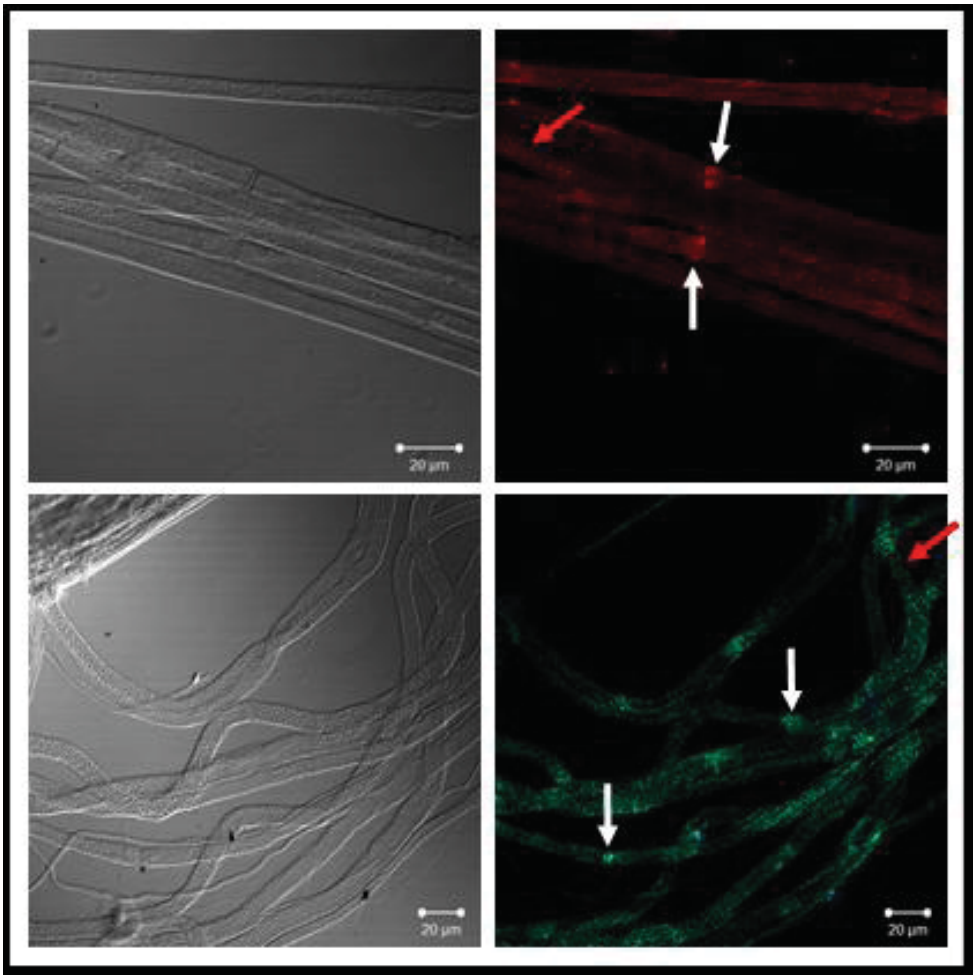

Figure R3-6 **| Immunofluorescence to detect Cx43 in teased mouse sciatic nerve**. Mice strand: C57BL6. Left: Phase contrast images corresponding to the image on their right. Right: Immunofluorescence against Cx43. Cx43 is expressed on some paranodes of peripheral nerves myelin sheath but not all of them. White arrows: Paranodes stained for Cx43, Red arrows: Paranodes without staining for Cx43. Red staining was obtained using secondary antibody linked to Alexa 594, green staining was obtained using secondary antibodies linked to Alexa 488.

We had the chance to work with Cx29 and Cx32 knock out mice, both developed in the University of Bonn, by the group of Prof. Dr. Klaus Willecke, from the Institut für Genetik. So we could perform immunofluorescence experiments with sciatic nerve teasing from those knock out mice. First we checked the specificity of the antibodies by immunostaining against Cx32 in sciatic nerve from Cx32 knock out mice (both male and female)

(*Figure R3-7*), and against Cx29 in sciatic nerve from Cx29 knock out mice (*Figure R3-8*).

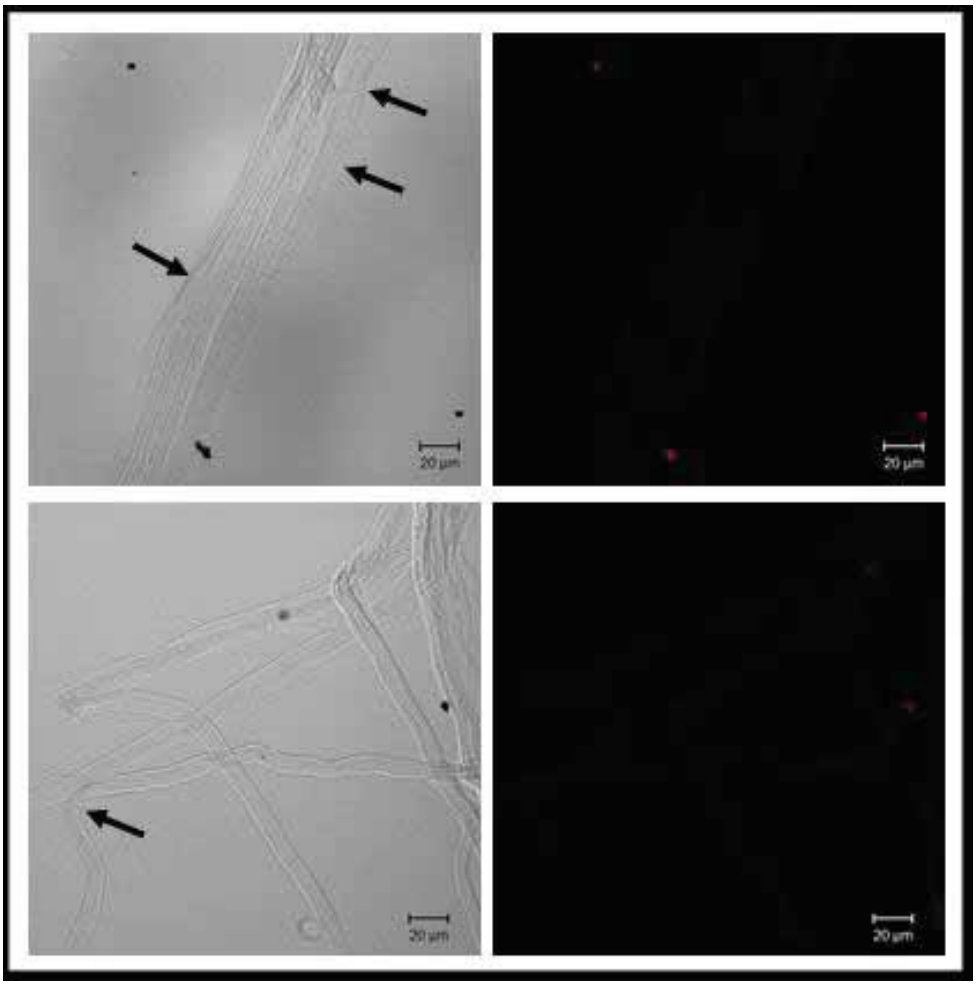

***Figure R3-7* | Immunofluorescence to detect Cx32 in teased C56BL6 Cx32-/- (female) and C56BL6 Cx32-/Y (male) mouse sciatic nerve**. Left: Phase contrast images corresponding to the image on their right. Right: Immunofluorescence against Cx32. There is no expression of Cx32 on the knock-out mice for this connexin in sciatic nerve. Top: C56BL6 Cx32-/- (female), bottom: C56BL6 Cx32-/Y (male). Arrows: Nodes of Ranvier.

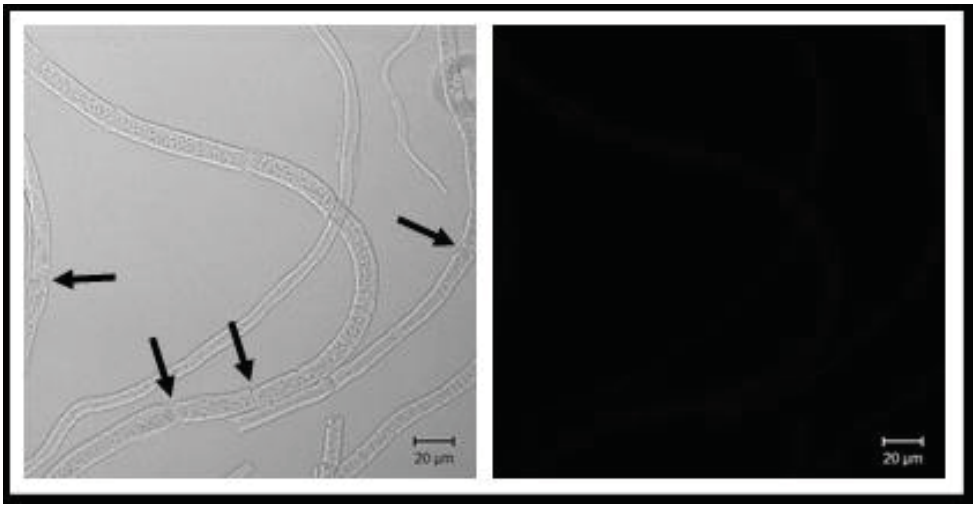

Figure R3-8 **| Immunofluorescence to detect Cx29 in teased C56BL6 Cx29-/- mouse sciatic nerve**. Mice strand: C56BL6. Left: Phase contrast images corresponding to the image on their right. Right: Immunofluorescence against Cx29. There is no visible staining for Cx29, so there is no expression (or low expression below the detection sensitivity of this method) of Cx29, indicating that there is no expression on the knock-out mice for this connexin in sciatic nerve. Black arrows: Nodes of Ranvier.

As expected, we could see no mark in those immunofluorescences, discarding the possibility of unspecific staining of the antibodies.

Then we did the same experiments we had done with wild type mice teased fibres but now directed to detect Cx32 in Cx29 knock out mice and Cx29 in Cx32 knock out mice. Figure *R3-9* shows that we could detect Cx32 in Cx29 knock out mice with the same pattern that we found before in wild type mice, namely an intense mark in the paranodes and the Schmidt-Lanterman incisures. So we could detect no differences in Cx32 expression or localization in mice lacking Cx29, indicating that expression and localization of Cx32 is independent from Cx29 and when this connexin is missed, Cx32 is not affected or overexpressed to supply the Cx29 lost function.

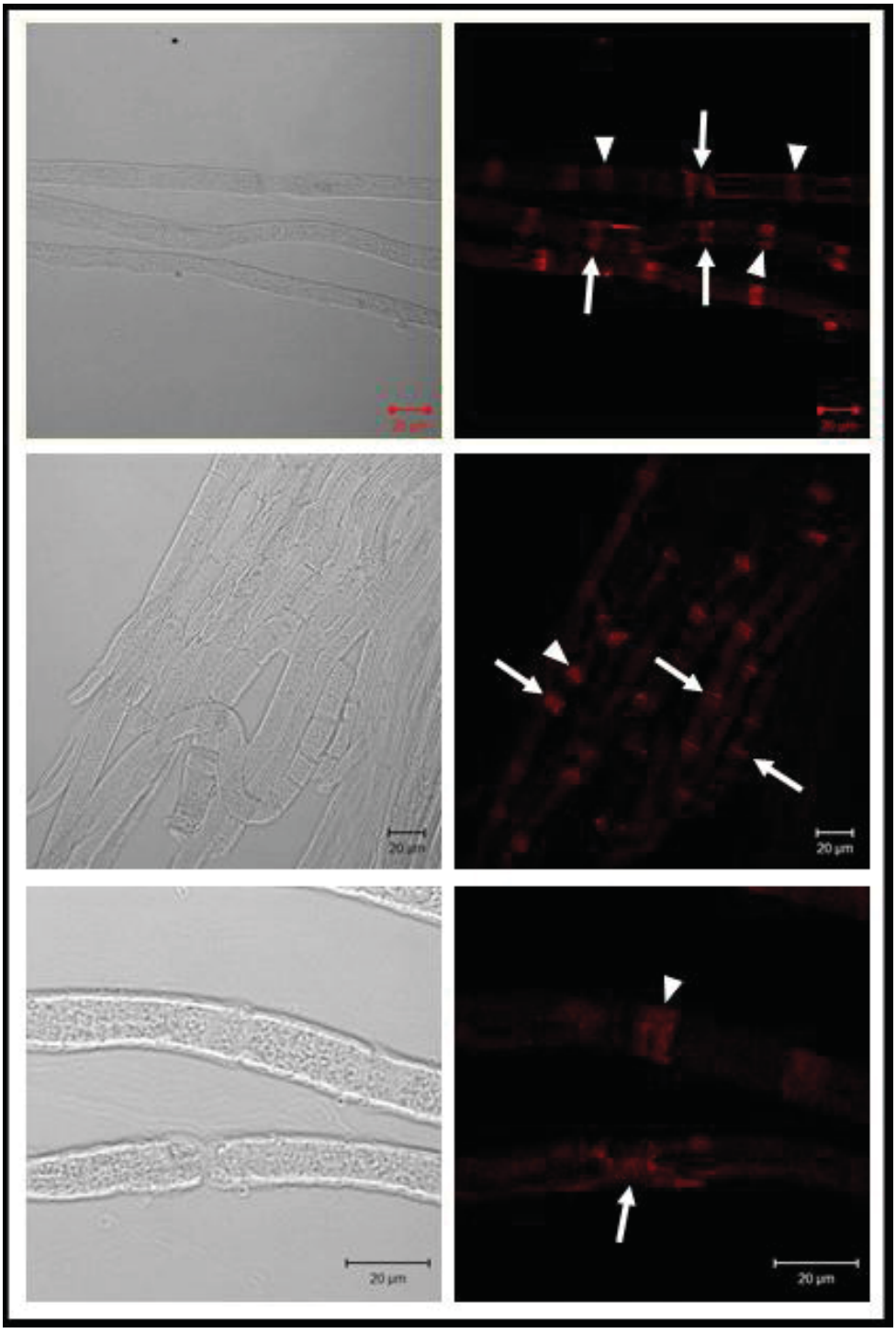

Figure R3-9 **| Immunofluorescence to detect Cx32 in teased C56BL6 Cx29-/- mouse sciatic nerve**. Mice strand: C56BL6. Left: Phase contrast images corresponding to the image on their right. Right: Immunofluorescence against Cx32. Cx32 is expressed on paranodes and Schmidt-Lanterman incisures of peripheral nerves myelin sheath as in wild type mice. Arrows: Nodes of Ranvier, Arrowheads: Schmidt-Lanterman incisures.

When we performed the same kind of immunofluorescences but this time against Cx29 in Cx32 knock out mice teased sciatic nerve fibres (both from female (*Figure R3-10*) and male (*Figure R3-11*) mice, as Cx32 is codified in the X chromosome and differences could appear). We had again a mark in the paranodes but it appeared weaker than the control sciatic nerve from wild type mice.

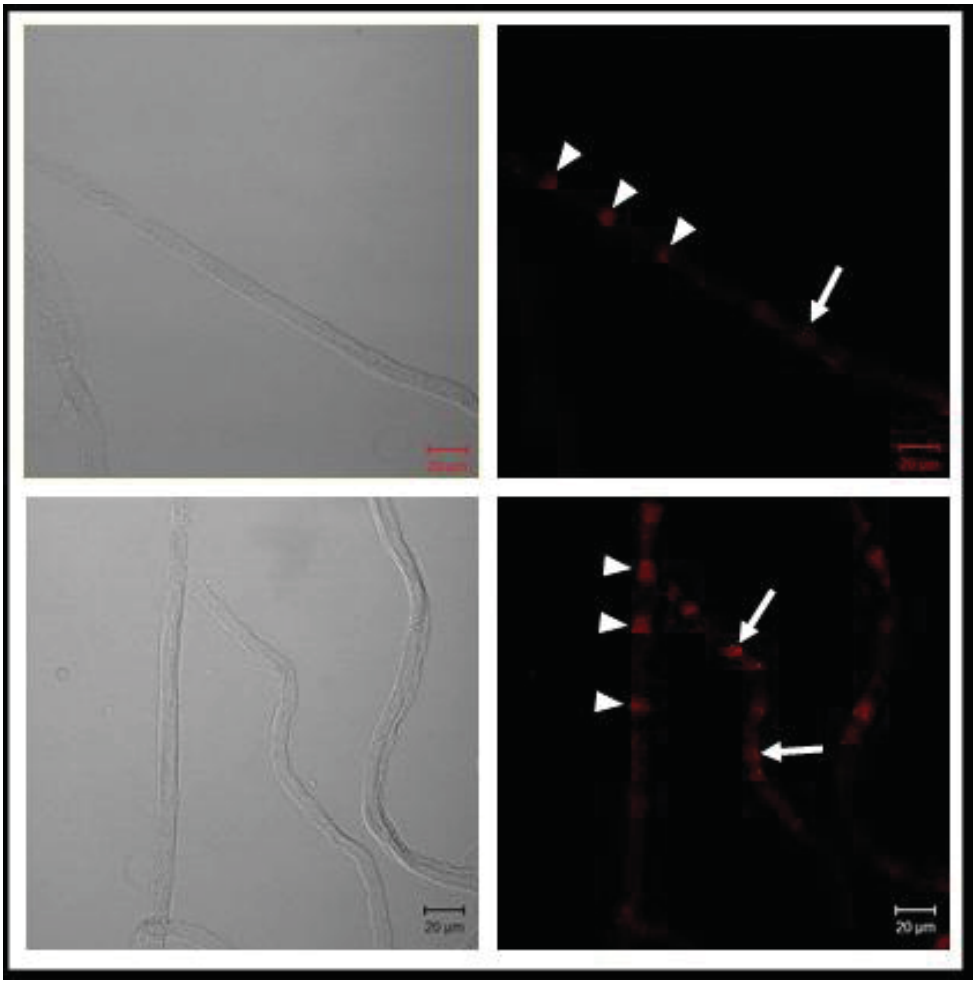

Figure R3-10 **| Immunofluorescence to detect Cx29 in teased C56BL6 Cx32-/- (female) mouse sciatic nerve**. Mice strand: C56BL6. Left: Phase contrast images corresponding to the image on their right. Right: Immunofluorescence against Cx29. Cx29 is expressed in Ranvier nodes and Schmidt-Lanterman incisures of peripheral nerves myelin sheath, but this expression appears to be weaker than in wild type mice. Arrows: Nodes of Ranvier.

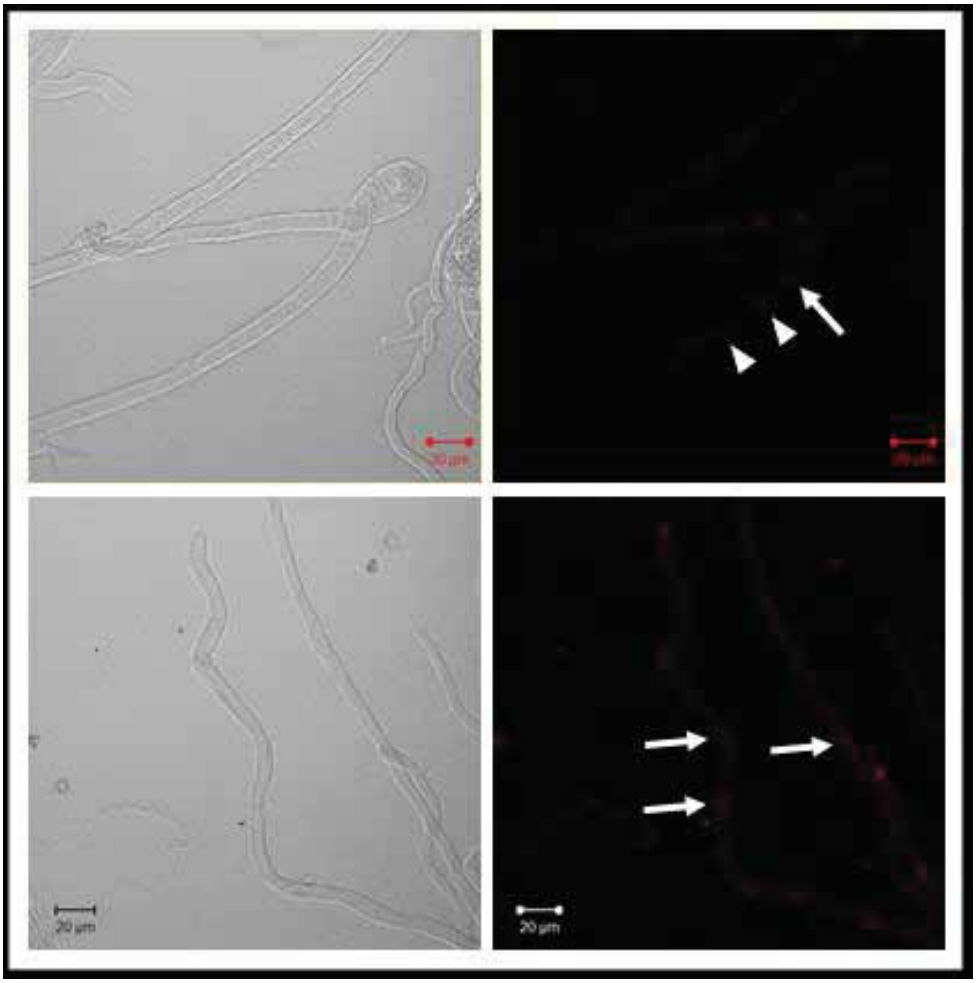

Figure R3-11 **| Immunofluorescence to detect Cx29 in teased C56BL6 Cx32 -/Y (male) mouse sciatic nerve**. Mice strand: C56BL6. Left: Phase contrast images corresponding to the image on their right. Right: Immunofluorescence against Cx29. Cx29 is expressed in Ranvier nodes and Schmidt-Lanterman incisures of peripheral nerves myelin sheath, this expression appears to look weaker than in wild type mice. Arrows: Nodes of Ranvier, arrowheads: Schmidt-Lanterman incisures.

We could even notice a slightly weaker mark in males compared with females from Cx32 knock out mice, which would be consistent with the fact that the male mice for this experiments were 7 months old, while the females were only 4 months old. These results support the idea that Cx29 is down regulated with age.

3.2 Cultured Schwann cells

Schwann cells primary cultures from adult mice sciatic nerves were obtained as described in materials and methods. We used CD1 mice strain for the primary cultures. To test the Schwann cell purity of our cultures immunofluorescences against S-100, a widely used marker for Schwann cells [200], were done: Most cells in our cultures expressed S-100 (data not shown), so we had highly pure (90%) Schwann cell primary cultures with only few fibroblast. The Schwann cells cultured in our conditions did not form myelin. Immunofluorescences to test the presence of connexins (Cx32, Cx29; Cx43) were performed on primary cultures of Schwann cells grown on glass coverslips. We had already detected the three connexins expressed by Schwann cells when forming the myelin sheath on peripheral nerves (See section 2.1 of results), and we wanted to test if our non-myelinating, cultured Schwann cells expressed those connexins. As far as we could observe, the most apparent and expressed connexin in our cultured, non myelinating cells, was Cx32 (as it happens in the myelin sheath, where it is also the most expressed connexin) but Cx29 and 43 were also expressed. Staining for Cx32 was detected all over the plasma membrane and the cytoplasm (*Figure R3-12*), and we could not detect any patch of gap junction, which means that this cultured Schwann cells are not coupled.

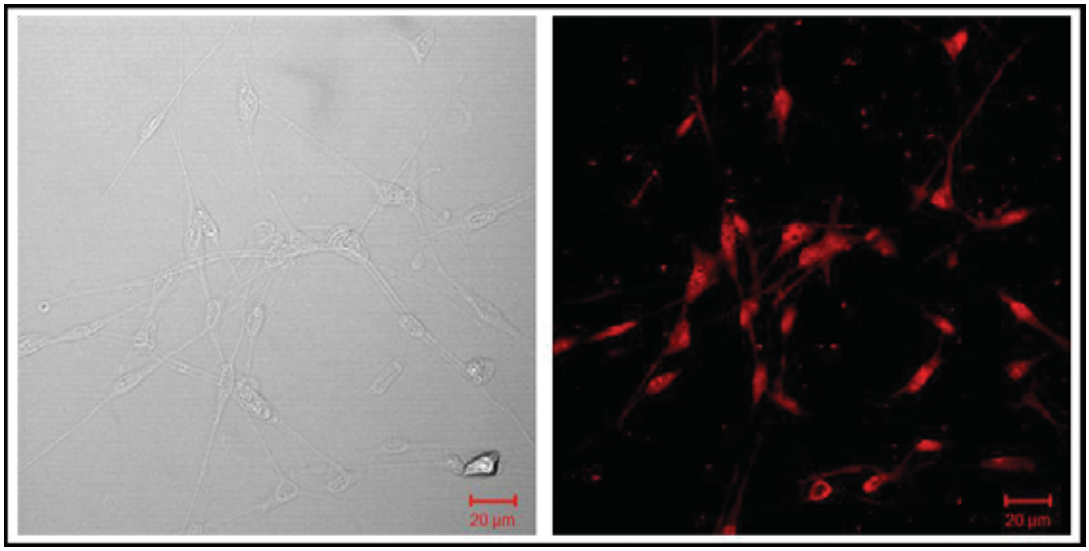

***Figure R3-12* | Immunofluorescence to detect Cx32 in cultured Schwann cells isolated from mouse sciatic nerve**. Mice strand: Swiss CD1. Left: Phase contrast image of the right picture Right: Cx32 is expressed homogeneously in the plasma membrane and the cytoplasm even though in culture do not form myelin. Interestingly connexins are not clustered and apparently no gap junctions are established between cells.

The same kind of staining in the plasma membrane and mainly in the cytoplasm detected for Cx32 was detected for Cx29 (*Figure R3-13*), even though it was not as abundant as Cx32.

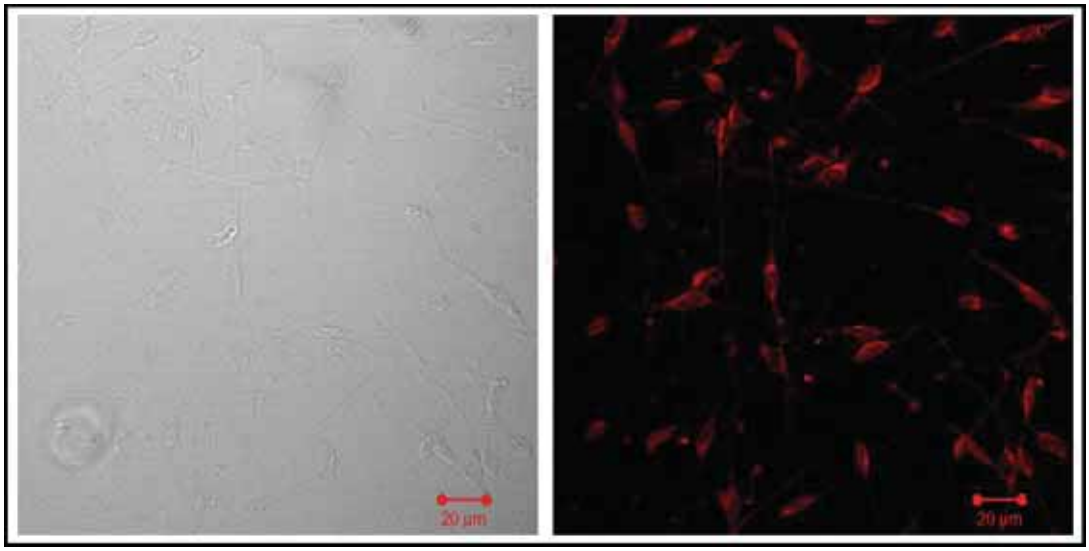

***Figure R3-13* | Immunofluorescence to detect Cx29 in cultured Schwann cells isolated from mouse sciatic nerve**. Mice strand: Swiss CD1. Left: Phase contrast image of the right picture Right: Cx29 is express homogeneously in the cytoplasm and the plasma membrane even though in culture don not form myelin. Again, connexins are not clustered and apparently no gap junctions are established between cells.

On the other hand, staining for Cx43 was apparently cytoplasmatic, and seemed to have preference for the perinuclear area (*Figure R3-14*).

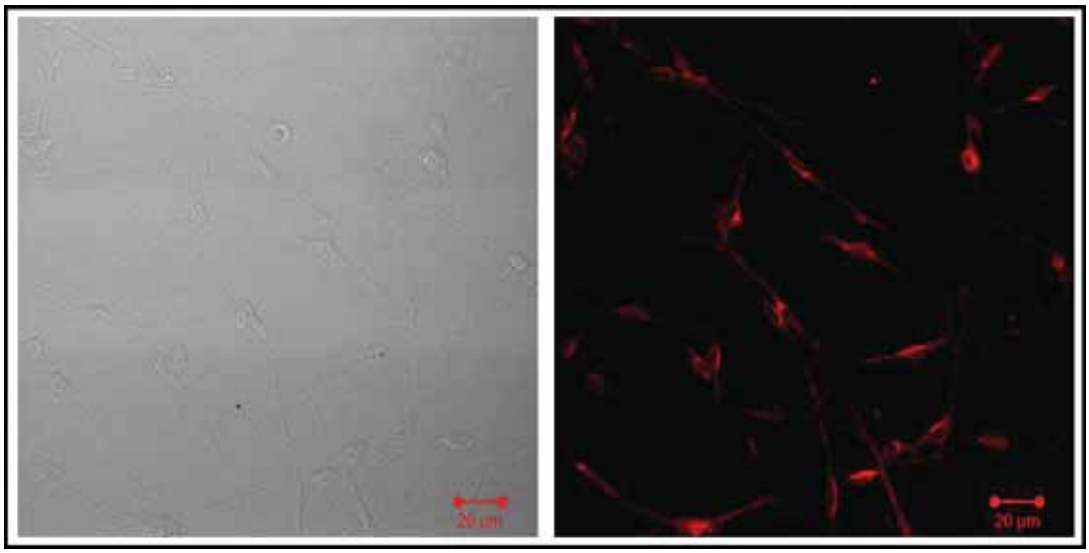

***Figure R3-14* | Immunofluorescence to detect Cx43 in cultured Schwann cells from mouse sciatic nerve**. Mice strand: Swiss CD1. Left: Phase contrast image of the right picture Right: Cx43 is express in the cytoplasm with preference for the perinuclear area.

With the immunofluorescences of cultured Schwann cells we could see that all Cx43, and much of the Cx29 and Cx32 do not reach the cultured Schwann cell plasma membrane. A possible explanation is that, because cultured Schwann cells do not form myelin, most of the connexins which would normally be localized in the myelin sheath are retained in the cytoplasm, and only few connexins reach the plasma membrane.

We also tried to culture Schwann cells from wild type C56BL6 mice but cells were unable to divide and died within few days in culture. It indicated us that something in the C56BL6 strain genetic background made Schwann cells unable to survive using our culture protocol. As Cx29 and Cx32 null mice belong to these

mice strain we unfortunately were unable to obtain cultures from Cx29 or Cx32 null Schwann cells, to be compared to those obtained with CD1 mice strain.

4. ATP RELEASE FROM SCIATIC NERVE

4.1 Whole sciatic nerve stimulation

In our TEVC experiments we saw ATP release through Cx32 hemichannels when the plasma membrane was depolarized, the physiological stimulus that opens Cx32 hemichannels during an action potential transmission. We wanted to see if we could also record ATP release from Schwann cells, the cells where Cx32 is naturally expressed. For that we used sciatic nerves from rats and mice and we used a suction electrode connected to a stimulator to trigger a nerve depolarization (see material and methods, section 7.2). We used again the luciferin-luciferase reaction to detect ATP and we captured the light produced after electrical stimulations with an ORCA II camera. Using this experimental approach, we detected the release of ATP from both, rat (*Figure R4-1*) and mice (*Figure R4-2*) sciatic nerves electrically stimulated.

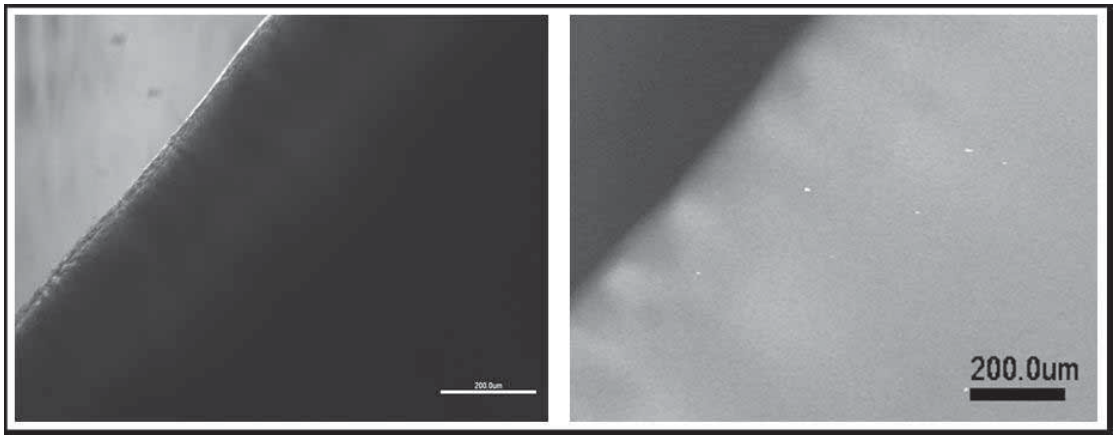

Figure R4-1 **| Imaging ATP release from rat sciatic nerve**. Left: Isolated rat sciatic nerve observed by transilumination. Right: Rat sciatic nerve was electrically stimulated and the ATP release detected by the luciferine-luciferase luminescent reaction and captured using an ORCA II hamamatsu camera. Stimuli: 4Hz, 15V, 10min. Scale bars: 200µm.

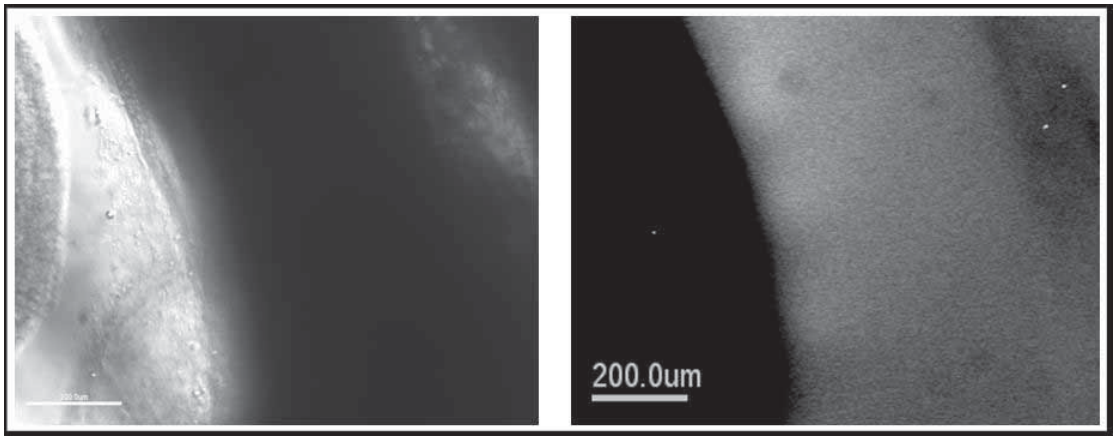

***Figure R4-2* | Imaging ATP release from mouse sciatic nerve**. Left: Isolated mice sciatic nerve observed by transilumination. Right: Mouse sciatic nerve was electrically stimulated and the ATP release detected by the luciferine-luciferase luminescent reaction and captured using an ORCA II hamamatsu camera. Stimuli: 2Hz, 15V, 10min. Scale bars: 200μm.

This release was not homogenous and there were some regions were it was more intense. Stimuli were applied for 10 to 30 min, with pulses of supramaximal intensity (usually 15 V), duration of 50-100 μs and a frequency of 2-4 Hz.

We also tried a mechanical stimulus on mice sciatic nerve and captured again the release of ATP. For that, Na^+ free buffer (30±5 mOsm) was added to the preparation of sciatic nerve bathed with isotonic buffer (280±10 mOsm) in order to cause a hypotonic shock (the ratio isotonic buffer: Na+ free buffer was 1:1). The preparation was stabilized during 2 min. To detect the luminescence due to the reaction of ATP and luciferin-luciferase, the shutter of the camera was maintained in the opening position for long periods of time, usually 30 min or more (*Figure R4-3*). We could record a release of ATP but we could not appreciate if in this condition this release is also focused on

some regions.

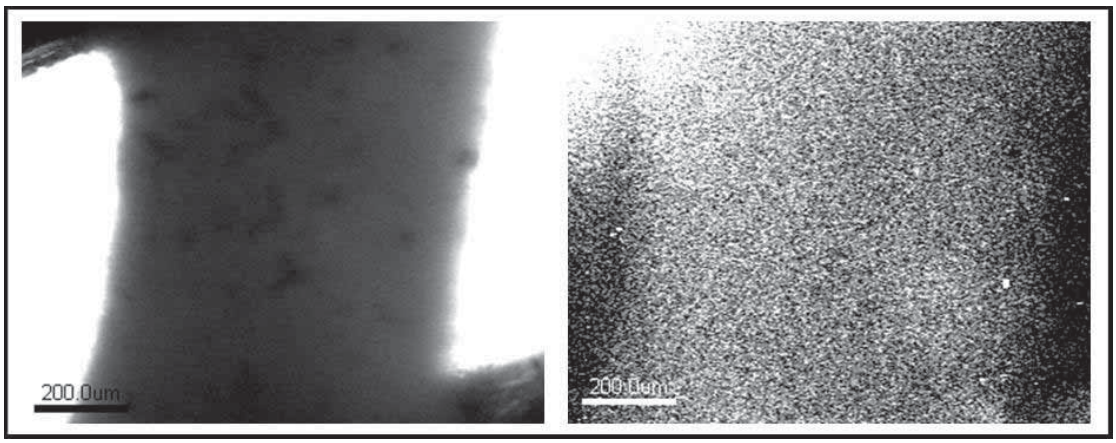

***Figure R4-3* | Imaging ATP release from whole mouse sciatic nerve due to a mechanic stimulation.** Right: Phase contrast image of sciatic nerve fragment. Left: Image of luminescence (ATP) from a sciatic nerve segment. The time of exposure was 30 min. A faint light was detected with a profile coincident with the sciatic nerve fragment shown in the right picture. Note that the upper left part of the picture is lighter that the rest, this effect is due to the thermal noise of the camera and is not related to an actual release of ATP. (Picture obtained by E. Mas).

4.2 Electrical stimulation of teased fibres from mouse sciatic nerves.

Using the whole nerve preparation we could see differentiated regions for the ATP release, and in order to distinguish which regions are responsible for the majority of ATP release, we teased one end of the nerve and electrically stimulated the other end with the suction electrode. We applied stimuli of 7-15 V and 1-4 Hz for 10 min, and again captured images of ATP release using an ORCA II camera and the luciferin-luciferase reaction. We could see some ATP release (*Figure R4-4*) but we could not distinguish if this ATP was released due to the electrical stimuli or the mechanical stimulation applied with the suction electrode as the preparation

was very sensitive to any movement or mechanical stimulus. However, we could see some regional heterogeneity in ATP release, with some brighter points were the ATP release was more intense. However, we could not determine for sure if those regions correspond to the paranodes as the images suggested, because they were not static and teased nerve moved in the buffer solution during the expositions.

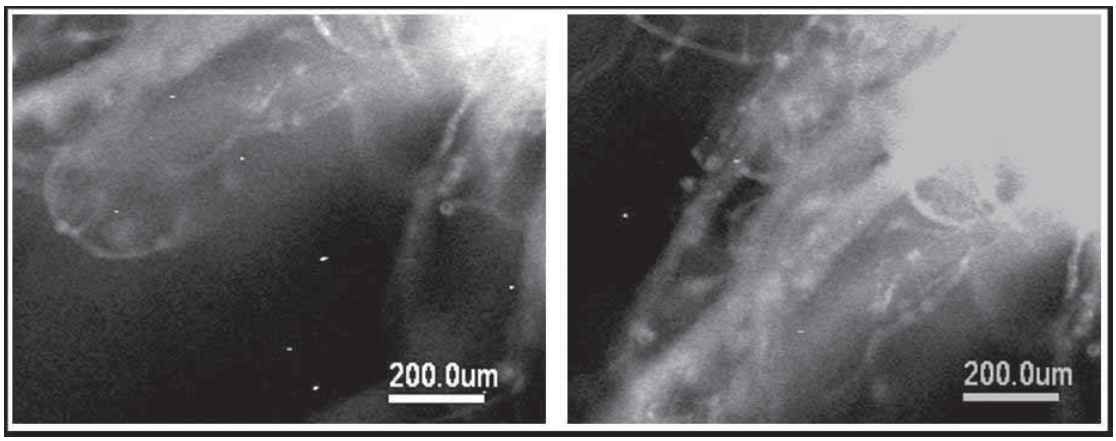

Figure R4-4 **| Imaging ATP release from mouse teased sciatic nerve**. Mouse sciatic nerve teasings were electrically stimulated with a suction electrode and ATP release detected by the luciferine-luciferase luminescent reaction and captured using an ORCA II Hamamatsu camera. Stimuli: 4 Hz, 15 V, 10 min. The signal registered is not clear and it's most likely due to the mechanical stimuli of the suction electrode than to the electrical stimuli. Scale bars: 200 μm.

5. HYPOTONIC SHOCK & ATP RELEASE

5.1 Hypotonic shock on cultured Schwann cells

Because we found that peripheral nerves release ATP under hypotonic conditions, we wanted to check the possible ability of cultured Schwann cells to release ATP under hypotonic stimulus. Primary Schwann cell cultures in 12 wells culture plates were tested as described on materials and methods (section 12). We could determine that Schwann cells under a hypotonic shock released ATP. This release was quick, just after the stimulus was applied, and quickly returned to basal levels, even tough the hyposmotic media was not removed, which indicates a fast, transient response of the cells (*Figure R5-1*).

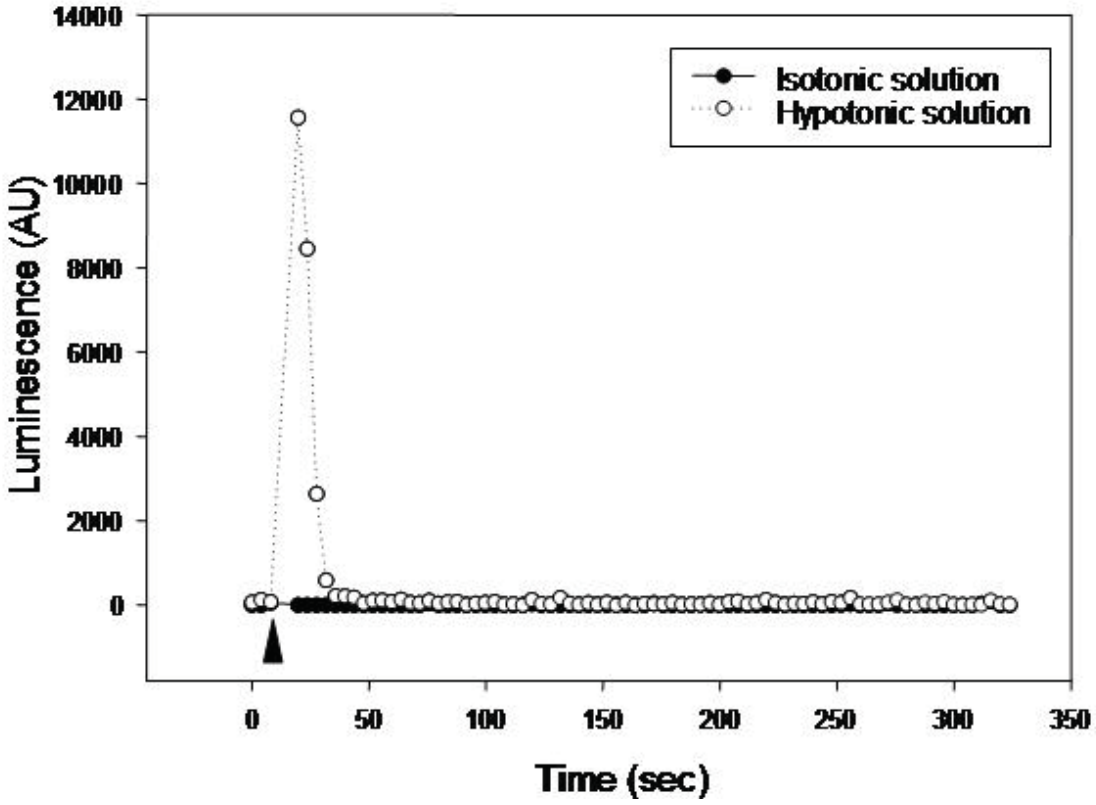

***Figure R5- 1*|** Graphic representation of luminescence detected in Schwann cells primary cultures after a hypotonic shock. Luminescence data reflects the amount of ATP released. The black arrowhead signals the moment when either hypotonic or isotonic solution is added to the cultured cells. AU: arbitrary units.

Comparing control Schwann cells (bathed with isotonic solution) with those that received a hypotonic shock, the differences on ATP release were significant (p=0.024), with 8 times more ATP released from cells under the hypotonic shock (*Figure R5-2*). The mean of ATP released by control Schwann cells group was $3.03x10^{-5}\pm 2.4x10^{-5}$ fmole/10^4cells, while the mean of ATP released by Schwann cells after a hypotonic shock was $25x10^{-5}\pm 11.7x10^{-5}$ fmole/10^4cells.

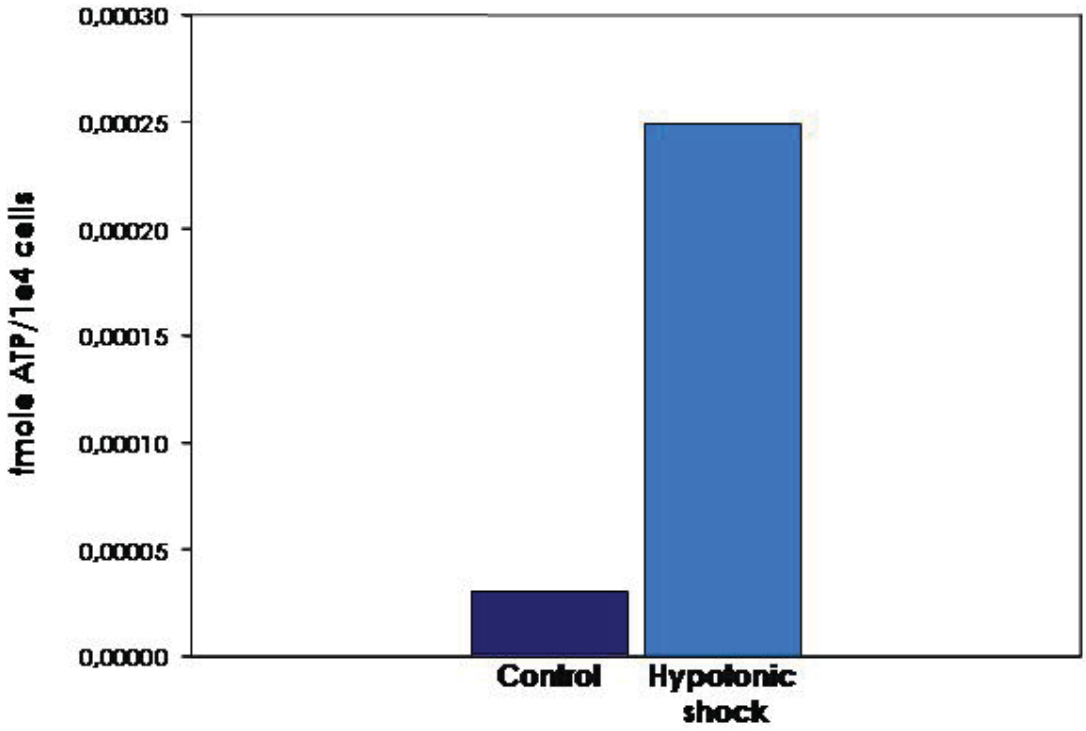

Figure R5-2 **|** Histogram representation of the ATP released from Schwann cell primary cultures subject to a hypotonic shock and its controls. The differences in ATP released are significant, with p=0.024. Control, n=6, Hypotonic shock, n=12.

5.2 Hypotonic shock on HeLa cells.

To further study the possible implication of Cx32 in the ATP release we did the same hypotonic shock experiments with WT HeLa and HeLa stable transfected with hCx32. First, we checked

again the Cx32 expression in hCx32 stable transfected HeLa cells, but this time by western blot and not immunofluorescence. We confirmed that the cells expressed hCx32 and that no hCx32 expression was detected by western blot in wild type HeLa cells (*Figure R5-3*).

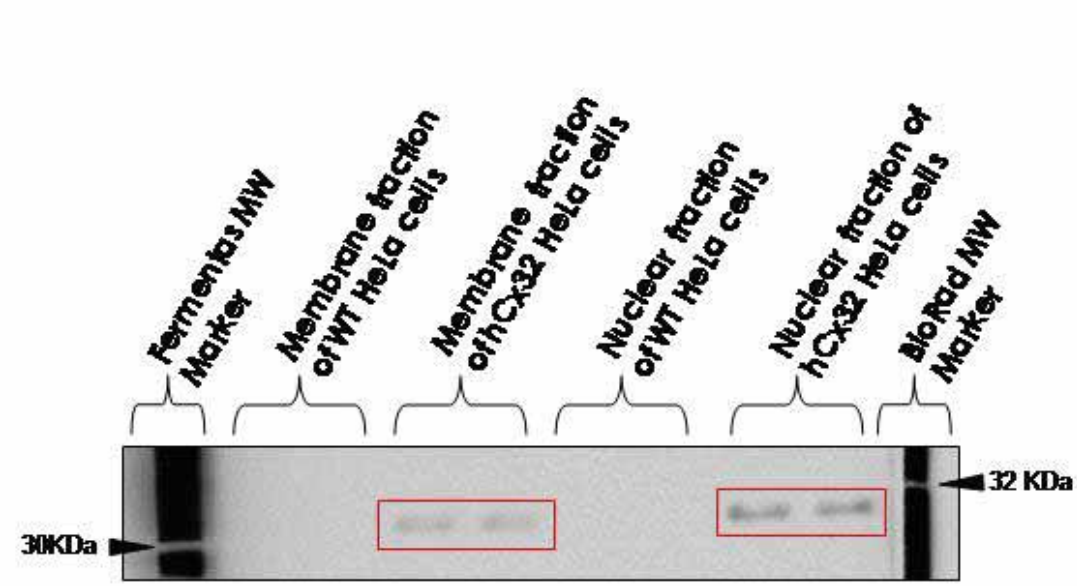

***Figure R5-3* | Western blot image of Cx32 from wild type and hCx32 transfected HeLa cells**. HeLa cells homogenates were fractionated between membrane and nuclear fractions. HeLa wild type cells do not express Cx32 while Cx32 is detected in hCx32 transfected HeLa cells both in the membrane and the nuclear fraction. The expression in the nuclear fraction is likely a contamination with membrane fraction (see section 6.2 on materials and methods).

When applying the hypotonic shock in the same way we had done before in experiments with cultured Schwann cells, we detected ATP release in response to this mechanical stimulus. The ATP release was rapid like the one observed with cultured Schwann cells. This release was not observed in control groups both of WT HeLa and hCx32 transfected HeLa cells (*Figure R5-4*).

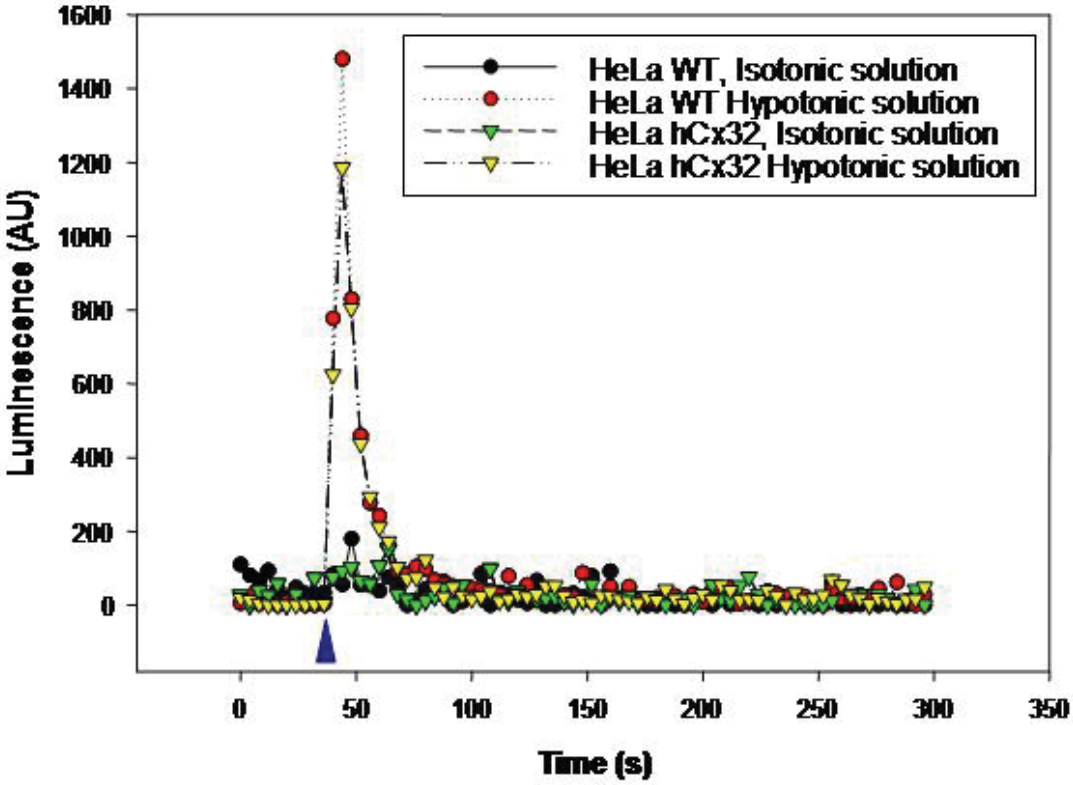

Figure R5-4 **|** Graphic representation of luminescence detected in WT and hCx32 transfected HeLa cells cultures after a hypotonic shock. Luminiscence data reflects the amount of ATP released. Blue arrowhead: injection of solutions. AU: arbitrary units.

Table R5-1 shows the differences in ATP release, when cells are submitted to shear stress by adding the isotonic solution or by mechanical stress with the hypotonic solution. Either non transfected or hCx32 transfected cells, release ATP under hypotonic conditions. Moreover, hCx32 transfected cells did not release much more ATP than WT cells, which is contrary to what we expected. These data are also represented in a histogram form in *figure R5-5*.

ATP fmole/10^4cells	Hela WT	HeLa hCx32
Isotonic solution	$4.08x10^{-3}$±0.012 n=16	$4.03x10^{-3}$±0,0115 n=16
Hypotonic solution	$11.7x10^{-3}$±0.02* n=32	$10.2x10^{-3}$±0.016* n=32

Table R5-1 **|** Table of ATP released from HeLa cells in response to a hypotonic shock. *: the differences compared to the isotonic solution are significant, p<0.005.

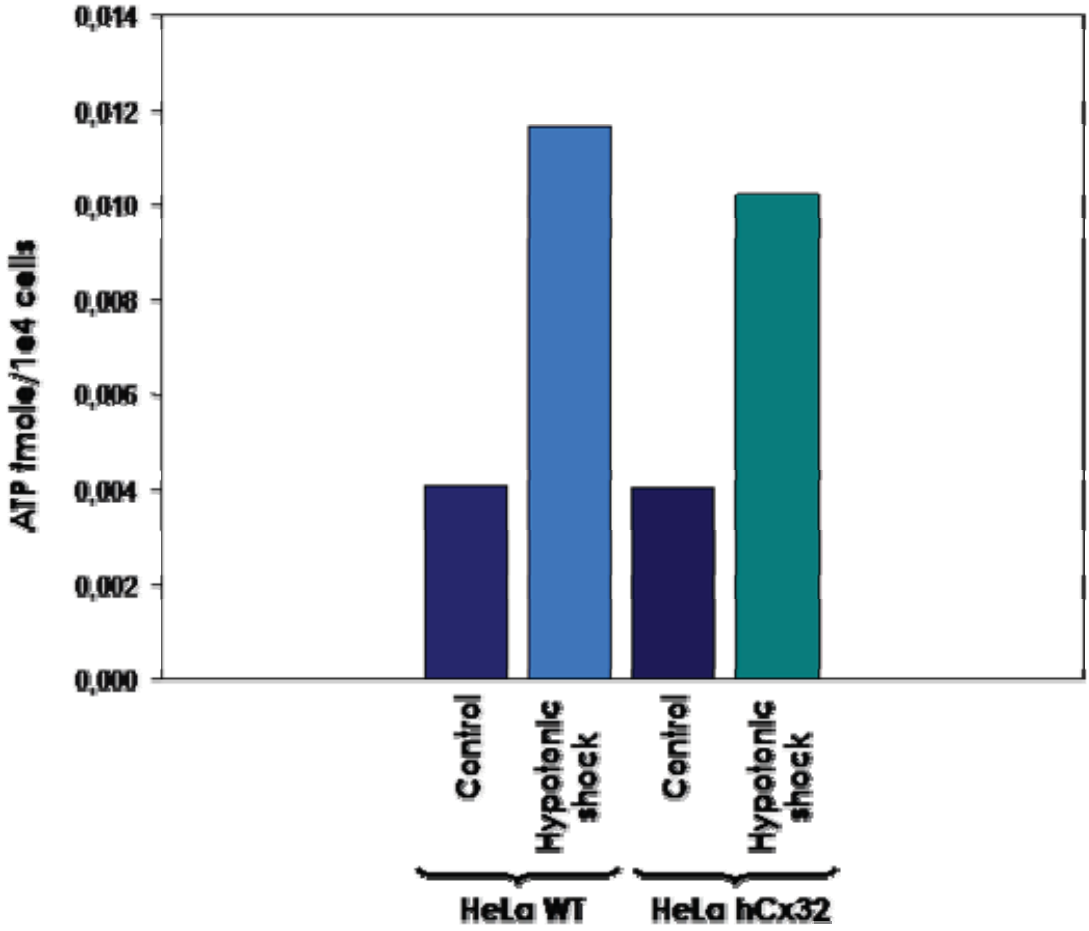

Figure R5-5 **|** Histogram representation of the ATP released from HeLa cells subjected to a hypotonic shock and its controls. The differences in ATP released due to the hypotonic shock are significant compared to the control groups, with p<0,001 both for HeLa WT cells and HeLa hCx32 transfected cells. There are no significant differences between HeLa WT cells and HeLa hCx32 transfected cells.

5.2.1 Hypotonic shock on HeLa cells preincubated with Brefeldin A.

After these results we wanted to test if exocytosis is the main pathway for the release of ATP in the hypotonic shock assays. For that, we treated WT and hCx32 transfected HeLa cells with Brefeldin A, a drug that disrupts the Golgi apparatus and inhibits the exocytosis. We performed again hypotonic shock assays with cultured WT HeLa cells preincubated or not with Brefeldin A 5µM as described in materials and methods (see section 12.2.2). In these assays, we saw again a quick ATP release from WT HeLa cells after the hypotonic shock. Indeed, the same levels of ATP release were recorded from BFA and non BFA preincubated WT HeLa cells (*Figure R5-6*).

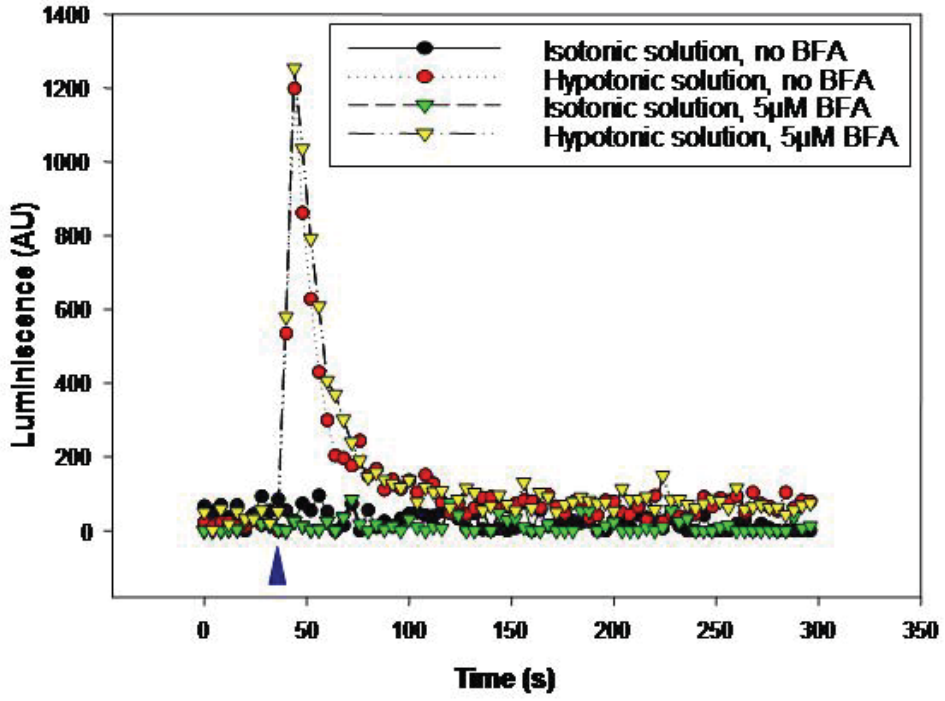

Figure R5-6 **|** Graphic representation of the ATP released from WT HeLa cells subjected to a hypotonic shock, and its controls, with and without Brefeldin A preincubation. Blue arrowhead: injection of solutions. AU: arbitrary units.

We made the same assays we had done for WT HeLa cells with hCx32 stable transfected HeLa cells. When performed the hypotonic shock assays with and without previous BFA preincubation we saw the same response we had seen for WT HeLa cells and no differences were detected when comparing ATP released from cells princubated with BFA with ATP released from control, non-preincubated cells (*Figure R5-7*).

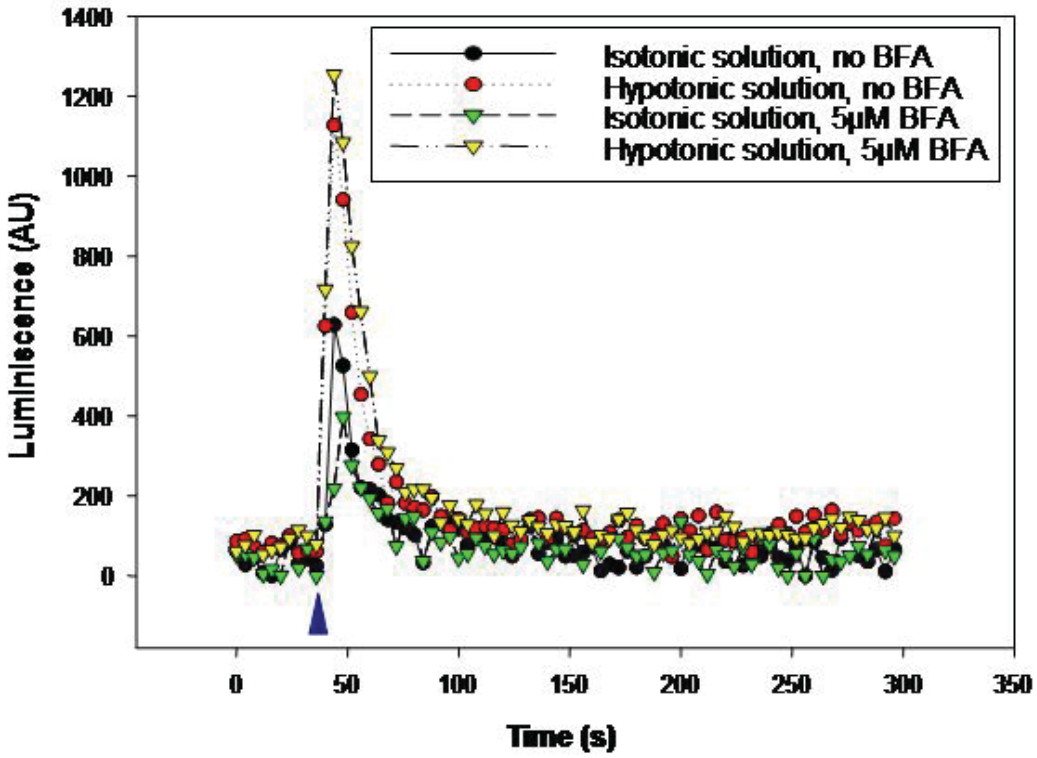

Figure R5-7 **|** Graphic representation of the ATP released from HeLa hCx32 transfected cells subjected to a hypotonic shock and its controls, with and without Brefeldin A preincubation. Blue arrowhead: injection of solutions. AU: arbitrary units.

Table R5-2 summarizes the results obtained. Hypotonic conditions increased the release of ATP in WT and hCx32 transfected HeLa cells, which is insensitive to BFA preincubation. Again, the ATP released under hypotonic shock was no significantly different when compared WT and hCx32 transfected

HeLa cells. However, the basal release of ATP due to shear stress in WT HeLa cells is decreased by BFA ($p<0.05$), which indicates that this release of ATP triggered by shear stress is due to exocytosis. In Cx32 transfected cells, the mean ATP release is increased, but not significantly, in BFA condition.

ATP	HeLa WT		HeLa hCx32	
fmole/10^4cells	No BFA	5µM BFA	No BFA	5µM BFA
Isotonic solution	$17x10^{-3}$ $\pm10x10^{-3}$ n=4	$9.49x10^{-3}$ $\pm3.87x10^{-3}$ n=5	$18.9x10^{-3}$ $\pm0.9x10^{-3}$ n=4	$21.1x10^{-3}$ $\pm5.76x10^{-3}$ n=5
Hypotonic solution	$34x10^{-3}$ $\pm10.8x10^{-3}$* n=8	$29.6x10^{-3}$ $\pm8.83x10^{-3}$* n=10	$33x10^{-3}$ $\pm7.33x10^{-3}$* n=8	$34.4x10^{-3}$ $\pm7.92x10^{-3}$ n=10

Table R5-2 **|** Table of ATP released from HeLa cells in response to a hypotonic shock, with and without preincubation with 5µM Brefeldin A. *: the differences compared to the isotonic solution are significant, $p<0.005$.

The same data is represented in a histogram graphic in the next figure (*Figure R5-8*):

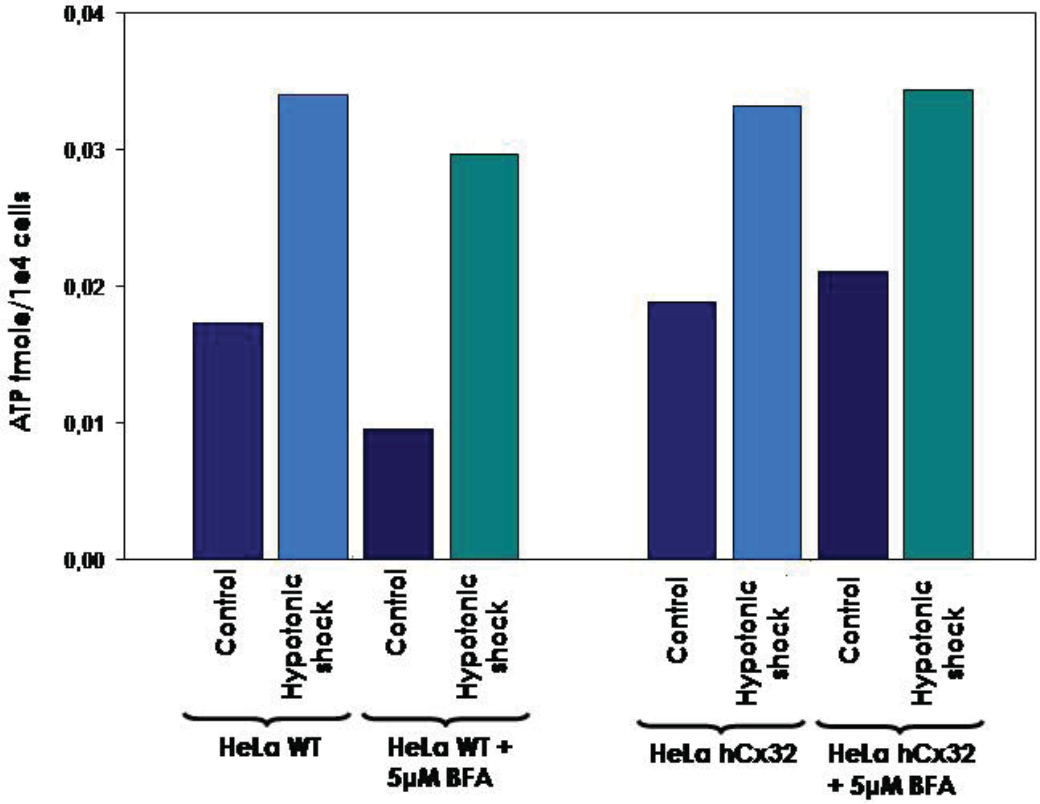

Figure R5-8 **| Histogram representation of the ATP released from WT and hCx32transfected HeLa cells subjected to a hypotonic shock with and without BFA 5 µM preincubation**. **Left**: ATP released from WT HeLa cells. The differences in ATP released due to the hypotonic shock are significant compared to the control groups, both for WT HeLa without and with BFA preincubation. There are also significant differences between the two isotonic (without hypotonic shock) groups (without and with BFA preincubation) with a p=0.018. **Right**: ATP released from hCx32 transfected HeLa cells. The differences in ATP released due to the hypotonic shock are significant compared to the isotonic groups; both for HeLa WT without and with BFA preincubation but there are no differences between both hypotonic shock groups, with and without BFA preincubation. There are no significant differences between the two isotonic groups.

5.2.2 Hypotonic shock on HeLa cells transfected with Syntaxin 1A.

Finally, we also performed the hypotonic shock assays with WT and hCx32 transfected HeLa transiently transfected with the SNARE protein syntaxin 1A, as we had already seen an inhibitory effect of the syntaxin 1A upon the hCx32 in the experiments

performed with *Xenopus* oocytes. We did again hypotonic shock assays with cultured WT HeLa cells with and without previous transfection with Syntaxin 1A as explained on materials and methods (see section 12.2.1). In these assays we saw once more a quick ATP release from WT HeLa cells after the hypotonic shock compared to the isotonic groups. We obtained the same response from S1A transfected WT HeLa cells 24 hours after transfection (*Figure R5-9*).

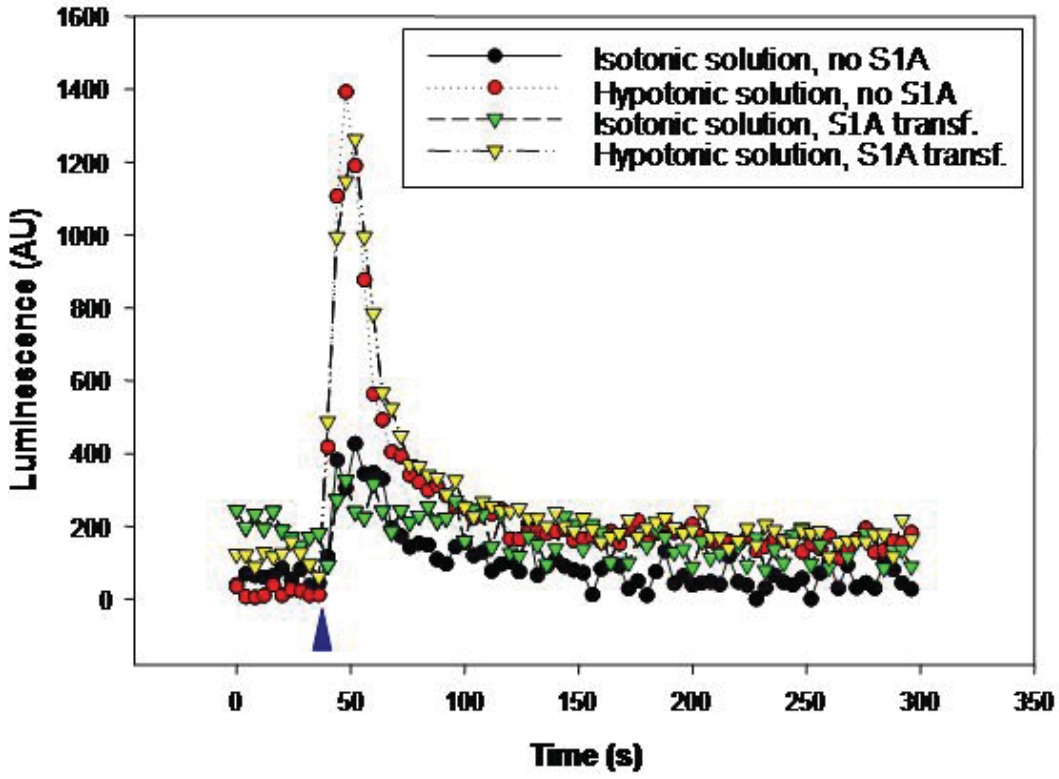

Figure R5-9 **|** Graphic representation of the ATP released from HeLa WT cells subjected to a hypotonic shock and its controls, with and without transient transfection with S1A. Blue arrowhead: injection of solutions. AU: arbitrary units.

Again, we made the same assays we had done for WT HeLa cells with hCx32 stable transfected HeLa cells. When we transiently transfected the hCx32 transfected HeLa cells with

S1A and performed the hypotonic shock assays we saw the same response we had for WT HeLa cells: a quick release of ATP after the hypotonic shock. There were no differences between the cells transiently transfected with S1A and the cells that were not transfected (*Figure R5-10*).

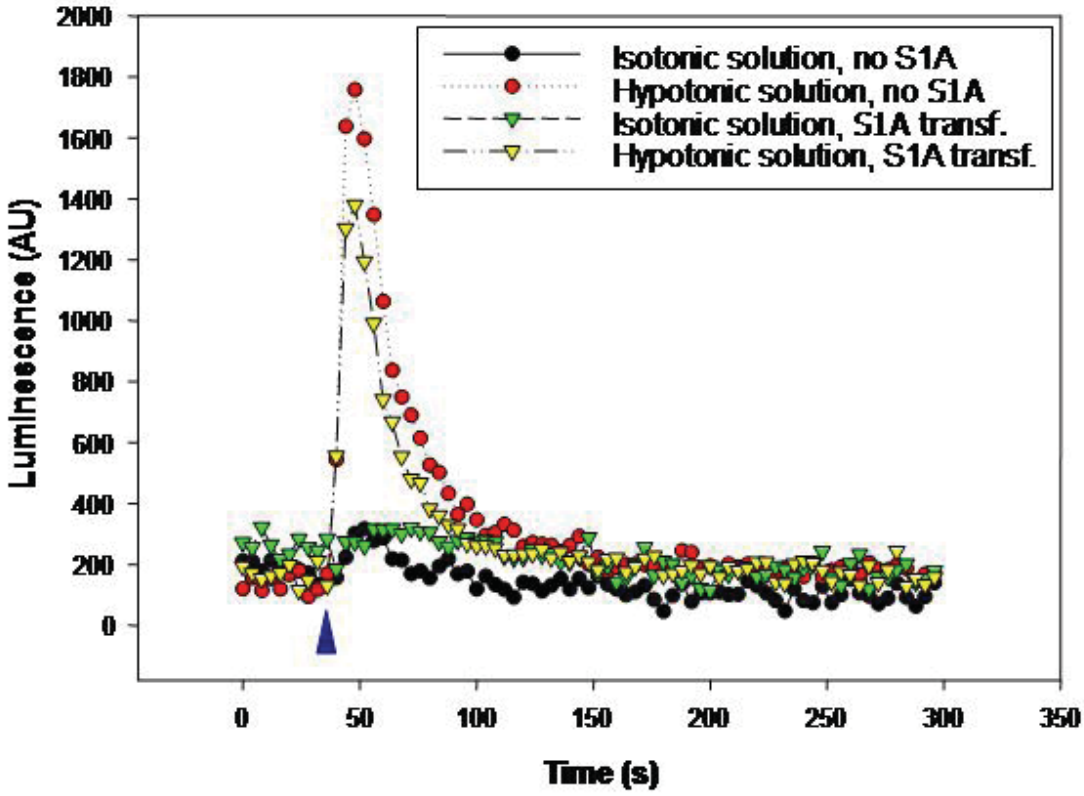

Figure R5-10 **|** Graphic representation of the ATP released from HeLa hCx32 cells subjected to a hypotonic shock and its controls, with and without transient S1A transfection. Blue arrowhead: injection of solutions. AU: arbitrary units.

Table R5-3 summarizes the results obtained. Hypotonic conditions increased the release of ATP in WT and hCx32 transfected HeLa cells, and these release is not affected by S1A transfection. Again, the ATP released under hypotonic shock was no significantly different when compared WT and hCx32 transfected HeLa cells. The basal release of ATP due to shear

stress in WT HeLa cells is significantly increased by transfection with S1A ($p<0.05$), which was not in Cx32 transfected cells.

ATP fmole/10^4cells	HeLa WT		HeLa hCx32	
	No S1A	S1A Transf.	No S1A	S1A Transf.
Isotonic solution	$2.71x10^{-3}$ $\pm0.64x10^{-3}$ n=3	$5.63x10^{-3}$ $\pm2.35x10^{-3}$ n=4	$1.64x10^{-3}$ $\pm0.22x10^{-3}$ n=4	$4.15x10^{-3}$ $\pm2.45x10^{-3}$ n=4
Hypotonic solution	$6.41x10^{-3}$ $\pm1.39x10^{-3}$* n=8	$7.49x10x^{-3}$ $\pm1.026x10^{-3}$ n=8	$8.49x10x^{-3}$ $\pm1.85x10^{-3}$* n=8	$6.36x10^{-3}$ $\pm1.27x10^{-3}$ n=8

Table R5-3 **|** Table of ATP released from HeLa cells in response to a hypotonic shock, with and without transfection with Syntaxin 1A. *: the differences compared to the isotonic solution are significant, $p<0.005$.

The same data is represented in a histogram graphic in *Figure R5-11*.

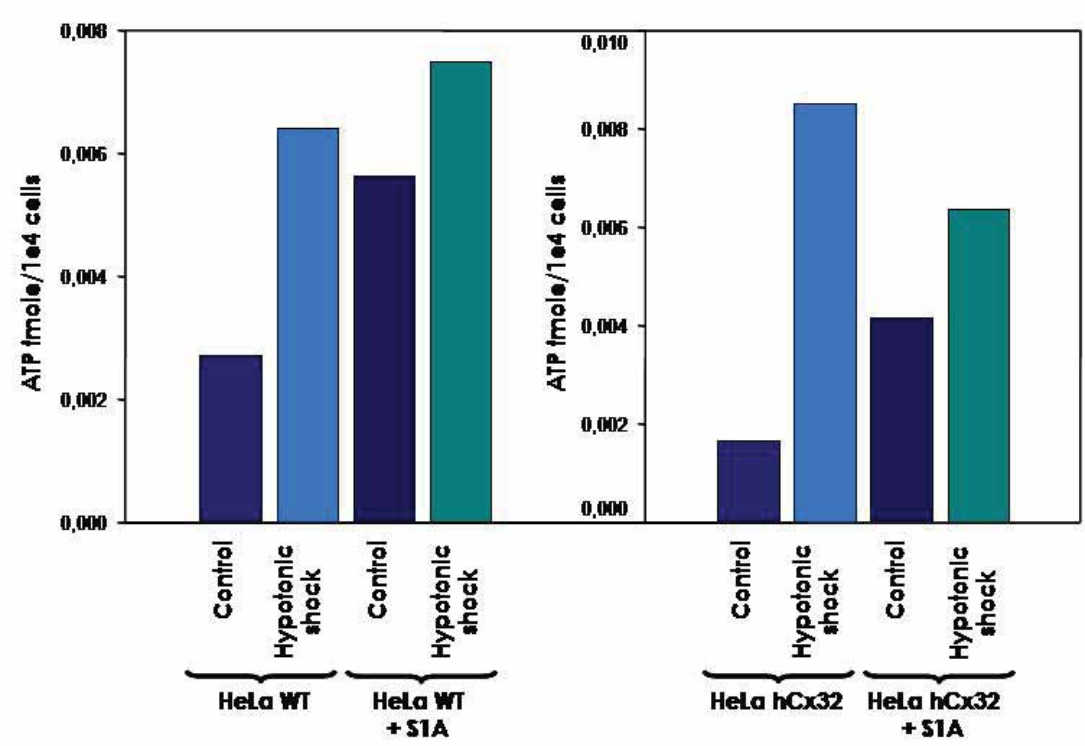

Figure R5-11 **| Histogram representation of the ATP released from WT and hCx32 HeLa cells subjected to a hypotonic shock with and without transient transfection with S1A**. **Left:** ATP released from WT HeLa cells. There are significant differences between the control-isotonic group and hypotonic shock group of WT HeLa cells ($p<0.005$) but there are not significant differences between the isotonic and hypotonic shock group of WT HeLa cells transiently transfected with S1A, probably due to the increase of ATP release in the control-isotonic group compared to the untransfected control-isotonic group, as there are significant differences between the two control-isotonic groups (without and with S1A transfection), $p<0.05$. There are no significant differences between the ATP released after a hypotonic shock from HeLa WT cells without and with S1A transfection. **Right:** ATP released from hCx32 HeLa cells. There are significant differences between the control-isotonic and hypotonic shock group of hCx32 HeLa cells ($p<0.001$) but there are not significant differences between the control-isotonic and hypotonic shock group of hCx32 HeLa cells transiently transfected with S1A, again, probably due to the increase of ATP release in the control group. There are no significant differences between the ATP released after a hypotonic shock from hCx32 transfected HeLa cells without and with S1A transfection.

DISCUSSION

Gap junctions allow electrical and metabolical communication between adjacent cells. One gap junction is composed of two hemichannels, each one expressed in the plasma membrane of each adjacent cell. One hemichannel is composed of six connexins. As it has been reported, hemichannels can form gap junctions together with another hemichannels [8, 11], or can have other functions as independent ionic channels in the cell plasma membrane [12, 17, 201]. Several groups have suggested that ATP can be released via connexin hemichannels in cells like astrocytes, osteoblasts or corneal endothelial cells [14, 16, 18, 129, 134, 135], where ATP release has been related to propagation of calcium waves. This role of connexin hemichannels in ATP release had to be demonstrated against a historical background of other ATP-release mechanisms like exocytosis [112, 132, 202], ABC (ATP-binding cassette) transporters [203], diffusion via $P2X_7$ [133, 203] receptor channels, etc.

In previous studies in our laboratory, ATP release through the *Xenopus laevis* oocyte endogenous connexin (Cx38) was already documented [138] in response to low calcium concentration, together with an outward current which had been previously reported [204-207]. This current was reversibly inactivated by calcium presence and was inhibited by gap junctions unspecific inhibitors like octanol and fluflenamic acid, and by Cx38 antisense oligonucleotide injection. Parallel to this calcium-sensitive currents ATP release from the oocytes was also recorded, and, like the currents, was inhibited by octanol, flufenamic acid and Cx38 antisense oligonucleotide injection.

With these results in hand we wanted to know if other connexin hemichannels could also release ATP. We kept on using the *Xenopus laevis* experimental model because is easy to express other connexins only injecting the cRNA, and we could record ionic currents and ATP release simultaneously in one single cell.

As ATP release has already been documented for Cx43 [16] and Cx38, and human Cx32 has been related to the X-linked form of Charcot-Marie-Tooth disease [4] we wanted to know if hCx32 was permeable to ATP, and if there is any relation between ATP release through Cx32 hemichannels and CMTX symptoms. For that hCx32 was expressed in *Xenopus* oocytes and was activated using a depolarizing protocol. In response we recorded an outward current characteristic for hCx32 [22, 36]. The possible inteferences of endogenous oocyte Cx38 were abolished injecting Cx38 antisense oligonucleotide together with hCx32 cRNA 48 hours before the recordings were actually performed. The outward currents recorded became inward currents abruptly once the depolarization stimuli ended and membrane potential went back to resting potential, and a long lasting tail current appeared. It was during this tail current that ATP release was detected. This ATP release during the tail current makes sense, because in our experimental conditions the equilibrium potential for ATP is highly positive, and extracellular ATP concentration is nearly zero. During the depolarization stimulus the potential is positive and ATP do not cross through hemichannels even when they are in their open state, because membrane potential is

close to ATP equilibrium potential. But during the tail current the membrane potential returns to negative values while hCx32 hemichannels are still in an open state, allowing ATP to cross the membrane and be released (*Figure D1*).

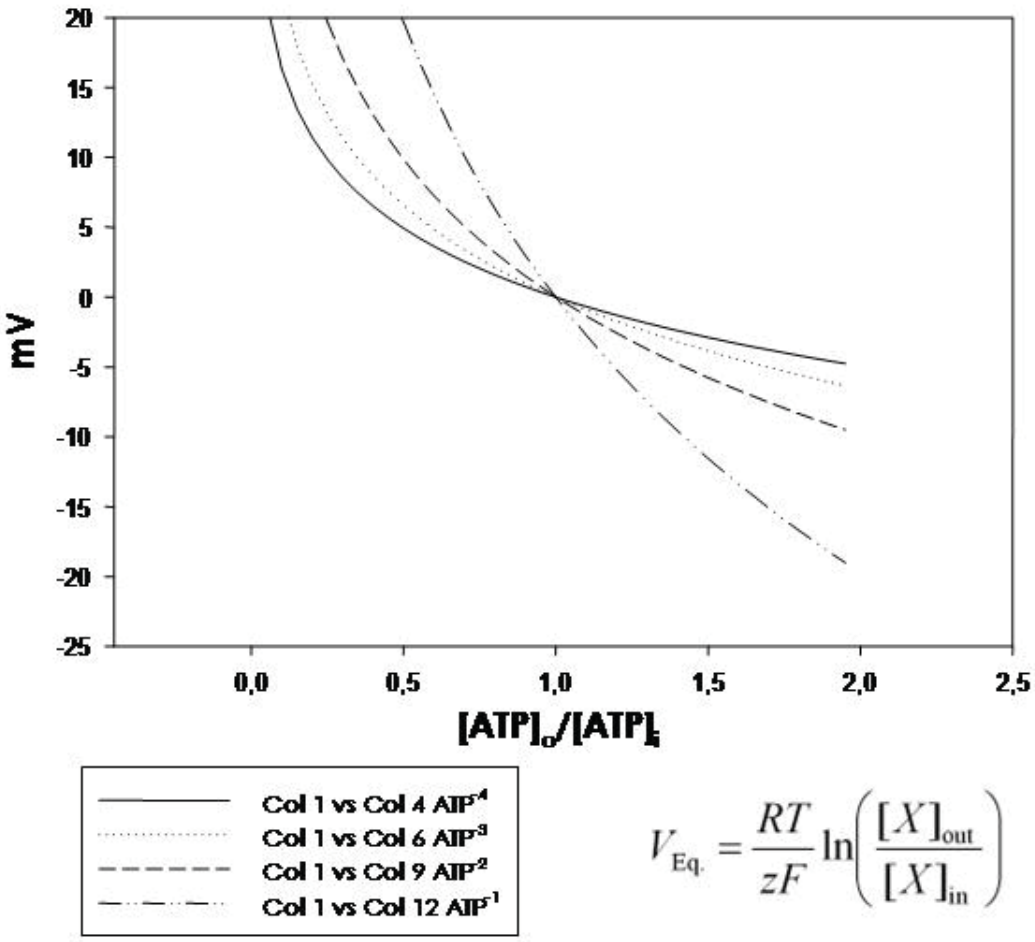

Figure D1 **|** Graphic representation of the ATP reversal potential calculated using the Nernst equation (bottom, right). When the extracellular ATP concentration is close to zero, the equilibrium potential is very positive.

We could establish a direct relation between the tail current electric charge and the amount of ATP released. As we had already seen in our laboratory, this relation is enforced when we applied the depolarizing protocol using a calcium free buffer, which enhances hCx32 hemichannels opening [22]. Under this

condition, we could observe not only a greater outward and tail currents but also higher amounts of ATP release. Moreover, to be sure that ATP was released through hemichannels and not by exocytosis [208], the assays were repeated after treating the *Xenopus* oocytes with Brefeldin A. ATP release was unaffected by this treatment, discarding the exocytic pathway for the majority of the recorded ATP release. After all these results obtained in our laboratory, we can say that hCx32 expressed in *Xenopus laevis* oocytes can be activated by depolarization and that, under this condition, ATP is released.

As Cx32 is expressed in Schwann cells among other cell types [209], and after demonstrating that hCx32 can release ATP when expressed in *Xenopus* oocytes, we wanted to know if Schwann cells can release ATP through Cx32. For this study we decided to use sciatic nerves from mice and rats, which have intact myelinating Schwann cells wrapping the axons. Plasma membrane depolarization opens hCx32 hemichannel. Accordingly, a depolarizing stimulus was applied to the whole nerve with a suction electrode, trying to imitate action potentials, the physiological stimulus that might trigger Cx32 hemichannels opening *in vivo*. We used a cooled high sensitive camera and the luciferin-luciferase reaction to capture the ATP release from the sciatic nerve. With this approach, we observed ATP release in response to electrical stimuli, which seemed to be focalized to certain periodical regions along the nerve. We hypothesized then that these ATP-release regions could correspond to the nodes of Ranvier, as they are also distributed periodically along axons of

nerves and Cx32 is highly expressed in the paranodal regions [176]. We performed immunofluorescences to find connexins (section 8 on materials and methods), and we could confirm that Cx32 is expressed in paranodes and Schmidt-Lanterman incisures of teased mice sciatic nerves. Together with Cx32 localization, we also performed immunostainings for the two other connexins described to be expressed in Schwann cells: Cx29 and Cx43.

Cx29 was reported to be expressed in paranodes and Schmidt-Lanterman incisures [59, 179], an expression pattern that we could confirm from our immunostainings, although it has also been reported to be expressed in the juxtaparanode [59], which we could not confirm as we observed no immunostaining for Cx29 in juxtaparanodal regions of mice sciatic nerve. Previous studies using freeze-fracture replica and immunogold labelling of sciatic nerve had reported that Cx29 is expressed in the innermost layers of myelin, while Cx32 is expressed in the outermost layers of myelin [179]. These results could not be either confirmed or rejected in our studies due to the immunostaining resolution.

On the other hand, Cx43 had been reported to be expressed but at low intensity along the myelin sheath of rat sciatic nerve [70]. But, although we also detected its expression along the myelin sheath and this expression was lower compared to Cx32 or Cx29 staining, the Cx43 localization was more intense in paranodal regions that in the rest of the myelin sheath, an observation that has not been reported before.

The function of Cx29 and Cx43 within Schwann cells myelin

sheath is yet unclear but Cx29 has been proposed to also contribute to the radial pathway described for Cx32 hemichannels [14], as in Cx32 null-mice still there's low mass weight dye diffusion through this pathway [40]. However, and as Cx32 null-mice develop a late-onset progressive demyelination neuropathy similar to CMTX [52], Cx29 can not fully replace Cx32 function and it must have another role in the peripheral myelin sheath physiology.

The function of Cx43 is even more mysterious at this time but it has been related to the Wallerian degeneration and remyelination processes after a nerve injury [180], as its expression is enhanced under these circumstances, and gets back to low basal expression in regenerated myelin sheaths after injury.

Considering that sciatic nerve releases ATP under depolarizing stimulus and that we detected the expression of three different connexins in paranodal zones, which are periodically repeated along axons, we wanted to make sure that the ATP release that we saw was from Schwann cells itself and not from other nerve components, that's why we started to culture Schwann cells from adult mice sciatic nerve. We wanted to check the connexin expression in cultured Schwann cells. It had been described that they still express Cx32 and Cx43 [70], and though there's no data about Cx29 it was presumed that they also expressed this connexin. We did immunostainings for these three connexin and found expression of all of them in Schwann cell primary cultures. Staining was localized all along the cell bodies, Cx32 showed the highest expression level, whereas Cx43

showed the lowest expression with a more intense mark around nuclei.

Once demonstrated that cultured Schwann cells express connexins, and that the most intensively connexin expressed is Cx32, it was the moment to activate Cx32 hemichannels on the Schwann cell membrane. As mechanical stimuli have been described to trigger hemichannel opening [20, 21], and release of ATP through hemichannels has been described in osteoblasts [134] and corneal epithelial cells [135] under mechanical stimulation, we decided to stimulate Schwann cell primary cultures with an hypotonic shock. Moreover, hypotonic conditions induce cell swelling and, in this condition, ATP is a necessary signal for the cells to recover their volume through a process known as regulated volume decreased (RVD). This process implies an autocrine and paracrine ATP effect through purinergic receptors (both P2Y and P2X), that would activate G-coupled proteins and an eventual intracellular Ca^{2+} increase, which would activate K^+ and Cl^- extrusion, necessary for the cell volume recovery [210]. The mechanism by which ATP is released after the hypotonic stimulus is yet unclear. Exocytosis, ionic channels and transporters have been proposed, and it is thought nowadays that multiple release mechanism are involved [211].

ATP release was detected using luciferin-luciferase luminescent reaction and we could see a fast ATP release response from Schwann cell to a hypotonic shock. The amount of ATP released was of $2.5x\ 10^{-4}$ fmole/10^4cells, which is significantly greater ($p=0.024$) than the ATP released from

control Schwann cells, that didn't received the hypotonic shock, which released 3.03x 10^{-5} fmole/10^4cells. However, it was not clear if this ATP was released across Cx32 hemichannels.

To further study the possible implication on Cx32 in ATP release we repeated the hypotonic shock assays with hCx32 stable transfected HeLa cells, using as a control group WT HeLa cells. We worked with HeLa cells because they are widely used for connexin-transfection studies [212-214], because wild type HeLa cells do not form gap junctions [215, 216] and have a very low expression of endogenous connexins. So, we used WT HeLa cells as biological model, and performed the hypotonic assays both with WT and hCx32 transfected HeLa cells. We could record a significant ATP release from cells that had undergone the hypotonic shock, compared to those that had not, but we could not see significant differences between wild type and hCx32 transfected HeLa cells. Cells suffering the hypotonic shock showed a mean ATP release of 0.0117 fmole/10^4 cells for HeLa WT cells, while there was a mean ATP release of 0.0102 fmole/10^4 cells for hCx32 transfected HeLa cells. So our results indicated that ATP released in response to hypotonic shock was not mainly released through Cx32 hemichannels in HeLa cells. To check if it could be released by the exocytic pathway, the assays were repeated but with a previous incubation of both WT and hCx32 transfected HeLa cells with Brefeldin A, a drug that disrupts the Golgi apparatus, and, in consequence, exocytosis [208, 217]. But we could not find significant differences between the ATP released in response to the hypotonic shock, either for WT

or for hCx32 transfected HeLa cells when we compared the assays without BFA preincubation with the ones that were preincubated for 5-7 hours with an isotonic solution containing 5μM BFA. We concluded the ATP release from these cells in response a hypotonic shock is not released through exocytosis, but by another pathway probably involving different channels. Interestingly, in these assays we could detect a change in the ATP release from the control cells that did not received the hypotonic shock but had the shear stress stimuli triggered by the injection of solution in the cultured wells. In this case the HeLa cells preincubated with BFA showed a reduction in the ATP release compared with the controls not preincubated with BFA (although it was only significant for WT HeLa cells, hCx32 transfected HeLa cells preincubated with BFA also had a smaller mean of ATP released), indicating that exocytosis could be the main mechanism by which ATP is release in response to shear stress.

In this study there are many open doors to new experimental approaches to research upon Cx32 and ATP release, and ATP release mechanisms from Schwann cells and sciatic nerve. However, the present work has also generated new tools to keep on with this study: First, five hCx32 mutated forms, all of them in a *Xenopus laevis* expression plasmid and in a eukaryotic expression plasmid.

All mutations (S26L, P87A, Del111-16, D178Y, and R220St) were described in patients with CMTX and have been, in a more

or less extent, described before [22, 41-43]. For more information on the characteristics of each mutation see introduction (section 2.5). The constructs into the *Xenopus* expression vector (pBxG) are ready to obtain cRNA and perform TEVC experiments with Xenopus oocytes injected with the mutated forms of Cx32, and record currents and ATP release. These experiments could tell us if any of the mutations affect or not the ability of hCx32 to release ATP under a depolarizing stimulus, and if so, if it could be a part of the mechanism leading to CMTX phenotype. Constructs into the eukaryotic expression vector (pMJgreen) are also ready to be transfected to HeLa, Neuro 2A or another cell line with connexin low expression to perform further analysis of hCx32 mutations behaviour by performing more hypotonic shock assays or other experiments.

Second, WT hCx32, P87A and S26L stable transfected HeLa cells, which can be used in hypotonic shock assays or other kinds of assays to test hCx32 behaviour. The other constructs (Del 111-16, D178Y and R220St) have no stable transfected cell line but are ready to perform transient or stable transfections in eukaryotic cells.

In our laboratory we have been working with the hypothesis that ATP release could be involved with CMTX disease. But how could this happen?

In Schwann cells ATP release has already been described in response to glutamate [193] and UTP [192], and this release has been related to exocytosis and anionic channels. In other glial cells,

such as astrocytes, different mechanisms for ATP release have been described: exocytosis [218], anionic channels [202] and hemichannels [16]. We think that Schwann cells can also release ATP by different mechanism, among them, Cx32 hemichannels.

As it has been described before (see section 5.2 on the introduction), Cx32 in Schwann cells is expressed in paranodal regions, close to the axon. In this location Cx32 could sense the depolarization triggered by action potentials and become active, open hemichannel pores and release ATP to the extracellular medium. This ATP would, in turn, activate $P2X_7$ and $P2Y_2$ purinergic receptors, also expressed in Schwann cells [157, 185, 186].

However, $P2X_7$ receptor needs high ATP concentrations (in the range of millimolar), and would normally be in a low conductance state [219, 220]. On the other hand, $P2Y_2$ can be activated at lower ATP concentrations, and trigger an increase of intracellular calcium concentration, which would activate other intracellular signals, some of them presumably involved in Schwann cell surviving.

Considering all these data and according to our hypothesis, when Cx32 is mutated, as it has been described in CMTX disease [4, 41, 46], two different alterations could occur to this signalling pathway (*Figure D-2*): (B) an increase or (C) a decrease of ATP release through Cx32 hemichannels.

On one hand, mutations on Cx32 that affect trafficking or lead to non-functional hemichannels would disrupt the ATP release through Cx32 hemichannels, and the amount of extracellular ATP would decrease, and so would do $P2Y_2$

activation, leading to cell death by a lack of survival stimulation (*Figure D-2, C*).

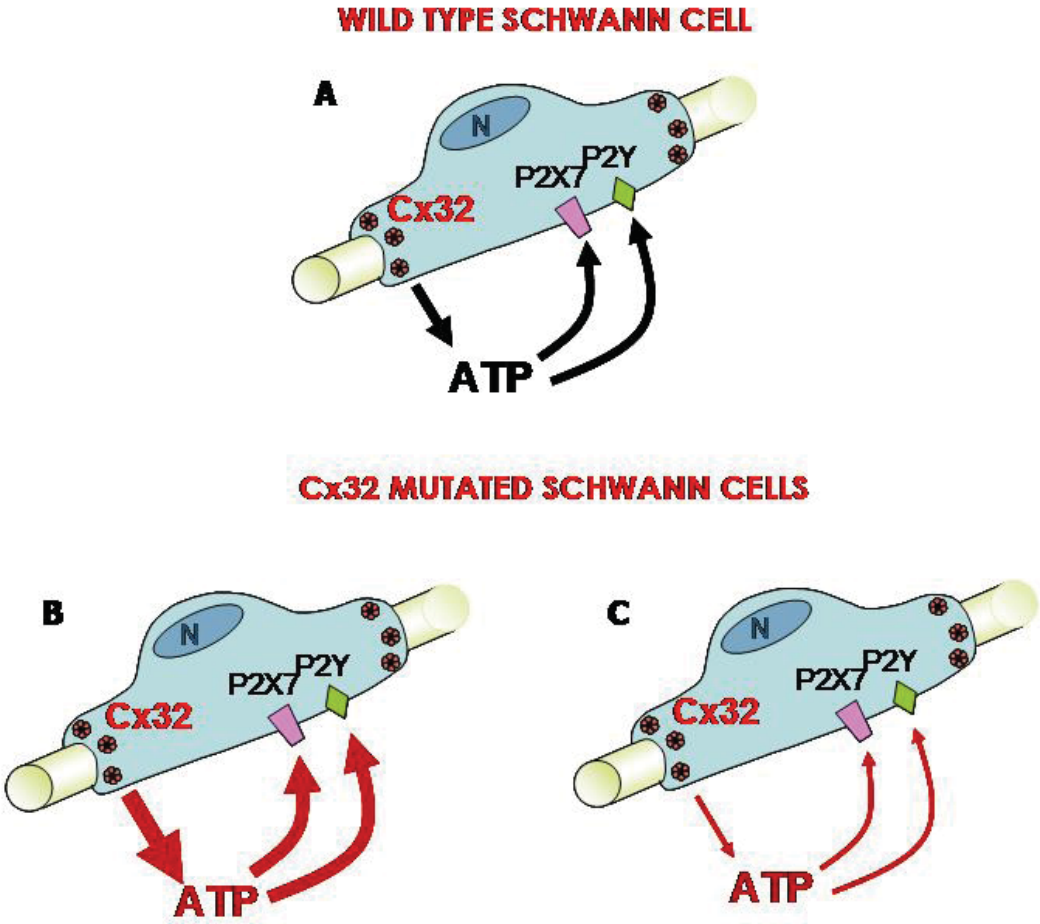

***Figure D-2* | Schematic representation of a Schwann cell in three different situations. A:** Schwann cell expressing wild type Cx32, through its hemichannels ATP is released for the correct cell function. **B:** Schwann cell expressing a Cx32 mutations that increase ATP release through hemichannels, triggering a greater activation of $P2X_7$ and P2Y purinergic receptors **C:** Schwann cell expressing a Cx32 mutations that inhibits or reduce the ATP release through hemichannels, leading to a reduced (and insufficient) activation of $P2X_7$ and/or P2Y receptors.

On the other hand, Cx32 mutations that form functional but altered hemichannels with a higher open probability would increase the total amount of extracellular ATP which would activate not only $P2Y_2$ receptors, but also the high conductance

of $P2X_7$ receptors, which has been related with necrosis and apoptosis [221, 222], and would lead to cell death (*Figure D-2, B*).

A similar hypothesis has been formulated to explain CNS glial cells response to injury [223]. So it would be interesting to characterise the hCx32 mutations regarding its capacity to release ATP, to see if at least one of these situations could actually occur, opening a new field of research for CMTX disease mechanisms. Another interesting approach to test this hypothesis would be to alter extracellular ATP concentrations in primary Schwann cell cultures and see if that leads to cell death or apoptosis.

And last but not least, a first glimpse of a possible interaction between Cx32 and S1A has been explored. As it as been explained in the introduction (section 3) S1A is a SNARE protein, and its first studied role was within the exocytotic machinery and the formation of the SNARE complex [92], together with SNAP 25 and synaptobrevin/VAMP1 and 2, responsible for the fusion of vesicles with the plasma membrane [94]. Later, many studies supported the idea that syntaxin 1A was able to regulate, through inhibition, many different kinds of ionic channels like R-,N- and L-type calcium channels [97-99], $K_v1.2$ potassium channels [101], calcium activated potassium channels (BKCa) [102], epithelial sodium channels (ENaC) [103] and CFTR channels [104]. Moreover, previous studies in our laboratory indicated that S1A was also able to inhibit currents generated by *Xenopus laevis* endogenous connexin (Cx38) (unpublished data).

With these antecedents we wanted to check if S1A could affect other connexins besides Cx38. Both cRNA coding for hCx32 and S1A were injected into Xenopus oocytes together with antisense against endogenous Cx38. TEVC recordings on oocytes coexpressing hCx32 and S1A were performed, again using a depolarizing stimulus to trigger hCx32 hemichannels opening. Outward currents and ATP release were simultaneously recorded and results were compared to those obtained from oocytes injected only with the hCx32 cRNA. We could see that S1A was able to partially inhibit outward currents (a 15% inhibition was observed). However, the most striking result was found both in ATP release, where an inhibition of about 45 % was obtained, and in the tail current electric charge, which had a 52% inhibition, which is much greater than the inhibition observed for the outward currents.

Although connexins are rather non-specific channels, and it has been reported that everything smaller than 1000Da can cross them [12], different connexins have different conductance values and different permeabilities, which would permit the discrimination of ions and second messengers [224]. It has been described that, in some connexins, certain charges at the cytoplasmic amino terminal [225] or extracellular loops [226] may contribute to ion and metabolite selectivity. Some studies support the idea that permeability does not only depend on pore size, and suggest charge interactions [227] and/or the molecular structure of the permeants [212] as discriminating factors. Thus, although Cx32 is one of the biggest among the connexin family

[10], it has been reported to have preference for adenosine and, in a less extent, for ATP [10]. Together with the fact that Cx32 has been described as an anionic channel [12], and ATP has negative charge (ATP^{-4}), our results could be due to a special feature that allows Cx32 to release ATP, which would be affected by S1A in a different way than merely altering hemichannels open probability, as it could affect a determinate subconductance state. Moreover, we performed immunostainings of mice sciatic nerve to see the localization of Cx32 and S1A. We could see that they are closely expressed in some parts of that nerve. So a possible direct or indirect interaction between these two molecules would be possible in mice sciatic nerve.

To try to get more data about that possible interaction between Cx32 and S1A both WT and stable hCx32 transfected HeLa cells were transiently transfected with S1A and hypotonic assays were performed. No differences in the ATP released after the hypotonic shock were observed between S1A transfected (24 hours after transfection) and untransfected cells, neither in the assays performed with WT HeLa cells, nor with the ones performed with hCx32 transfected HeLa cells. Since there were also no differences between hCx32 and wild type HeLa cells under hypotonic shock, it can be considered that Cx32 is not (or very poorly) reacting to the hypotonic stimulus when expressed in HeLa cells. On the other hand, when we compared the control groups (cells that were treated with isotonic solution and did not suffer a hypotonic shock) we saw differences in the amount of ATP released. We had an increase in the measured ATP on

controls of S1A transfected cells compared to untransfected cells (again it was only significant for WT HeLa cells, but S1A transiently transfected hCx32 HeLa cells also showed a greater mean ATP released compared to the untransfected control). This increase could be a consequence of S1A overexpression, which would increase the pool of vesicle docked to the plasma membrane, thus increasing the rate of exocytosis activated in response to the shear stress generated by the injection of solution during the assays. The fact that we saw no differences between S1A transfected hCx32 HeLa cells and control hCx32 HeLa cells doesn't mean there is no interaction between them, since we had the same results with WT HeLa cells, suggesting that the ATP was not mainly released through hCx32 hemichannels. This rather suggests that this is not a good model assay to study hCx32 role in ATP release, and its possible interaction with S1A in the ATP release, so further experimental approaches should be performed to elucidate this hypothesis.

CONCLUSIONS

- ✓ Human Cx32 expressed in *Xenopus* oocytes is activated by depolarizing potentials, a non-specific outward current is generated and ATP is released.

- ✓ This ATP release is associated to a tail current activated when the membrane potential return to resting values after a depolarizing pulse.

- ✓ Syntaxin 1A partially inhibits outward currents from Xenopus oocytes expressing Cx32 hemichannels.

- ✓ Syntaxin 1A inhibits in a much more extent the tail current electric charge and ATP release from Xenopus oocytes expressing Cx32 hemichannels.

- ✓ Connexin 32 and connexin 29 are expressed on paranodal regions and Schmidt-Lanterman incisures in mice sciatic nerve. Connexin 43 showed a weaker detection, with preferential expression in paranodes.

- ✓ Connexin 29 null mice have a normal pattern of expression of Cx32 in sciatic nerves.

- ✓ Connexin 32 null mice exhibit a decreased amount of Cx29 in sciatic nerve, which is enhanced with age, even though the expression pattern remains unaltered.

- ✓ Cultured Schwann cells express Cx32, Cx29 and Cx43.

- ✓ Mice and Rat sciatic nerve release ATP in response to electrical stimulation with a suction electrode. This release is concentrated to specific areas of the nerve.

- ✓ Primary cultures of Schwann cells release ATP under hypotonic conditions.

- ✓ HeLa cells respond to hypotonic shock releasing ATP. There are no differences between wild type and stable hCx32 transfected HeLa cells after a hypotonic shock.

- ✓ Both WT and hCx32 HeLa cells preincubated with 5μM BFA do not show significant differences in ATP released in response to hypotonic shock compared to not BFA preincubated cells.

- ✓ There is a reduction in ATP released from HeLa WT cells control groups preincubated with BFA, compared to controls not preincubated.

- ✓ There is an increase in ATP released from HeLa WT cells control groups transiently transfected with S1A, compared to controls not transfected.

- ✓ Both WT and hCx32 HeLa cells transiently transfected with

S1A do not show significant differences in ATP released in response to hypotonic shock compared to not transfected cells.

BIBLIOGRAPHY

1. Tanaka, Y. & Hirokawa, N. Mouse models of Charcot-Marie-Tooth disease. *Trends Genet* **18**, S39-44 (2002).
2. Muller, H.W. et al. Advances in Charcot-Marie-Tooth disease research: cellular function of CMT-related proteins, transgenic animal models, and pathomechanisms. The European CMT Consortium. *Neurobiol Dis* **4**, 215-20 (1997).
3. Suter, U. & Scherer, S.S. Disease mechanisms in inherited neuropathies. *Nat Rev Neurosci* **4**, 714-26 (2003).
4. Bone, L.J., Deschenes, S.M., Balice-Gordon, R.J., Fischbeck, K.H. & Scherer, S.S. Connexin32 and X-linked Charcot-Marie-Tooth disease. *Neurobiol Dis* **4**, 221-30 (1997).
5. Young, P. & Suter, U. The causes of Charcot-Marie-Tooth disease. *Cell Mol Life Sci* **60**, 2547-60 (2003).
6. Sohl, G. & Willecke, K. Gap junctions and the connexin protein family. *Cardiovasc Res* **62**, 228-32 (2004).
7. Oyamada, M., Oyamada, Y. & Takamatsu, T. Regulation of connexin expression. *Biochim Biophys Acta* **1719**, 6-23 (2005).
8. Kumar, N.M. & Gilula, N.B. The gap junction communication channel. *Cell* **84**, 381-8 (1996).
9. Theis, M., Sohl, G., Eiberger, J. & Willecke, K. Emerging complexities in identity and function of glial connexins. *Trends Neurosci* **28**, 188-95 (2005).
10. Sosinsky, G.E. & Nicholson, B.J. Structural organization of gap junction channels. *Biochim Biophys Acta* **1711**, 99-125 (2005).
11. Evans, W.H. & Martin, P.E. Gap junctions: structure and function (Review). *Mol Membr Biol* **19**, 121-36 (2002).
12. Bennett, M.V., Contreras, J.E., Bukauskas, F.F. & Saez, J.C. New roles for astrocytes: gap junction hemichannels have something to communicate. *Trends Neurosci* **26**, 610-7 (2003).
13. Paul, D.L., Ebihara, L., Takemoto, L.J., Swenson, K.I. & Goodenough, D.A. Connexin46, a novel lens gap junction protein, induces voltage-gated currents in nonjunctional plasma membrane of Xenopus oocytes. *J Cell Biol* **115**, 1077-89 (1991).
14. Goodenough, D.A. & Paul, D.L. Beyond the gap: functions of unpaired connexon channels. *Nat Rev Mol Cell Biol* **4**, 285-94 (2003).
15. Saez, J.C., Retamal, M.A., Basilio, D., Bukauskas, F.F. & Bennett, M.V. Connexin-based gap junction hemichannels: gating mechanisms. *Biochim Biophys Acta* **1711**, 215-24 (2005).
16. Stout, C.E., Costantin, J.L., Naus, C.C. & Charles, A.C. Intercellular calcium signaling in astrocytes via ATP release through connexin hemichannels. *J Biol Chem* **277**, 10482-8 (2002).
17. Ebihara, L. New roles for connexons. *News Physiol Sci* **18**, 100-3 (2003).
18. Cotrina, M.L. et al. Connexins regulate calcium signaling by controlling ATP release. *Proc Natl Acad Sci U S A* **95**, 15735-40 (1998).
19. Li, H. et al. Properties and regulation of gap junctional hemichannels in the plasma membranes of cultured cells. *J Cell Biol* **134**, 1019-30

(1996).
20. Schlosser, S.F., Burgstahler, A.D. & Nathanson, M.H. Isolated rat hepatocytes can signal to other hepatocytes and bile duct cells by release of nucleotides. *Proc Natl Acad Sci U S A* **93**, 9948-53 (1996).
21. Bao, L., Sachs, F. & Dahl, G. Connexins are mechanosensitive. *Am J Physiol Cell Physiol* **287**, C1389-95 (2004).
22. Gomez-Hernandez, J.M., de Miguel, M., Larrosa, B., Gonzalez, D. & Barrio, L.C. Molecular basis of calcium regulation in connexin-32 hemichannels. *Proc Natl Acad Sci U S A* **100**, 16030-5 (2003).
23. Ripps, H., Qian, H. & Zakevicius, J. Pharmacological enhancement of hemi-gap-junctional currents in Xenopus oocytes. *J Neurosci Methods* **121**, 81-92 (2002).
24. Trexler, E.B., Bukauskas, F.F., Bennett, M.V., Bargiello, T.A. & Verselis, V.K. Rapid and direct effects of pH on connexins revealed by the connexin46 hemichannel preparation. *J Gen Physiol* **113**, 721-42 (1999).
25. Gonzalez, D., Gomez-Hernandez, J.M. & Barrio, L.C. Molecular basis of voltage dependence of connexin channels: an integrative appraisal. *Prog Biophys Mol Biol* **94**, 66-106 (2007).
26. Revilla, A., Castro, C. & Barrio, L.C. Molecular dissection of transjunctional voltage dependence in the connexin-32 and connexin-43 junctions. *Biophys J* **77**, 1374-83 (1999).
27. Bukauskas, F.F. et al. Clustering of connexin 43-enhanced green fluorescent protein gap junction channels and functional coupling in living cells. *Proc Natl Acad Sci U S A* **97**, 2556-61 (2000).
28. Stergiopoulos, K. et al. Hetero-domain interactions as a mechanism for the regulation of connexin channels. *Circ Res* **84**, 1144-55 (1999).
29. Liu, S. et al. A structural basis for the unequal sensitivity of the major cardiac and liver gap junctions to intracellular acidification: the carboxyl tail length. *Biophys J* **64**, 1422-33 (1993).
30. Homma, N. et al. A particle-receptor model for the insulin-induced closure of connexin43 channels. *Circ Res* **83**, 27-32 (1998).
31. Liu, F., Arce, F.T., Ramachandran, S. & Lal, R. Nanomechanics of hemichannel conformations: connexin flexibility underlying channel opening and closing. *J Biol Chem* **281**, 23207-17 (2006).
32. Revilla, A., Bennett, M.V. & Barrio, L.C. Molecular determinants of membrane potential dependence in vertebrate gap junction channels. *Proc Natl Acad Sci U S A* **97**, 14760-5 (2000).
33. Kumar, N.M. & Gilula, N.B. Cloning and characterization of human and rat liver cDNAs coding for a gap junction protein. *J Cell Biol* **103**, 767-76 (1986).
34. Paul, D.L. Molecular cloning of cDNA for rat liver gap junction protein. *J Cell Biol* **103**, 123-34 (1986).
35. Harris, A.L. Emerging issues of connexin channels: biophysics fills the gap. *Q Rev Biophys* **34**, 325-472 (2001).
36. Castro, C., Gomez-Hernandez, J.M., Silander, K. & Barrio, L.C. Altered formation of hemichannels and gap junction channels caused by C-terminal connexin-32 mutations. *J Neurosci* **19**, 3752-60 (1999).

37. De Vuyst, E. et al. Intracellular calcium changes trigger connexin 32 hemichannel opening. *EMBO J* **25**, 34-44 (2006).
38. Bergoffen, J. et al. Connexin mutations in X-linked Charcot-Marie-Tooth disease. *Science* **262**, 2039-42 (1993).
39. Scherer, S.S. et al. Connexin32 is a myelin-related protein in the PNS and CNS. *J Neurosci* **15**, 8281-94 (1995).
40. Balice-Gordon, R.J., Bone, L.J. & Scherer, S.S. Functional gap junctions in the schwann cell myelin sheath. *J Cell Biol* **142**, 1095-104 (1998).
41. Abrams, C.K., Oh, S., Ri, Y. & Bargiello, T.A. Mutations in connexin 32: the molecular and biophysical bases for the X-linked form of Charcot-Marie-Tooth disease. *Brain Res Brain Res Rev* **32**, 203-14 (2000).
42. Bicego, M. et al. Selective defects in channel permeability associated with Cx32 mutations causing X-linked Charcot-Marie-Tooth disease. *Neurobiol Dis* **21**, 607-17 (2006).
43. Ressot, C. & Bruzzone, R. Connexin channels in Schwann cells and the development of the X-linked form of Charcot-Marie-Tooth disease. *Brain Res Brain Res Rev* **32**, 192-202 (2000).
44. Kleopa, K.A., Yum, S.W. & Scherer, S.S. Cellular mechanisms of connexin32 mutations associated with CNS manifestations. *J Neurosci Res* **68**, 522-34 (2002).
45. Murru, M.R. et al. A novel Cx32 mutation causes X-linked Charcot-Marie-Tooth disease with brainstem involvement and brain magnetic resonance spectroscopy abnormalities. *Neurol Sci* **27**, 18-23 (2006).
46. Bondurand, N. et al. Human Connexin 32, a gap junction protein altered in the X-linked form of Charcot-Marie-Tooth disease, is directly regulated by the transcription factor SOX10. *Hum Mol Genet* **10**, 2783-95 (2001).
47. Houlden, H. et al. Connexin 32 promoter P2 mutations: a mechanism of peripheral nerve dysfunction. *Ann Neurol* **56**, 730-4 (2004).
48. Nelles, E. et al. Defective propagation of signals generated by sympathetic nerve stimulation in the liver of connexin32-deficient mice. *Proc Natl Acad Sci U S A* **93**, 9565-70 (1996).
49. Stumpel, F., Ott, T., Willecke, K. & Jungermann, K. Connexin 32 gap junctions enhance stimulation of glucose output by glucagon and noradrenaline in mouse liver. *Hepatology* **28**, 1616-20 (1998).
50. Temme, A. et al. High incidence of spontaneous and chemically induced liver tumors in mice deficient for connexin32. *Curr Biol* **7**, 713-6 (1997).
51. Scherer, S.S. et al. Connexin32-null mice develop demyelinating peripheral neuropathy. *Glia* **24**, 8-20 (1998).
52. Anzini, P. et al. Structural abnormalities and deficient maintenance of peripheral nerve myelin in mice lacking the gap junction protein connexin 32. *J Neurosci* **17**, 4545-51 (1997).
53. Scherer, S.S. et al. Transgenic expression of human connexin32 in myelinating Schwann cells prevents demyelination in connexin32-null mice. *J Neurosci* **25**, 1550-9 (2005).
54. Neuberg, D.H., Sancho, S. & Suter, U. Altered molecular architecture

of peripheral nerves in mice lacking the peripheral myelin protein 22 or connexin32. *J Neurosci Res* **58**, 612-23 (1999).
55. Nicholson, S.M., Gomes, D., de Nechaud, B. & Bruzzone, R. Altered gene expression in Schwann cells of connexin32 knockout animals. *J Neurosci Res* **66**, 23-36 (2001).
56. Melanson-Drapeau, L. et al. Oligodendrocyte progenitor enrichment in the connexin32 null-mutant mouse. *J Neurosci* **23**, 1759-68 (2003).
57. Sutor, B., Schmolke, C., Teubner, B., Schirmer, C. & Willecke, K. Myelination defects and neuronal hyperexcitability in the neocortex of connexin 32-deficient mice. *Cereb Cortex* **10**, 684-97 (2000).
58. Sohl, G., Eiberger, J., Jung, Y.T., Kozak, C.A. & Willecke, K. The mouse gap junction gene connexin29 is highly expressed in sciatic nerve and regulated during brain development. *Biol Chem* **382**, 973-8 (2001).
59. Altevogt, B.M., Kleopa, K.A., Postma, F.R., Scherer, S.S. & Paul, D.L. Connexin29 is uniquely distributed within myelinating glial cells of the central and peripheral nervous systems. *J Neurosci* **22**, 6458-70 (2002).
60. Huang, Y., Sirkowski, E.E., Stickney, J.T. & Scherer, S.S. Prenylation-defective human connexin32 mutants are normally localized and function equivalently to wild-type connexin32 in myelinating Schwann cells. *J Neurosci* **25**, 7111-20 (2005).
61. Eiberger, J. et al. Expression pattern and functional characterization of connexin29 in transgenic mice. *Glia* **53**, 601-11 (2006).
62. Rodriguez-Sinovas, A. et al. The modulatory effects of connexin 43 on cell death/survival beyond cell coupling. *Prog Biophys Mol Biol* **94**, 219-32 (2007).
63. Iino, S., Asamoto, K. & Nojyo, Y. Heterogeneous distribution of a gap junction protein, connexin43, in the gastroduodenal junction of the guinea pig. *Auton Neurosci* **93**, 8-13 (2001).
64. Zhang, C., Finger, T.E. & Restrepo, D. Mature olfactory receptor neurons express connexin 43. *J Comp Neurol* **426**, 1-12 (2000).
65. Willecke, K. et al. Structural and functional diversity of connexin genes in the mouse and human genome. *Biol Chem* **383**, 725-37 (2002).
66. Dhein, S., Polontchouk, L., Salameh, A. & Haefliger, J.A. Pharmacological modulation and differential regulation of the cardiac gap junction proteins connexin 43 and connexin 40. *Biol Cell* **94**, 409-22 (2002).
67. Gourdie, R.G. et al. The spatial distribution and relative abundance of gap-junctional connexin40 and connexin43 correlate to functional properties of components of the cardiac atrioventricular conduction system. *J Cell Sci* **105 (Pt 4)**, 985-91 (1993).
68. Schulz, R. et al. Connexin 43 in ischemic pre- and postconditioning. *Heart Fail Rev* **12**, 261-6 (2007).
69. Boengler, K., Schulz, R. & Heusch, G. Connexin 43 signalling and cardioprotection. *Heart* **92**, 1724-7 (2006).
70. Mambetisaeva, E.T., Gire, V. & Evans, W.H. Multiple connexin

expression in peripheral nerve, Schwann cells, and Schwannoma cells. *J Neurosci Res* **57**, 166-75 (1999).
71. Yoshimura, T., Satake, M. & Kobayashi, T. Connexin43 is another gap junction protein in the peripheral nervous system. *J Neurochem* **67**, 1252-8 (1996).
72. Chandross, K.J. Nerve injury and inflammatory cytokines modulate gap junctions in the peripheral nervous system. *Glia* **24**, 21-31 (1998).
73. Gimlich, R.L., Kumar, N.M. & Gilula, N.B. Sequence and developmental expression of mRNA coding for a gap junction protein in Xenopus. *J Cell Biol* **107**, 1065-73 (1988).
74. Ebihara, L., Beyer, E.C., Swenson, K.I., Paul, D.L. & Goodenough, D.A. Cloning and expression of a Xenopus embryonic gap junction protein. *Science* **243**, 1194-5 (1989).
75. Gimlich, R.L., Kumar, N.M. & Gilula, N.B. Differential regulation of the levels of three gap junction mRNAs in Xenopus embryos. *J Cell Biol* **110**, 597-605 (1990).
76. Yoshizaki, G. & Patino, R. Molecular cloning, tissue distribution, and hormonal control in the ovary of Cx41 mRNA, a novel Xenopus connexin gene transcript. *Mol Reprod Dev* **42**, 7-18 (1995).
77. Landesman, Y., Postma, F.R., Goodenough, D.A. & Paul, D.L. Multiple connexins contribute to intercellular communication in the Xenopus embryo. *J Cell Sci* **116**, 29-38 (2003).
78. Yen, M.R. & Saier, M.H., Jr. Gap junctional proteins of animals: the innexin/pannexin superfamily. *Prog Biophys Mol Biol* **94**, 5-14 (2007).
79. Panchin, Y.V. Evolution of gap junction proteins--the pannexin alternative. *J Exp Biol* **208**, 1415-9 (2005).
80. Baranova, A. et al. The mammalian pannexin family is homologous to the invertebrate innexin gap junction proteins. *Genomics* **83**, 706-16 (2004).
81. Phelan, P. & Starich, T.A. Innexins get into the gap. *Bioessays* **23**, 388-96 (2001).
82. Bruzzone, R., Hormuzdi, S.G., Barbe, M.T., Herb, A. & Monyer, H. Pannexins, a family of gap junction proteins expressed in brain. *Proc Natl Acad Sci U S A* **100**, 13644-9 (2003).
83. Dvoriantchikova, G., Ivanov, D., Panchin, Y. & Shestopalov, V.I. Expression of pannexin family of proteins in the retina. *FEBS Lett* **580**, 2178-82 (2006).
84. Dahl, G. & Locovei, S. Pannexin: to gap or not to gap, is that a question? *IUBMB Life* **58**, 409-19 (2006).
85. Locovei, S., Bao, L. & Dahl, G. Pannexin 1 in erythrocytes: function without a gap. *Proc Natl Acad Sci U S A* **103**, 7655-9 (2006).
86. Huang, Y.J. et al. The role of pannexin 1 hemichannels in ATP release and cell-cell communication in mouse taste buds. *Proc Natl Acad Sci U S A* **104**, 6436-41 (2007).
87. Thompson, R.J., Zhou, N. & MacVicar, B.A. Ischemia opens neuronal gap junction hemichannels. *Science* **312**, 924-7 (2006).
88. Pelegrin, P. & Surprenant, A. Pannexin-1 mediates large pore formation and interleukin-1beta release by the ATP-gated P2X7

receptor. *EMBO J* **25**, 5071-82 (2006).
89. Pelegrin, P. & Surprenant, A. Pannexin-1 couples to maitotoxin- and nigericin-induced interleukin-1beta release through a dye uptake-independent pathway. *J Biol Chem* **282**, 2386-94 (2007).
90. Locovei, S., Wang, J. & Dahl, G. Activation of pannexin 1 channels by ATP through P2Y receptors and by cytoplasmic calcium. *FEBS Lett* **580**, 239-44 (2006).
91. Shestopalov, V.I. & Panchin, Y. Pannexins and gap junction protein diversity. *Cell Mol Life Sci* **65**, 376-94 (2008).
92. Rizo, J. & Sudhof, T.C. Snares and Munc18 in synaptic vesicle fusion. *Nat Rev Neurosci* **3**, 641-53 (2002).
93. Hayashi, T. et al. Synaptic vesicle membrane fusion complex: action of clostridial neurotoxins on assembly. *EMBO J* **13**, 5051-61 (1994).
94. Jahn, R. & Sudhof, T.C. Membrane fusion and exocytosis. *Annu Rev Biochem* **68**, 863-911 (1999).
95. Margittai, M., Fasshauer, D., Jahn, R. & Langen, R. The Habc domain and the SNARE core complex are connected by a highly flexible linker. *Biochemistry* **42**, 4009-14 (2003).
96. Fujiwara, T. et al. Analysis of knock-out mice to determine the role of HPC-1/syntaxin 1A in expressing synaptic plasticity. *J Neurosci* **26**, 5767-76 (2006).
97. Arien, H., Wiser, O., Arkin, I.T., Leonov, H. & Atlas, D. Syntaxin 1A modulates the voltage-gated L-type calcium channel (Ca(v)1.2) in a cooperative manner. *J Biol Chem* **278**, 29231-9 (2003).
98. Wiser, O., Cohen, R. & Atlas, D. Ionic dependence of Ca2+ channel modulation by syntaxin 1A. *Proc Natl Acad Sci U S A* **99**, 3968-73 (2002).
99. Catterall, W.A. Interactions of presynaptic Ca2+ channels and snare proteins in neurotransmitter release. *Ann N Y Acad Sci* **868**, 144-59 (1999).
100. Li, Q. et al. A syntaxin 1, Galpha(o), and N-type calcium channel complex at a presynaptic nerve terminal: analysis by quantitative immunocolocalization. *J Neurosci* **24**, 4070-81 (2004).
101. Michaelevski, I. et al. Direct interaction of target SNAREs with the Kv2.1 channel. Modal regulation of channel activation and inactivation gating. *J Biol Chem* **278**, 34320-30 (2003).
102. Ling, S., Sheng, J.Z., Braun, J.E. & Braun, A.P. Syntaxin 1A co-associates with native rat brain and cloned large conductance, calcium-activated potassium channels in situ. *J Physiol* **553**, 65-81 (2003).
103. Condliffe, S.B., Zhang, H. & Frizzell, R.A. Syntaxin 1A regulates ENaC channel activity. *J Biol Chem* **279**, 10085-92 (2004).
104. Ganeshan, R., Di, A., Nelson, D.J., Quick, M.W. & Kirk, K.L. The interaction between syntaxin 1A and cystic fibrosis transmembrane conductance regulator Cl- channels is mechanistically distinct from syntaxin 1A-SNARE interactions. *J Biol Chem* **278**, 2876-85 (2003).
105. Cherian, P.P. et al. Mechanical strain opens connexin 43 hemichannels in osteocytes: a novel mechanism for the release of

prostaglandin. *Mol Biol Cell* **16**, 3100-6 (2005).
106. Takemura, H. et al. Hypotonicity-induced ATP release is potentiated by intracellular Ca2+ and cyclic AMP in cultured human bronchial cells. *Jpn J Physiol* **53**, 319-26 (2003).
107. Mitchell, C.H., Carre, D.A., McGlinn, A.M., Stone, R.A. & Civan, M.M. A release mechanism for stored ATP in ocular ciliary epithelial cells. *Proc Natl Acad Sci U S A* **95**, 7174-8 (1998).
108. Boudreault, F. & Grygorczyk, R. Cell swelling-induced ATP release is tightly dependent on intracellular calcium elevations. *J Physiol* **561**, 499-513 (2004).
109. Knight, G.E., Bodin, P., De Groat, W.C. & Burnstock, G. ATP is released from guinea pig ureter epithelium on distension. *Am J Physiol Renal Physiol* **282**, F281-8 (2002).
110. Braet, K. et al. Pharmacological sensitivity of ATP release triggered by photoliberation of inositol-1,4,5-trisphosphate and zero extracellular calcium in brain endothelial cells. *J Cell Physiol* **197**, 205-13 (2003).
111. Arcuino, G. et al. Intercellular calcium signaling mediated by point-source burst release of ATP. *Proc Natl Acad Sci U S A* **99**, 9840-5 (2002).
112. Lazarowski, E.R., Boucher, R.C. & Harden, T.K. Mechanisms of release of nucleotides and integration of their action as P2X- and P2Y-receptor activating molecules. *Mol Pharmacol* **64**, 785-95 (2003).
113. Sorensen, C.E. & Novak, I. Visualization of ATP release in pancreatic acini in response to cholinergic stimulus. Use of fluorescent probes and confocal microscopy. *J Biol Chem* **276**, 32925-32 (2001).
114. Burnstock, G. The past, present and future of purine nucleotides as signalling molecules. *Neuropharmacology* **36**, 1127-39 (1997).
115. Evans, R.J., Derkach, V. & Surprenant, A. ATP mediates fast synaptic transmission in mammalian neurons. *Nature* **357**, 503-5 (1992).
116. Ballerini, P. et al. Glial cells express multiple ATP binding cassette proteins which are involved in ATP release. *Neuroreport* **13**, 1789-92 (2002).
117. Reigada, D. & Mitchell, C.H. Release of ATP from retinal pigment epithelial cells involves both CFTR and vesicular transport. *Am J Physiol Cell Physiol* **288**, C132-40 (2005).
118. Sprague, R.S., Ellsworth, M.L., Stephenson, A.H., Kleinhenz, M.E. & Lonigro, A.J. Deformation-induced ATP release from red blood cells requires CFTR activity. *Am J Physiol* **275**, H1726-32 (1998).
119. Abraham, E.H. et al. Cystic fibrosis transmembrane conductance regulator and adenosine triphosphate. *Science* **275**, 1324-6 (1997).
120. Hazama, A. et al. Swelling-induced, CFTR-independent ATP release from a human epithelial cell line: lack of correlation with volume-sensitive cl(-) channels. *J Gen Physiol* **114**, 525-33 (1999).
121. Watt, W.C., Lazarowski, E.R. & Boucher, R.C. Cystic fibrosis transmembrane regulator-independent release of ATP. Its implications for the regulation of P2Y2 receptors in airway epithelia. *J Biol Chem* **273**, 14053-8 (1998).
122. Donaldson, S.H. et al. Basal nucleotide levels, release, and

metabolism in normal and cystic fibrosis airways. *Mol Med* **6**, 969-82 (2000).
123. Sauer, H., Hescheler, J. & Wartenberg, M. Mechanical strain-induced Ca(2+) waves are propagated via ATP release and purinergic receptor activation. *Am J Physiol Cell Physiol* **279**, C295-307 (2000).
124. Hisadome, K. et al. Volume-regulated anion channels serve as an auto/paracrine nucleotide release pathway in aortic endothelial cells. *J Gen Physiol* **119**, 511-20 (2002).
125. Sabirov, R.Z., Dutta, A.K. & Okada, Y. Volume-dependent ATP-conductive large-conductance anion channel as a pathway for swelling-induced ATP release. *J Gen Physiol* **118**, 251-66 (2001).
126. Bodas, E. et al. ATP crossing the cell plasma membrane generates an ionic current in xenopus oocytes. *J Biol Chem* **275**, 20268-73 (2000).
127. Abraham, E.H. et al. Erythrocyte membrane ATP binding cassette (ABC) proteins: MRP1 and CFTR as well as CD39 (ecto-apyrase) involved in RBC ATP transport and elevated blood plasma ATP of cystic fibrosis. *Blood Cells Mol Dis* **27**, 165-80 (2001).
128. Guthrie, P.B. et al. ATP released from astrocytes mediates glial calcium waves. *J Neurosci* **19**, 520-8 (1999).
129. Cotrina, M.L., Lin, J.H., Lopez-Garcia, J.C., Naus, C.C. & Nedergaard, M. ATP-mediated glia signaling. *J Neurosci* **20**, 2835-44 (2000).
130. Jorgensen, N.R. et al. Intercellular calcium signaling occurs between human osteoblasts and osteoclasts and requires activation of osteoclast P2X7 receptors. *J Biol Chem* **277**, 7574-80 (2002).
131. Stout, C., Goodenough, D.A. & Paul, D.L. Connexins: functions without junctions. *Curr Opin Cell Biol* **16**, 507-12 (2004).
132. Coco, S. et al. Storage and release of ATP from astrocytes in culture. *J Biol Chem* **278**, 1354-62 (2003).
133. Suadicani, S.O., Brosnan, C.F. & Scemes, E. P2X7 receptors mediate ATP release and amplification of astrocytic intercellular Ca2+ signaling. *J Neurosci* **26**, 1378-85 (2006).
134. Romanello, M., Veronesi, V. & D'Andrea, P. Mechanosensitivity and intercellular communication in HOBIT osteoblastic cells: a possible role for gap junction hemichannels. *Biorheology* **40**, 119-21 (2003).
135. Gomes, P., Srinivas, S.P., Van Driessche, W., Vereecke, J. & Himpens, B. ATP release through connexin hemichannels in corneal endothelial cells. *Invest Ophthalmol Vis Sci* **46**, 1208-18 (2005).
136. Pearson, R.A., Dale, N., Llaudet, E. & Mobbs, P. ATP released via gap junction hemichannels from the pigment epithelium regulates neural retinal progenitor proliferation. *Neuron* **46**, 731-44 (2005).
137. Zhao, H.B., Yu, N. & Fleming, C.R. Gap junctional hemichannel-mediated ATP release and hearing controls in the inner ear. *Proc Natl Acad Sci U S A* **102**, 18724-9 (2005).
138. Bahima, L. et al. Endogenous hemichannels play a role in the release of ATP from Xenopus oocytes. *J Cell Physiol* **206**, 95-102 (2006).
139. Holton, P. The liberation of adenosine triphosphate on antidromic stimulation of sensory nerves. *J Physiol* **145**, 494-504 (1959).
140. Burnstock, G., Campbell, G., Satchell, D. & Smythe, A. Evidence that

adenosine triphosphate or a related nucleotide is the transmitter substance released by non-adrenergic inhibitory nerves in the gut. *Br J Pharmacol* **40**, 668-88 (1970).
141. Burnstock, G. Purinergic nerves. *Pharmacol Rev* **24**, 509-81 (1972).
142. Bardoni, R., Goldstein, P.A., Lee, C.J., Gu, J.G. & MacDermott, A.B. ATP P2X receptors mediate fast synaptic transmission in the dorsal horn of the rat spinal cord. *J Neurosci* **17**, 5297-304 (1997).
143. Nieber, K., Poelchen, W. & Illes, P. Role of ATP in fast excitatory synaptic potentials in locus coeruleus neurones of the rat. *Br J Pharmacol* **122**, 423-30 (1997).
144. Pankratov, Y., Castro, E., Miras-Portugal, M.T. & Krishtal, O. A purinergic component of the excitatory postsynaptic current mediated by P2X receptors in the CA1 neurons of the rat hippocampus. *Eur J Neurosci* **10**, 3898-902 (1998).
145. Burnstock, G. Autonomic neuromuscular junctions: current developments and future directions. *J Anat* **146**, 1-30 (1986).
146. Silinsky, E.M., Gerzanich, V. & Vanner, S.M. ATP mediates excitatory synaptic transmission in mammalian neurones. *Br J Pharmacol* **106**, 762-3 (1992).
147. Schwiebert, E.M. & Zsembery, A. Extracellular ATP as a signaling molecule for epithelial cells. *Biochim Biophys Acta* **1615**, 7-32 (2003).
148. Gachet, C. Regulation of platelet functions by P2 receptors. *Annu Rev Pharmacol Toxicol* **46**, 277-300 (2006).
149. Raffaghello, L., Chiozzi, P., Falzoni, S., Di Virgilio, F. & Pistoia, V. The P2X7 receptor sustains the growth of human neuroblastoma cells through a substance P-dependent mechanism. *Cancer Res* **66**, 907-14 (2006).
150. Fredholm, B.B. et al. Towards a revised nomenclature for P1 and P2 receptors. *Trends Pharmacol Sci* **18**, 79-82 (1997).
151. Abbracchio, M.P. & Burnstock, G. Purinoceptors: are there families of P2X and P2Y purinoceptors? *Pharmacol Ther* **64**, 445-75 (1994).
152. Ralevic, V. & Burnstock, G. Receptors for purines and pyrimidines. *Pharmacol Rev* **50**, 413-92 (1998).
153. Kidd, E.J. et al. Localization of P2X purinoceptor transcripts in the rat nervous system. *Mol Pharmacol* **48**, 569-73 (1995).
154. Kanjhan, R. et al. Distribution of the P2X2 receptor subunit of the ATP-gated ion channels in the rat central nervous system. *J Comp Neurol* **407**, 11-32 (1999).
155. Garcia-Guzman, M., Stuhmer, W. & Soto, F. Molecular characterization and pharmacological properties of the human P2X3 purinoceptor. *Brain Res Mol Brain Res* **47**, 59-66 (1997).
156. Garcia-Guzman, M., Soto, F., Gomez-Hernandez, J.M., Lund, P.E. & Stuhmer, W. Characterization of recombinant human P2X4 receptor reveals pharmacological differences to the rat homologue. *Mol Pharmacol* **51**, 109-18 (1997).
157. Grafe, P., Mayer, C., Takigawa, T., Kamleiter, M. & Sanchez-Brandelik, R. Confocal calcium imaging reveals an ionotropic P2 nucleotide receptor in the paranodal membrane of rat Schwann cells. *J Physiol*

515 (Pt 2), 377-83 (1999).
158. von Kugelgen, I. & Wetter, A. Molecular pharmacology of P2Y-receptors. *Naunyn Schmiedebergs Arch Pharmacol* **362**, 310-23 (2000).
159. Jessen, K.R. Glial cells. *Int J Biochem Cell Biol* **36**, 1861-7 (2004).
160. Jessen, K.R. & Mirsky, R. Signals that determine Schwann cell identity. *J Anat* **200**, 367-76 (2002).
161. Bhatheja, K. & Field, J. Schwann cells: origins and role in axonal maintenance and regeneration. *Int J Biochem Cell Biol* **38**, 1995-9 (2006).
162. Jessen, K.R. & Mirsky, R. The origin and development of glial cells in peripheral nerves. *Nat Rev Neurosci* **6**, 671-82 (2005).
163. Voyvodic, J.T. Target size regulates calibre and myelination of sympathetic axons. *Nature* **342**, 430-3 (1989).
164. Snipes, G.J. & Suter, U. Molecular anatomy and genetics of myelin proteins in the peripheral nervous system. *J Anat* **186 (Pt 3)**, 483-94 (1995).
165. Arroyo, E.J. & Scherer, S.S. On the molecular architecture of myelinated fibers. *Histochem Cell Biol* **113**, 1-18 (2000).
166. Ritchie, J.M. & Rogart, R.B. Density of sodium channels in mammalian myelinated nerve fibers and nature of the axonal membrane under the myelin sheath. *Proc Natl Acad Sci U S A* **74**, 211-5 (1977).
167. Ariyasu, R.G., Nichol, J.A. & Ellisman, M.H. Localization of sodium/potassium adenosine triphosphatase in multiple cell types of the murine nervous system with antibodies raised against the enzyme from kidney. *J Neurosci* **5**, 2581-96 (1985).
168. Einheber, S. et al. The axonal membrane protein Caspr, a homologue of neurexin IV, is a component of the septate-like paranodal junctions that assemble during myelination. *J Cell Biol* **139**, 1495-506 (1997).
169. Menegoz, M. et al. Paranodin, a glycoprotein of neuronal paranodal membranes. *Neuron* **19**, 319-31 (1997).
170. Poliak, S. et al. Caspr2, a new member of the neurexin superfamily, is localized at the juxtaparanodes of myelinated axons and associates with K+ channels. *Neuron* **24**, 1037-47 (1999).
171. Chiu, S.Y. & Ritchie, J.M. Potassium channels in nodal and internodal axonal membrane of mammalian myelinated fibres. *Nature* **284**, 170-1 (1980).
172. Mi, H., Deerinck, T.J., Ellisman, M.H. & Schwarz, T.L. Differential distribution of closely related potassium channels in rat Schwann cells. *J Neurosci* **15**, 3761-74 (1995).
173. Vabnick, I. & Shrager, P. Ion channel redistribution and function during development of the myelinated axon. *J Neurobiol* **37**, 80-96 (1998).
174. Smart, S.L. et al. Deletion of the K(V)1.1 potassium channel causes epilepsy in mice. *Neuron* **20**, 809-19 (1998).
175. Zhou, L., Zhang, C.L., Messing, A. & Chiu, S.Y. Temperature-sensitive neuromuscular transmission in Kv1.1 null mice: role of potassium channels under the myelin sheath in young nerves. *J Neurosci* **18**,

7200-15 (1998).
176. Meier, C., Dermietzel, R., Davidson, K.G., Yasumura, T. & Rash, J.E. Connexin32-containing gap junctions in Schwann cells at the internodal zone of partial myelin compaction and in Schmidt-Lanterman incisures. *J Neurosci* **24**, 3186-98 (2004).
177. Chanson, M., Chandross, K.J., Rook, M.B., Kessler, J.A. & Spray, D.C. Gating characteristics of a steeply voltage-dependent gap junction channel in rat Schwann cells. *J Gen Physiol* **102**, 925-46 (1993).
178. Li, J. et al. Analysis of connexin expression during mouse Schwann cell development identifies connexin29 as a novel marker for the transition of neural crest to precursor cells. *Glia* **55**, 93-103 (2007).
179. Li, X. et al. Connexin29 expression, immunocytochemistry and freeze-fracture replica immunogold labelling (FRIL) in sciatic nerve. *Eur J Neurosci* **16**, 795-806 (2002).
180. Chandross, K.J. et al. Altered connexin expression after peripheral nerve injury. *Mol Cell Neurosci* **7**, 501-18 (1996).
181. Roscoe, W.A., Messersmith, E., Meyer-Franke, A., Wipke, B. & Karlik, S.J. Connexin 43 gap junction proteins are up-regulated in remyelinating spinal cord. *J Neurosci Res* **85**, 945-53 (2007).
182. Maier, M., Berger, P. & Suter, U. Understanding Schwann cell-neurone interactions: the key to Charcot-Marie-Tooth disease? *J Anat* **200**, 357-66 (2002).
183. Chojnowski, A. et al. Silencing of the Charcot-Marie-Tooth associated MTMR2 gene decreases proliferation and enhances cell death in primary cultures of Schwann cells. *Neurobiol Dis* **26**, 323-31 (2007).
184. Berger, P., Niemann, A. & Suter, U. Schwann cells and the pathogenesis of inherited motor and sensory neuropathies (Charcot-Marie-Tooth disease). *Glia* **54**, 243-57 (2006).
185. Colomar, A. & Amedee, T. ATP stimulation of P2X(7) receptors activates three different ionic conductances on cultured mouse Schwann cells. *Eur J Neurosci* **14**, 927-36 (2001).
186. Lyons, S.A., Morell, P. & McCarthy, K.D. Schwann cells exhibit P2Y purinergic receptors that regulate intracellular calcium and are up-regulated by cyclic AMP analogues. *J Neurochem* **63**, 552-60 (1994).
187. Baker, M.D. Electrophysiology of mammalian Schwann cells. *Prog Biophys Mol Biol* **78**, 83-103 (2002).
188. Stevens, B. & Fields, R.D. Response of Schwann cells to action potentials in development. *Science* **287**, 2267-71 (2000).
189. Mayer, C., Quasthoff, S. & Grafe, P. Differences in the sensitivity to purinergic stimulation of myelinating and non-myelinating Schwann cells in peripheral human and rat nerve. *Glia* **23**, 374-82 (1998).
190. Fields, R.D. & Stevens, B. ATP: an extracellular signaling molecule between neurons and glia. *Trends Neurosci* **23**, 625-33 (2000).
191. Fields, R.D. & Burnstock, G. Purinergic signalling in neuron-glia interactions. *Nat Rev Neurosci* **7**, 423-36 (2006).
192. Liu, G.J., Werry, E.L. & Bennett, M.R. Secretion of ATP from Schwann cells in response to uridine triphosphate. *Eur J Neurosci* **21**, 151-60 (2005).

193. Liu, G.J. & Bennett, M.R. ATP secretion from nerve trunks and Schwann cells mediated by glutamate. *Neuroreport* **14**, 2079-83 (2003).
194. Barrio, L.C. et al. Gap junctions formed by connexins 26 and 32 alone and in combination are differently affected by applied voltage. *Proc Natl Acad Sci U S A* **88**, 8410-4 (1991).
195. McElroy, W.D. The Energy Source for Bioluminescence in an Isolated System. *Proc Natl Acad Sci U S A* **33**, 342-5 (1947).
196. Gonzalez-Sistal, A. et al. Ionic dependence of the velocity of release of ATP from permeabilized cholinergic synaptic vesicles. *Neuroscience* **149**, 251-5 (2007).
197. Brockes, J.P., Fields, K.L. & Raff, M.C. Studies on cultured rat Schwann cells. I. Establishment of purified populations from cultures of peripheral nerve. *Brain Res* **165**, 105-18 (1979).
198. Serra, E. et al. Schwann cells harbor the somatic NF1 mutation in neurofibromas: evidence of two different Schwann cell subpopulations. *Hum Mol Genet* **9**, 3055-64 (2000).
199. Rosenbaum, T. et al. Long-term culture and characterization of human neurofibroma-derived Schwann cells. *J Neurosci Res* **61**, 524-32 (2000).
200. Spreca, A. et al. Immunocytochemical localization of S-100b protein in degenerating and regenerating rat sciatic nerves. *J Histochem Cytochem* **37**, 441-6 (1989).
201. Evans, W.H., De Vuyst, E. & Leybaert, L. The gap junction cellular internet: connexin hemichannels enter the signalling limelight. *Biochem J* **397**, 1-14 (2006).
202. Abdipranoto, A., Liu, G.J., Werry, E.L. & Bennett, M.R. Mechanisms of secretion of ATP from cortical astrocytes triggered by uridine triphosphate. *Neuroreport* **14**, 2177-81 (2003).
203. Faria, R.X., Defarias, F.P. & Alves, L.A. Are second messengers crucial for opening the pore associated with P2X7 receptor? *Am J Physiol Cell Physiol* **288**, C260-71 (2005).
204. Arellano, R.O., Woodward, R.M. & Miledi, R. A monovalent cationic conductance that is blocked by extracellular divalent cations in Xenopus oocytes. *J Physiol* **484 (Pt 3)**, 593-604 (1995).
205. Reifarth, F.W., Amasheh, S., Clauss, W. & Weber, W. The Ca2+-inactivated Cl- channel at work: selectivity, blocker kinetics and transport visualization. *J Membr Biol* **155**, 95-104 (1997).
206. Zhang, Y., McBride, D.W., Jr. & Hamill, O.P. The ion selectivity of a membrane conductance inactivated by extracellular calcium in Xenopus oocytes. *J Physiol* **508 (Pt 3)**, 763-76 (1998).
207. Zhang, Y. & Hamill, O.P. Calcium-, voltage- and osmotic stress-sensitive currents in Xenopus oocytes and their relationship to single mechanically gated channels. *J Physiol* **523 Pt 1**, 83-99 (2000).
208. Maroto, R. & Hamill, O.P. Brefeldin A block of integrin-dependent mechanosensitive ATP release from Xenopus oocytes reveals a novel mechanism of mechanotransduction. *J Biol Chem* **276**, 23867-72 (2001).

determinant of charge selectivity in connexin46 channels. *Biophys J* **79**, 3036-51 (2000).

227. Cao, F. et al. A quantitative analysis of connexin-specific permeability differences of gap junctions expressed in HeLa transfectants and Xenopus oocytes. *J Cell Sci* **111 (Pt 1)**, 31-43 (1998).